Authors: Subcommittee on Biologic Markers in Urinary Toxicology, National Reseach Council

those scenarios differ in species (animal-to-human extrapolation), in magnitude of exposure (dose extrapolation), or in route of exposure (route-to-route extrapolation). Again, it is assumed, lacking data to the contrary, that a relationship observed in one scenario is valid in the other. Risk can be stated as the magnitude of exposure that is estimated to be without substantial likelihood of harmful effect, or stated as the probability of occurrence of harmful effect.

The remainder of this chapter concerns answers to two questions: What is the basis for concluding that extrapolation is reasonable? Can it be said that one approach to extrapolation is better than another approach? It is in relation to the second question that the relevance and utility of biologic markers in risk assessment become apparent.

Basis of Extrapolation

Animal Studies

A fundamental principle of toxicology is that results of animal studies can be applied to humans. The scientific basis for assuming that animals are good surrogates for humans and therefore a suitable basis for extrapolation to humans is overwhelming. If one considers that the genetic makeup of a mouse or a rat is more than 95% and of a monkey is more than 99% identical with that of a human, it is reasonable to assume that these animals in particular and mammals, in general, will react to infectious agents and chemical stressors much as humans will. Among mammals, most of the host defense mechanisms (barrier and immune) and metabolic (anabolic and catabolic) systems are similar. In particular, the urinary systems of most mammals are very similar. Although specific, often subtle, differences between humans and other animals with respect to renal function have been demonstrated, the vast majority of human renal responses to xenobiotics mimic what has been observed in other species. Biologic markers of renal transport, concentrating, and metabolic functions of the kidney are reproduced in many species, including humans, although quantitative differences have been demonstrated. Therefore, it is reasonable to use animal models for extrapolation to humans unless specific information on specific chemicals dictates otherwise.

Many epidemiologic investigations have, in fact, been suggested as a result of animal studies, and the epidemiologic findings have tended to support the results of the animal studies. For example, several of the current epidemiologic studies of heavy-metal toxicity, including small exposures, were initiated in response to urinary toxicity observed in a large number of animal studies and were undertaken specifically because of the likelihood that the human response would mimic that seen in animal test species. Mechanistic studies of chemically induced nephrotoxicity in animals influenced or stimulated epidemiologic studies of a variety of substances, including many of the halogenated hydrocarbons, such as chloroform, hexa-

chlorobutadiene, and bromobenzene. Much of the epidemiologic investigation and mechanistic understanding of anesthetic, analgesic, and antibiotic nephropathy has been driven by observations of nephrotoxicity in animals. Classic examples of the direct application of animal studies to epidemiology of known nephrotoxicants are the use of antineoplastic and immunosuppressant drugs (e.g., cisplatin and cyclosporin, respectively).

Studies of carcinogenic responses in laboratory animals and in humans have revealed substantial correlations (Crump et al., 1989). The results suggest that there are reasonable approaches to extrapolating cancer responses observed in test species—approaches that appear to predict fairly well the responses in humans.

Identification of chemical hazards should include assimilation and evaluation of all relevant information. Appraisal of physical and chemical properties and structure-activity relationships can sometimes provide important indications of potential toxic characteristics. Markers of urinary function and chemical toxicity in experimental animals can be studied at various levels of tissue structure and organization (Table 5-1). This is in contrast with human studies, in which only noninvasive studies of renal function are possible. Markers identified through in vitro studies of systems that use animal and human cells or tissues in culture can often give insight into potential toxicity. However, because of the intricacy of the body, only whole-animal studies or observations in humans provide information on the operation of multiple cells, tissues, and organs under the influence of complicated feedback mechanisms. Animals are necessary in the study of chemical-induced toxicity and for the development and validation of markers because studies that involve modulation of cellular responses and tissue sampling cannot be performed in humans.

Traditionally, experimental animal studies have been of most value for identifying markers that can be used to predict target-organ effects, understand dose-response relationships, and study mechanisms of action. The studies include measurements of function, blood chemistry, urinalysis (including cytology), histopathology, and electron microscopy. Metabolism and transport peculiar to the kidney are often routine parts of such studies.

Animal models developed as surrogates for humans in the study of renal and urinary function should conform to some general principles, which are applicable to any organ system, although they are discussed here in the context of renal and urinary toxicology. They include the following:

- The animal model should be reproducible within and among laboratories. It should not be so complex that only a few laboratories could do the study.
- The model should be peculiar to the part of the urinary tract under consideration. This characteristic can be realized only with sophisticated procedures that permit study of discrete nephron segments.

- The model should be sensitive enough to differentiate normal from abnormal changes in structure or function.
- The model should be able to measure alterations in renal structure or function caused by exogenous agents.

Whole-animal studies are usually the first step in evaluating the potential toxicity of a given agent, and these studies involve assessment of urine and plasma for markers indicative of organ function and toxicity. Noninvasive or nondestructive studies can be followed by application of histopathologic techniques to determine markers of target-organ or tissue-site injury. In most cases, rodents suffice, but there might be instances when only a primate can properly represent the human situation. For example, the route of administration might be important if direct extrapolation to humans is likely. With nephrotoxicants as with other toxicants, acute, subchronic, and chronic exposures are used to determine potential toxicity. The determination of markers of urinary toxicity is generally easier with acute protocols than with subchronic or chronic exposures. Studies often involve single exposures of both sexes of at least two species, usually rodents. Depending on the results of the rodent studies and the questions being asked, one might decide to study the agent in higher mammals, such as dogs or monkeys. The use of subchronic or chronic exposure regimens is usually driven by the nature of the potential human exposure, the agent being studied, and the possibility of chronic toxicity, including carcinogenicity.

Renal Parenchymal Injury

The difficulties in diagnosing renal injury and predicting its health consequences are considerable. That is primarily because the kidney can undergo substantial chemically induced injury without any clinical manifestation; subtle injury can be negligible, given the considerable functional reserve of the kidney. For example, the single cross-sectional measurement of glomerular filtration rate (GFR) might show only severe acute or chronic renal damage, as discussed in Chapter 2. Most studies indicate that quantitative urinary-enzyme secretion patterns cannot reveal either the type or the severity of renal injury, and often they do not correlate with structural or functional changes, as discussed in greater detail in Chapter 4. The need, therefore, is for standard diagnostic criteria that are sensitive enough to serve as markers of renal damage in the presence of renal functional reserve.

Much of the nephrotoxicity that follows the administration of inert, relatively nontoxic chemicals is related to the formation of reactive electrophiles during their metabolism (Ford and Hook, 1984). It is thought that the electrophilic products can react covalently with various nucleophilic sites on renal macromolecules and, by some mechanism yet to be defined, lead to renal damage. Measurement of the re-

0090-9556/02/3005-505–512$7.00
DRUG METABOLISM AND DISPOSITION
Copyright © 2002 by The American Society for Pharmacology and Experimental Therapeutics
DMD 30:505–512, 2002

Vol. 30, No. 5
623/975196
Printed in U.S.A.

GLUCURONIDATION OF STATINS IN ANIMALS AND HUMANS: A NOVEL MECHANISM OF STATIN LACTONIZATION

THOMAYANT PRUEKSARITANONT, RAJU SUBRAMANIAN, XIAOJUN FANG, BENNETT MA, YUE QIU, JIUNN H. LIN, PAUL G. PEARSON, AND THOMAS A. BAILLIE

Department of Drug Metabolism, Merck Research Laboratories, West Point, Pennsylvania

(Received October 25, 2001; accepted January 18, 2002)

This article is available online at http://dmd.aspetjournals.org

ABSTRACT:

The active forms of all marketed hydroxymethylglutaryl (HMG)-CoA reductase inhibitors share a common dihydroxy heptanoic or heptenoic acid side chain. In this study, we present evidence for the formation of acyl glucuronide conjugates of the hydroxy acid forms of simvastatin (SVA), atorvastatin (AVA), and cerivastatin (CVA) in rat, dog, and human liver preparations in vitro and for the excretion of the acyl glucuronide of SVA in dog bile and urine. Upon incubation of each statin (SVA, CVA or AVA) with liver microsomal preparations supplemented with UDP-glucuronic acid, two major products were detected. Based on analysis by high-pressure liquid chromatography, UV spectroscopy, and/or liquid chromatography (LC)-mass spectrometry analysis, these metabolites were identified as a glucuronide conjugate of the hydroxy acid form of the statin and the corresponding δ-lactone. By means of an LC-NMR technique, the glucuronide structure was established to be a 1-*O*-acyl-β-D-glucuronide conjugate of the statin acid. The formation of statin glucuronide and statin lactone in human liver microsomes exhibited modest intersubject variability (3- to 6-fold; n = 10). Studies with expressed UDP glucuronosyltransferases (UGTs) revealed that both UGT1A1 and UGT1A3 were capable of forming the glucuronide conjugates and the corresponding lactones for all three statins. Kinetic studies of statin glucuronidation and lactonization in liver microsomes revealed marked species differences in intrinsic clearance (CL_{int}) values for SVA (but not for AVA or CVA), with the highest CL_{int} observed in dogs, followed by rats and humans. Of the statins studied, SVA underwent glucuronidation and lactonization in human liver microsomes, with the lowest CL_{int} (0.4 μl/min/mg of protein for SVA versus ~3 μl/min/mg of protein for AVA and CVA). Consistent with the present in vitro findings, substantial levels of the glucuronide conjugate (~20% of dose) and the lactone form of SVA [simvastatin (SV); ~10% of dose] were detected in bile following i.v. administration of [^{14}C]SVA to dogs. The acyl glucuronide conjugate of SVA, upon isolation from an in vitro incubation, underwent spontaneous cyclization to SV. Since the rate of this lactonization was high under conditions of physiological pH, the present results suggest that the statin lactones detected previously in bile and/or plasma following administration of SVA to animals or of AVA or CVA to animals and humans, might originate, at least in part, from the corresponding acyl glucuronide conjugates. Thus, acyl glucuronide formation, which seems to be a common metabolic pathway for the hydroxy acid forms of statins, may play an important, albeit previously unrecognized, role in the conversion of active HMG-CoA reductase inhibitors to their latent δ-lactone forms.

HMG[1]-CoA reductase inhibitors, also called "statins", which target the rate-limiting enzyme in cholesterol biosynthesis, are used widely for the treatment of hypercholesterolemia and hypertriglyceridemia (Mauro, 1993). Except for simvastatin (SV) and lovastatin (LV), all currently available statins are administered as the pharmacologically active hydroxy acid forms. SV and LV are inactive δ-lactones, which, upon conversion to their respective hydroxy acids (SVA and LVA), serve as potent competitive inhibitors of HMG-CoA reductase (Duggan and Vickers, 1990). All statins undergo varying degrees of metabolism in both animals and humans (Vickers et al., 1990b; Everett et al., 1991; Dain et al., 1993; Halpin et al., 1993; Cheng et al., 1994; Le Couteur et al., 1996; Boberg et al., 1998; Black et al., 1999), catalyzed primarily by the cytochrome P450 system (Wang et al., 1991; Boberg et al., 1997; Prueksaritanont et al., 1997, 1999). Other reported biotransformation pathways include lactonization of statin hydroxy acids and β-oxidation at the common dihydroxy heptanoic or heptenoic acid side chain (Vickers et al., 1990b; Halpin et al., 1993; Boberg et al., 1997; Black et al., 1999; Prueksaritanont et al., 2001); in recent studies, it has been shown that the CoA thioester conjugate of the hydroxy acid side chain probably serves as an intermediate in these processes (Prueksaritanont et al., 2001).

In a recent study, glucuronide conjugates of CVA have been reported in animals (Boberg et al., 1998), indicating that the heptenoic acid side chain also may be subject to glucuronidation. To date, however, no other marketed statins have been reported to form glucuronides in animals or humans. In preliminary studies on the metabolism of SVA in dogs, we found high levels of SV and modest

[1] Abbreviations used are: HMG, hydroxymethylglutaryl; SV, simvastatin; LV, lovastatin; SVA, hydroxy acid form of simvastatin; LVA, hydroxy acid form of lovastatin; CVA, cerivastatin; UGT, UDP glucuronosyltransferase; AVA, atorvastatin; UDPGA, UDP-glucuronic acid; HPLC, high-pressure liquid chromatography; ACN, acetonitrile; LC-MS, liquid chromatography-mass spectrometry; CL_{int}, intrinsic clearance; AV, the lactone form of atorvastatin; CV, the lactone form of cerivastatin; P450, cytochrome P450.

Address correspondence to: Dr. Thomayant Prueksaritanont, Department of Drug Metabolism, Merck Research Laboratories, WP 75-100, West Point, PA 19486. E-mail: thomayant_prueksaritanont@merck.com

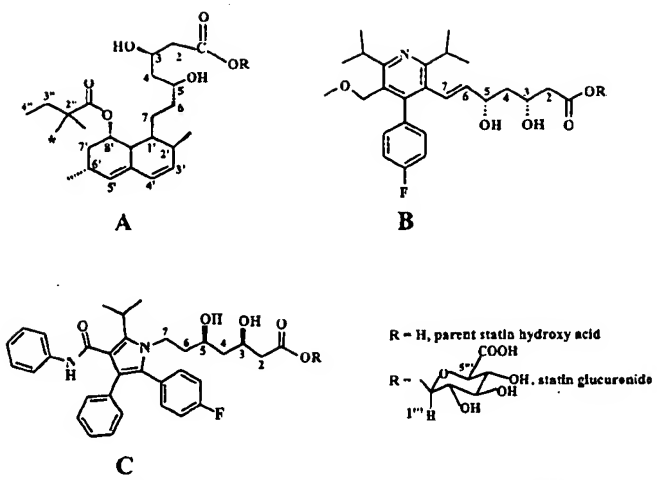

FIG. 1. *Structures of statin hydroxy acids and their acyl glucuronide conjugates for SVA (A), CVA (B), and AVA (C).*

*, indicates the position of ^{14}C label.

concentrations of SVA glucuronide in specimens of bile. Moreover, the glucuronide conjugate of SVA seemed to be unstable upon standing. Based on these observations, we speculated that acyl glucuronidation might be a common metabolic pathway for statins and that spontaneous cyclization of the resulting conjugate may contribute to the lactonization observed for all statins.

Based upon these considerations, we set out to characterize the glucuronidation of statins using SVA, AVA, and CVA as model compounds in liver microsomal preparations from both animals and humans. These three statins were selected for study since they have been reported to undergo significant lactonization in vivo in animals and/or humans (Vickers et al., 1990a,b; Boberg et al., 1998; Kantola et al., 1998). The identity of the UGTs, which catalyze the glucuronidation of these agents, was investigated with the aid of expressed enzymes, and the stability of the acyl glucuronide in vitro was studied in the case of the SVA conjugate. Finally, the significance of the glucuronidation pathway in the disposition of SVA in vivo was examined using the dog as an animal model.

Experimental Procedures

Materials. SV, SVA, and [^{14}C]SVA, with a specific activity of 50 μCi/μmol (Fig. 1), were synthesized at Merck Research Laboratories (Rahway, NJ). AVA and CVA were extracted from commercial sources, and their identity and purity were confirmed by infrared and NMR spectroscopy. Brij 58 and UDPGA were obtained from Sigma Chemical Co. (St. Louis, MO). CD_3CN (99.8 atom % D) and D_2O (99.8 atom % D) were purchased from Isotec, Inc. (Miamisburg, OH), and CF_3COOD (99.5 atom % D) was obtained from Aldrich Chemical Co. (Milwaukee, WI). All other reagents were of analytical or HPLC grade. Human recombinant UGTs were obtained from GENTEST (Woburn, MA) and Panvera (Madison, WI). Human liver microsomes were purchased from XenoTech, LLC (Kansas City, KS) and GENTEST, whereas those from male Sprague-Dawley rats (~260–320 g) and beagle dogs (9–11 kg) were prepared in-house, as described previously (Prueksaritanont et al., 1997), and were pooled from four to six animals before use.

In Vitro Metabolism of Statins. A typical incubation mixture, in a final volume of 0.3 ml, contained 0.3 mg (dog) or 0.45 mg (human or rat) of liver microsomal protein, preincubated for 15 min with 0.045 mg of Brij 58, 20 mM MgCl, 5 mM UDPGA, and 0.05 M Tris buffer, pH 7.0. The preincubation step with Brij 58 was found to be optimal for high enzyme activity. Unless otherwise specified, the reaction was started by the addition of SVA, AVA, or CVA following a 3-min preincubation at 37°C and was conducted for up to 60 min. Control experiments were performed by excluding either the microsomes or UDPGA from the incubation mixtures. The reaction was terminated at appropriate time intervals by the addition of 0.8 ml of acetonitrile (ACN). The ACN extracts were evaporated to dryness and reconstituted, just before analysis, in the mobile phase (20% ACN in 25 mM ammonium acetate buffer, pH 4.5) for analysis by the HPLC method described below. Kinetic studies were conducted using 0.2 to 200 μM statins in liver microsomal preparations from humans, rats, and dogs. The incubation mixtures were incubated for 45 min at 37°C.

Incubations with human recombinant UGTs were performed using the same conditions as described above for human liver microsomes, except that the mixture contained 0.3 mg of UGTs and was incubated for up to 60 min. Control incubations using microsomes isolated from the same cell line containing the vector, but without a cDNA insert, also were included.

For the purpose of isolation and purification of the statin glucuronides, large-scale incubations of the statins (100 μM; 20 × 0.5-ml incubation) were carried out with dog liver microsomes (2 mg/ml) and UDPGA (5 mM) for 60 min. The ACN extracts were evaporated to dryness and reconstituted for analysis by LC-MS and LC-NMR spectroscopy.

Stability of SVA Acyl Glucuronide. The acyl glucuronide of SVA was isolated by HPLC (see *Analytical Procedures* for conditions) from an in vitro incubation with dog liver microsomes, SVA (100 μM), and UDPGA (5 mM). Duplicate 0.5-min fractions (~0.5 ml) containing the SVA glucuronide were collected by a fraction collector (Foxy 200; ISCO, Inc., Lincoln, NE) into tubes containing 0.3 ml of buffer, with a specific pH value between 4 to 8. The resulting mixtures then were injected immediately onto an HPLC column (with an autosampler set at 5°C) at about 2.5-h intervals over an 8-h period. For each pH mixture, the time for the first injection was considered as the starting time (time = 0).

In Vivo Metabolism and Excretion of SVA. All studies were reviewed and approved by the Merck Research Laboratories Institutional Animal Care and Use Committee. Beagle dogs (n = 3 each; 9–14 kg) were surgically prepared with common bile-duct cannulae and were housed individually in metabolism cages with an extracorporeal reservoir on their back for bile collection. [^{14}C]SVA was administrated intravenously at 1.2 mg/kg, and bile was collected in a bag containing 0.5 M ammonium acetate buffer, pH 4.5 (~10% of total bile volume), continuously every hour over a period of 10 h and during the next 10 to 24 h. Urine samples also were collected during 0 to 8, 8 to 24, and 24 to 48 h postdose. The bile and urine samples were frozen immediately on dry ice and kept at −20°C for later analysis.

Analytical Procedures for Statins and Metabolites. SVA, CVA, AVA, and their metabolites were analyzed using published HPLC methods (Prueksaritanont et al., 1999) with minor modifications. In brief, samples held in an autosampler set at 5°C were chromatographed on a C_{18} Zorbax column (150 × 4.6 mm, 5 μm; Waters, Inc., Milford, MA) preceded by a C_{18} guard column, with a linear gradient of ACN and 25 mM ammonium acetate, pH 4.5. The eluate was monitored by UV absorption at 240 nm (SVA and AVA) or 280 nm (CVA) and by an on-line β-RAM radioactivity detector (IN/US Systems, Tampa, FL). Due to the unavailability of authentic standards for glucuronide conjugates of statins, quantitation of these metabolites in the in vitro incubation mixtures was accomplished using standard curves for their respective parent statins, assuming identical extraction recoveries and extinction coefficients between the parent drug and its corresponding glucuronide conjugate. For the three statins, standard curves showed satisfactory linearity and precision (<15% coefficient of variation). The limits of assay detection were 5 pmol (on column) for all three statins.

Levels of total radioactivity in bile and urine samples were determined by direct measurement of samples using a scintillation counter (Packard Instrument Company, Inc., Downers Grove, IL). Concentrations of SV, SVA glucuronide, and SVA in bile samples were estimated based on total radioactivity and metabolite profiling studies (using HPLC with an on-line IN/US β-RAM radioactivity detector).

Identification of the statin metabolites was accomplished by using LC-MS techniques (HP-1050 gradient system; Hewlett Packard, San Fernando, CA; Finnigan MAT LCQ ion trap mass spectrometer; Thermo Finnigan MAT, San Jose, CA). Separation of the metabolites was carried out on a Betasil C_{18} column (2 × 150 mm, 5 μm), with a linear gradient of ACN and 0.1% formic acid (30% ACN to 80% ACN in 20 min) delivered at a constant flow rate of 0.2 ml/min. Mass spectral analyses were performed using electrospray ionization in the negative ion mode (for SVA and AVA glucuronide conjugates) or

positive ion mode (for statin lactones and CVA glucuronide). The electrospray ionization voltage was set at 4 kV, with the heated capillary temperature held at 230°C.

For NMR studies, the dried extract from in vitro incubates containing the metabolite were reconstituted in approximately 250 μl of 30% ACN/70% water in 1 mM ammonium acetate, pH 4.5 (SVA), or 10% ACN/90% water/0.1% CF_3COOD (AVA and CVA) before injection. All NMR spectra were acquired under stopped-flow conditions. Once the apex of the metabolite peak was detected, the HPLC pump was stopped after a precalibrated delay time, at the end of which the metabolite was located in the NMR flow cell. The HPLC conditions were optimized such that the LC peak volume matched that of the NMR flow cell volume (60 μl) to maximize the signal-to-noise ratio of the NMR spectrum. Deuterated mobile phase was used for all LC-NMR runs, and no solvent suppression techniques were applied. The following HPLC conditions were used for LC-NMR studies: Symmetry C_{18}, 5-μm, 3.9 × 150-mm column (SVA) or Phenomenex phenylhexyl, 5-μm, 2 × 150-mm column (AVA and CVA); flow rate, 1.0 ml/min (SVA) or 0.3 ml/min (CVA and AVA); and UV detection at 239 nm (SVA), 244 nm (AVA), or 283 nm (CVA). Separation of glucuronide metabolites from parent statins was achieved using the following gradient conditions: SVA, 0 to 1 min at 30% A, 1 to 18 min 30 to 81% A, 18 to 22 min at 81% A, and a 22.1-min return to 30% A; AVA/CVA, 0 to 3 min at 10% A, 3 to 30 min 10 to 64% A, 30.1 to 35 min at 90% A, and a 35.1-min return to 10% A, where A is 90% CD_3CN + 10% D_2O + 0.1% CF_3COOD and B is 90% D_2O + 10% CD_3CN + 0.1% CF_3COOD. The parent LC-NMR spectra were obtained by injecting ~25 μg of the corresponding statin under the same LC conditions as used for the metabolite. ^1H chemical shifts (in parts per million) are referenced relative to residual CD_2HCN at 1.99 ppm. NMR spectra were obtained using an Inova (11.7 T/500 MHz) 51-mm, narrow-bore spectrometer (Varian, Inc., Palo Alto, CA) equipped with a 60-μl flow probe (Varian, Inc.).

Data Analysis. Apparent K_m and V_{max} values were estimated using a nonlinear regression program (Enlit; Biosoft, Ferguson, MO). The CL_{int} values were estimated by dividing V_{max} by K_m.

Results

Glucuronidation of Statins in Dog Liver Microsomes. Figure 2A illustrates a typical HPLC chromatogram derived from incubates of SVA with dog liver microsomes in the presence of UDPGA. Two major products with an UV spectrum similar to that of SVA were observed. The nonpolar product, which eluted after SVA, was identified as the lactone SV based on the identical HPLC retention time and UV spectrum compared with the authentic standard. The more polar metabolite, upon LC-MS analysis, afforded an $[M - H]^-$ ion at *m/z* 611, 176 mass units higher than the $[M - H]^-$ ion of SVA, suggesting that it was a glucuronide conjugate of SVA. Except for a small amount of SV (<0.6% of initial concentration), the two metabolites were not detectable in control incubations that lacked liver protein or UDPGA. The results suggested that the glucuronide conjugate of SVA was formed enzymatically, whereas SV was formed both by enzymatic (major) and chemical (minor) processes under the conditions used. The enzymatic reaction for both products was mediated by UDPGA-dependent enzyme(s).

As was the case with SVA, two metabolites of AVA or CVA (one more polar and the other less polar than the corresponding parent) were detected when AVA or CVA was incubated with human liver microsomes supplemented with UDPGA (Fig. 2, B and C). Both metabolites afforded an UV spectrum identical to that of the corresponding parent and were not detected in the absence of microsomes or UDPGA. LC-MS analysis indicated that the more polar metabolites of AVA and CVA gave an $[M - H]^-$ ion at *m/z* 733 and an $[M + H]^+$ species at *m/z* 636, respectively, which corresponded to an addition of 176 mass units to their respective parent statin. In each case, collisional activation of these ions led a loss of 176 Da (data not shown), suggesting that the metabolites in question were the statin glucuronides. The nonpolar metabolites of AVA and CVA afforded $[M + H]^+$ ions at *m/z* 541 and 442, which were 18 mass units less than the corresponding ions from AVA and CVA, respectively. Based on the HPLC retention time and UV and MS spectra, the nonpolar metabolites were assigned as AV and CV, the lactone derivatives of AVA and CVA, respectively.

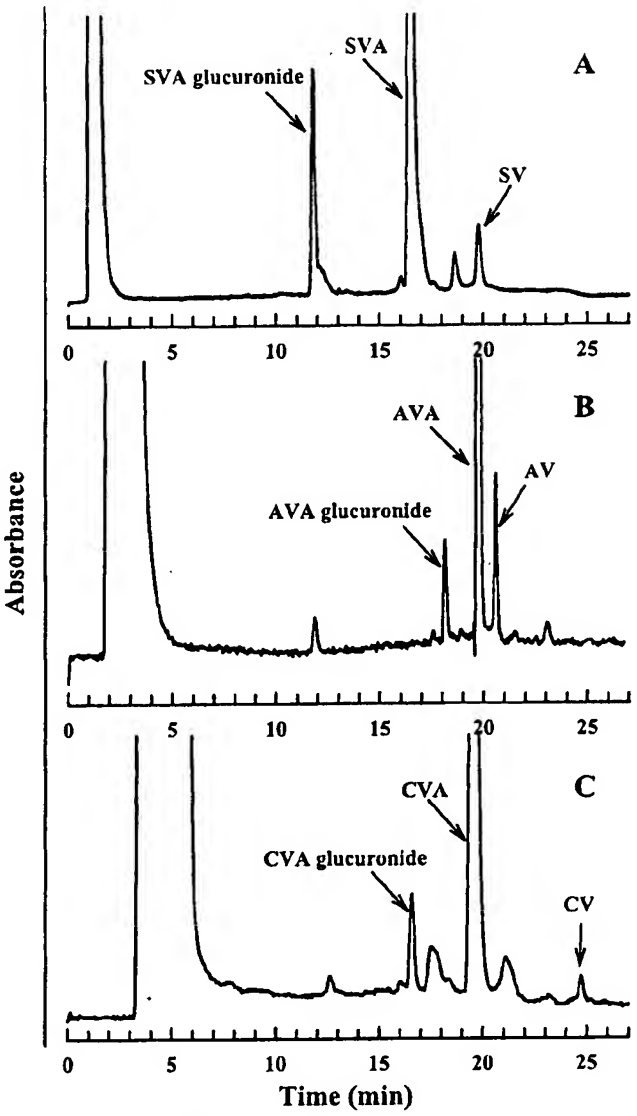

FIG. 2. *Representative HPLC-UV profiles of metabolites of SVA (A), AVA (B), and CVA (C) in dog liver microsomal incubates.*

Incubations were carried out at 37°C for 45 min using dog liver microsomes (1 mg/ml) and statins (100 μM) with UDPGA (5 mM).

For all three statins, formation of the glucuronide conjugate and lactone was linear with time up to 1 h. The formation of each glucuronide was highest at an incubation pH of 7.0 (data not shown). At incubation buffer pH values higher than 7, formation of the lactones became more prevalent compared with that of the glucuronide conjugates. Lactone formation also seemed to increase when the incubation mixture was left overnight at room temperature. For these reasons, all incubations in subsequent experiments were performed at pH 7.0, and samples were analyzed immediately (with an autosampler set at 5°C during analysis) after incubation.

NMR Identification of Statin Glucuronides. LC-NMR experiments were performed to identify the site of conjugation of the statin

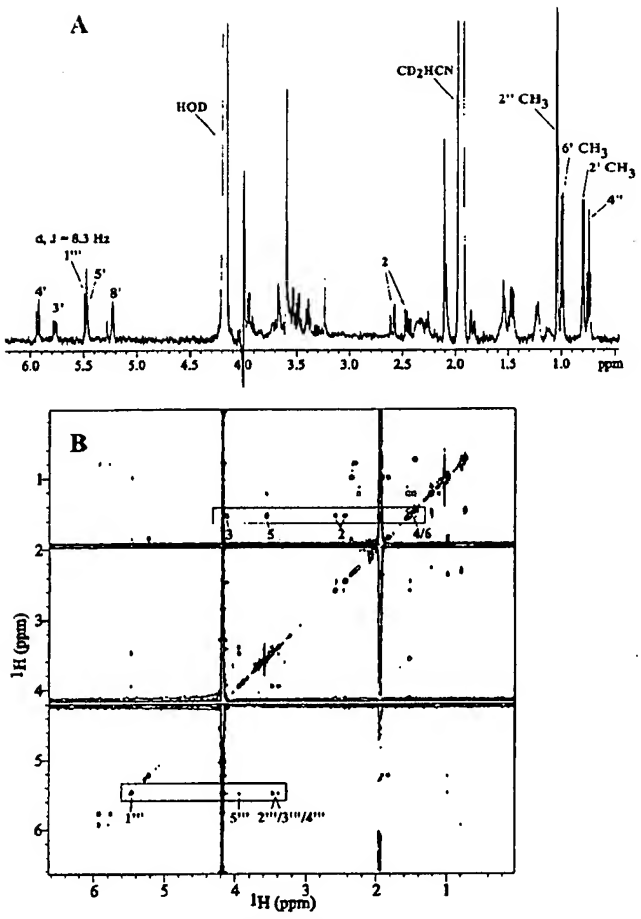

FIG. 3. *One-dimensional ^1H (A) and total correlation NMR spectroscopy (B) spectra of SVA glucuronide.*

Only key protons are identified in both spectra.

glucuronides. Under the HPLC conditions used for LC-NMR in this study, the full-width-at-half-height LC peak volumes for the glucuronides of SVA, CVA, and AVA were 156, 75, and 69 μl, respectively, which contained ~10 to 15 μg of the conjugates in the active volume of the flow cell. The results described below support the conclusion that the glucuronide conjugates of these statins formed upon incubation with dog liver microsomes are β-1-*O*-acyl glucuronides (Fig. 1). The anomeric proton (labeled 1‴) of SVA glucuronide exhibits a ^1H chemical shift of 5.48 ppm (Figs. 3, A and B; Table 1). Through-bond proton connectivities of the heptanoic acid side chain and the glucuronide moiety in SVA glucuronide are shown in Fig. 3B and were identified by total correlation NMR spectroscopy (Summers et al., 1986). Similar to the SVA glucuronide, the anomeric protons of the glucuronide conjugates of CVA and AVA have a ^1H chemical shift of 5.51 and 5.53 ppm, respectively. For all three statins, the 1‴ proton was a doublet, with a scalar coupling constant of 8.1 or 8.3 Hz indicative of a β-anomer. The 1‴ chemical shifts are consistent with an acyl glucuronide rather than an ether glucuronide at the 3 or 5 positions since the anomeric proton in an alkyl ether glucuronide would have a $\delta < 4.5$ ppm (Boberg et al., 1998). Relative to the parent statin, protons at position 2 (α to the carboxyl group) also underwent a concomitant downfield shift in the glucuronide conjugate (Table 1).

NMR also indicated that all three statin glucuronides were in the open acid form. Protons 3 and 5 have distinct chemical shifts characteristic of the lactone or the hydroxy acid form. For example, protons 3 and 5 appeared in SV (the lactone form of SVA) at 4.25 and 4.64 ppm, respectively, and in SVA at 4.19 and 3.58 ppm, respectively. The chemical shifts of methine protons 3 and 5 (Table 1) are indicative of the open acid forms in all three statin glucuronides. The chemical shifts of protons in the remainder of the statin molecules were practically unchanged.

Metabolism of Statins by Human Liver Microsomes. As was the case with dog liver microsomes, formation of the statin acyl glucuronide and the corresponding lactone in human liver microsomes was dependent on the presence of both microsomal protein and UDPGA. Due to the apparent instability of the acyl glucuronides of the three statins studied, the sum of the acyl glucuronide and the corresponding lactone was used to calculate rates of total glucuronidation for each statin. For all three statins, formation rates of the acyl glucuronide conjugates + the lactones in 10 human livers exhibited 3- to 6-fold variation and were higher with CVA than with SVA or AVA in most livers (Fig. 4). On average, the summed rates of glucuronidation + lactonization were 32 ± 13, 44 ± 27, and 88 ± 32 pmol/min/mg of protein for SVA, AVA, and CVA, respectively. The formation rates of glucuronide + lactone of AVA seemed to correlate with that of CVA (r^2, 0.7). However, no correlation was observed for the rates of glucuronidation + lactonization between SVA and CVA or between SVA and AVA (r^2, <0.2).

Metabolism of Statins by Recombinant UGT Isoforms. Studies on the metabolism of statins by commercially available human recombinant UGT isoforms indicated that both UGT1A1 and UGT1A3 catalyzed the formation of acyl glucuronide conjugates of SVA, AVA, and CVA. As was the case in the liver microsomal preparations, formation of the corresponding lactones also was observed with UGT1A1 and UGT1A3 in the presence of UDPGA. Per milligram of protein, the rate of glucuronidation and lactonization of SVA, AVA, or CVA was approximately the same for UGT1A1 (5–7 pmol/min/mg) and 1A3 (2 pmol/min/mg) under the experimental conditions used. All other UGTs tested (UGT1A4, UGT1A6, UGT2B7, and UGT2B15), as well as the control microsomes, failed to produce either the glucuronide or the lactone of any statin to appreciable extent (≤0.5 pmol/min/mg).

Kinetic Studies. The rates of formation of the acyl glucuronide conjugates and the lactones of the three statins in human, dog, and rat liver microsomes were best described by single-enzyme Michaelis-Menten kinetics over the substrate concentration range studied (Figs. 5, A–C). In the case of SVA, species differences were observed in the kinetics of UDPGA-dependent metabolism. In dogs, this reaction was mediated by an enzyme(s) of higher affinity and capacity than that in humans but of comparable affinity and higher capacity than that in rats (Table 2). As a result, the CL_{int} of SVA glucuronidation + lactonization was ~4- to 35-fold higher in dogs than in rats and humans, respectively. In contrast, species differences were not as marked for the UDPGA-dependent metabolism of AVA and CVA; the CL_{int} ranged from 2 to 6 μl/min/mg in all three species (Table 2). The glucuronidation of AVA was mediated by UGTs with high affinity (K_m, ~10–15 μM) in all species examined. In human liver microsomes, the rate of glucuronide + lactone formation was lower for SVA (0.4 μl/min/mg) than for either AVA or CVA (2.9–3.3 μl/min/mg).

Stability of SVA Acyl Glucuronide. The SVA acyl glucuronide isolated from in vitro incubations (Fig. 6A) was found to be relatively stable at 5°C in buffers over pH 4 to 5.6 for at least 8 h after isolation (Figs. 6B and 7). At pH values of 7 or higher, the isolated acyl glucuronide converted rapidly to SV (Figs. 6, C and D, and 7). In fact, formation of SV was observed in the first injection done immediately after the isolated glucuronide fraction was added to pH 8 buffer. Under the conditions (5°C) and in all buffers tested, there was no

TABLE 1

^{1}H Chemical shifts of key protons in the heptanoic/heptenoic acid side chain of all three statins and their corresponding glucuronides

All chemical shifts are referenced to residual CD_2HCN at 1.99 ppm.

Position	SVA	SVA Glucuronide	CVA	CVA Glucuronide	AVA	AVA Glucuronide
2	2.28, 2.38	2.46, 2.60	2.34, 2.39	2.53, 2.54	2.31, 2.38	2.46, 2.55
3	4.19	4.14	3.67	3.64	4.01	4.08
5	3.58	3.56	4.18	4.19	3.68	3.78
1‴		5.48		5.57		5.53

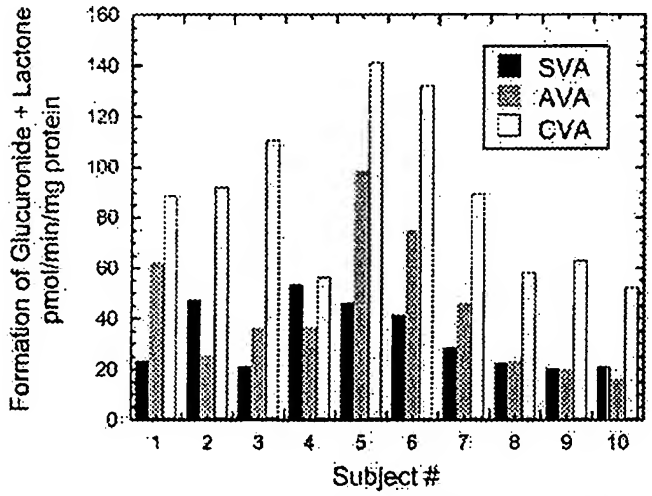

FIG. 4. *Formation of acyl glucuronide conjugates and lactones of SVA, AVA, and CVA in human liver microsomes obtained from 10 different individuals.*

Incubations were carried out in duplicate at 37°C for 40 min using liver microsomes (1.5 mg/ml) and statins (200 μM) with UDPGA (5 mM).

evidence for the formation of SVA or acyl migration products of the glucuronide conjugate of SVA (Fig. 6, B–D). At higher temperatures (37°C), however, the glucuronide levels decreased more rapidly, and at pH values >8, both SV and SVA were formed (data not shown).

In Vivo Formation of SVA Acyl Glucuronide in Dogs. In dogs, within 24 h following i.v. administration of [^{14}C]SVA, about 65 and 5% of total radioactivity was found in bile and urine, respectively. As was reported previously (Vickers et al., 1990a,b), metabolite profiling studies of bile and urine samples indicated that unchanged SVA accounted for less than 5% of the total radioactivity recovered, suggesting that SVA underwent extensive metabolism in dogs. The studies also indicated the presence of the acyl glucuronide conjugate of SVA and its lactone SV in bile (Fig. 8A). The identity of SVA glucuronide in bile was based on the HPLC retention time, the UV and LC-MS spectra, and the formation of free SVA upon treatment with β-glucuronidase. Unlike the chemical degradation process, which led to SV, the enzymatic hydrolysis of SVA glucuronide resulted in unchanged parent SVA (Fig. 8B). Using the present bile collection scheme, the acyl glucuronide (~20% of dose) and SV (~14% of dose) were among major metabolites in bile, accounting for about ~30 and ~20%, respectively, of the total radioactivity recovered (Table 3). As was the case in vitro, levels of the acyl glucuronide conjugate in bile decreased, and concentrations of SV increased when samples of bile were allowed to stand or when an aliquot of bile (which was initially buffered to pH 4.5 to prevent degradation) was treated with sodium hydroxide to pH 7 (Fig. 8C).

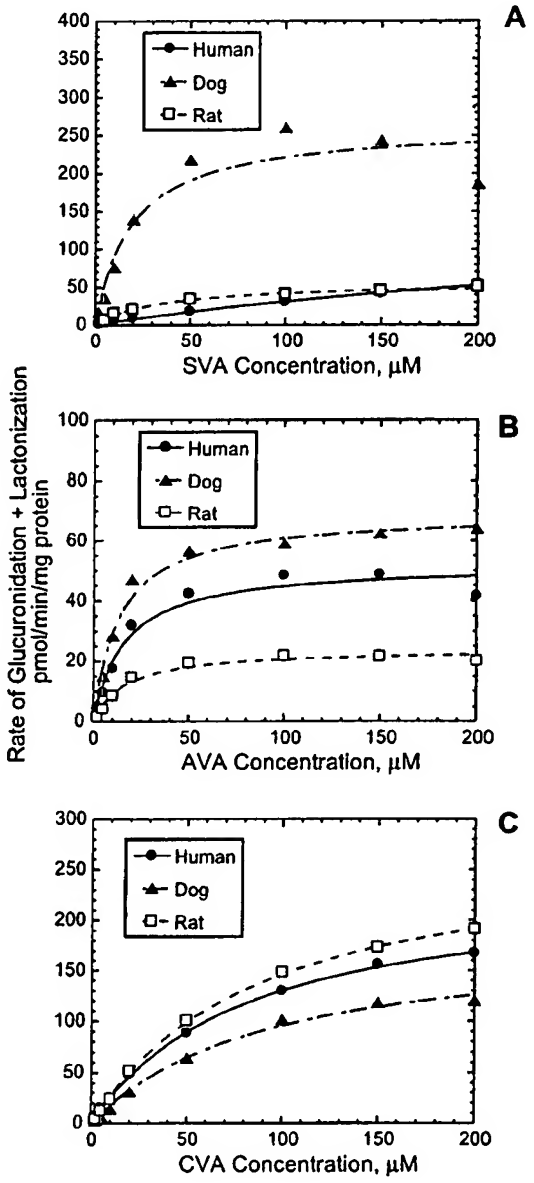

FIG. 5. *Formation of acyl glucuronide conjugates and lactones of SVA (A), AVA (B), and CVA (C) in dog, rat, and human liver microsomes as a function of the substrate concentration.*

Incubations were carried out in duplicate at 37°C for 40 min using liver microsomes (1.5–2 mg/ml) and various concentrations of statins with UDPGA (5 mM).

Discussion

This article provides the first experimental evidence for the glucuronidation of SVA, AVA, and CVA in liver microsomal preparations from animals and humans and of glucuronidation of SVA in vivo in dogs. To date, only glucuronide conjugates of CVA, but not AVA and SVA, have been documented in dog bile (Boberg et al., 1998), whereas significant lactone formation was reported to occur in vivo

TABLE 2

Kinetic parameters for UDPGA-dependent metabolism of statins in liver microsomal preparations

Incubations were performed in duplicate for each substrate concentration using pooled liver microsomes from humans (n = 20), dogs (n = 4), and rats (n = 6). Values are estimates ± S.E.

Statin	Species	K_m	V_{max}	CL_{int}
		μM	*pmol/min/mg*	*μl/min/mg*
SVA	Human	416 ± 80[a]	162 ± 23	0.4
	Dog	19 ± 8	263 ± 28	13.8
	Rat	35 ± 4	57 ± 2	1.6
AVA	Human	16 ± 4	52 ± 3	3.3
	Dog	13 ± 2	69 ± 3	5.3
	Rat	16 ± 3	24 ± 1	1.5
CVA	Human	83 ± 4	238 ± 4	2.9
	Dog	92 ± 15	184 ± 13	2.0
	Rat	90 ± 6	278 ± 8	3.1

[a] Extrapolated values.

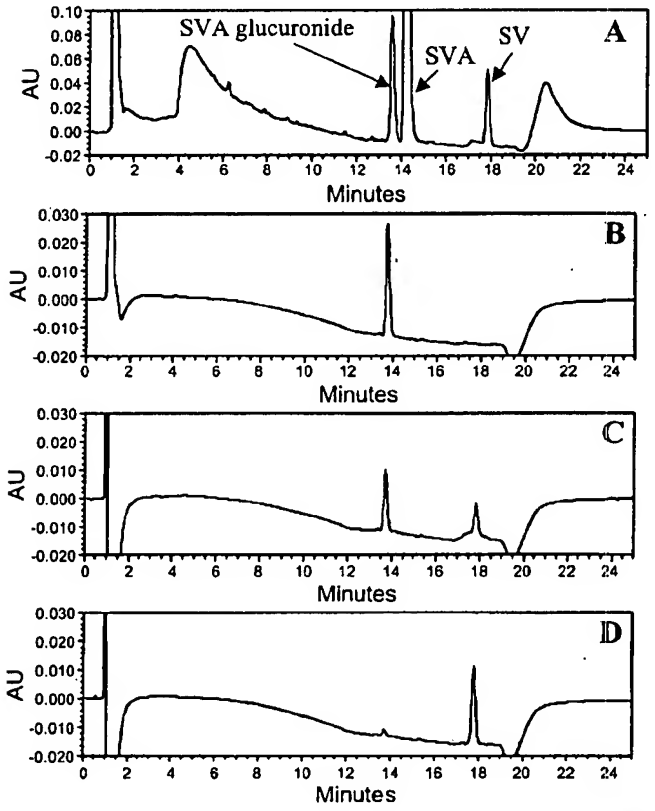

FIG. 6. *Representative HPLC-UV profiles of a dog liver microsomal incubate with SVA (200 μM) and UDPGA (5 mM) (A), an isolated fraction of SVA glucuronide collected in pH 4 buffer (B), an isolated fraction of SVA glucuronide collected in pH 7 buffer (C), and an isolated fraction of SVA glucuronide collected in pH 8 buffer (D).*

AU, absorbance unit.

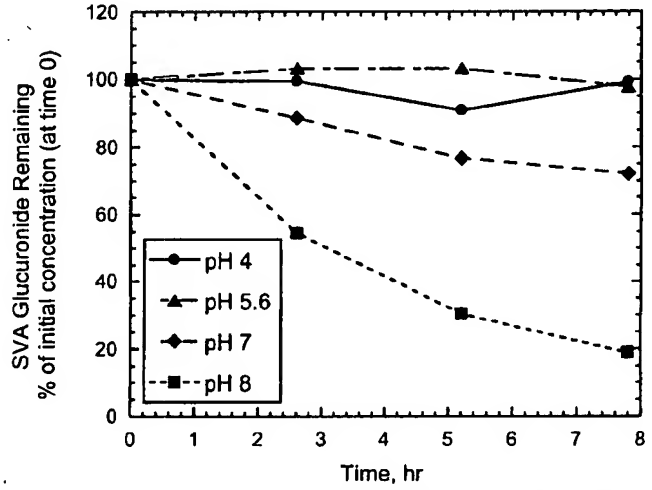

FIG. 7. *Stability of SVA glucuronide conjugate as a function of time in different pH buffers at 5°C.*

following administration of SVA or CVA to dogs (Vickers et al., 1990a; Boberg et al., 1998) and of CVA and AVA to humans (Kantola et al., 1998, 1999). Thus far, the lactonization of statins generally has been attributed to cyclization of acyl-CoA thioester intermediates (Halpin et al., 1993; Boberg et al., 1998) and to chemical equilibration processes (Kantola et al., 1999), and the former pathway has been confirmed recently in vitro (Prueksaritanont et al., 2001). Based on the present in vitro and in vivo results, we hypothesize that the lack of reports on glucuronidation of SVA and AVA (and possibly other statin acids) most likely is a consequence of the relative ease of spontaneous cyclization of the statin acyl glucuronides and that the glucuronidation pathway contributes, at least in part, to the formation of statin lactones.

In the current study, LC-NMR techniques were used to characterize the acyl glucuronide conjugates of three statins. LC-NMR is well suited to such applications since it has been demonstrated to be a powerful nondestructive tool for the structural characterization of unstable metabolites (Lindon et al., 2000). In the in vitro experiments, it was shown that the formation of each statin lactone was dependent on the presence of both microsomal protein and UDPGA, suggesting that lactonization of the statin hydroxy acid was mediated by glucuronidation followed by elimination of the glucuronic acid moiety. This glucuronidation-dependent lactonization was later confirmed when it was found that SVA glucuronide converted rapidly to SV upon standing. Since the glucuronide-to-lactone conversion occurred readily in the physiological pH range (pH 7–8), this mechanism has in vivo relevance and probably contributes to the formation of SV from SVA in vivo. Lactonization by the glucuronidation pathway also is expected to occur for AVA and CVA since both compounds undergo significant glucuronidation and lactonization under the same in vitro incubation conditions. In addition, the acyl glucuronide conjugates of these statins also were unstable and underwent conversion primarily to the corresponding lactone forms upon standing. In the case of CVA, the glucuronide conjugate was found to undergo hydrolysis to regenerate the parent statin at pH 7.4 or above (data not shown). The data suggest that, in vivo, CVA glucuronide would undergo conversion to CVA in addition to lactonization to CV. It is

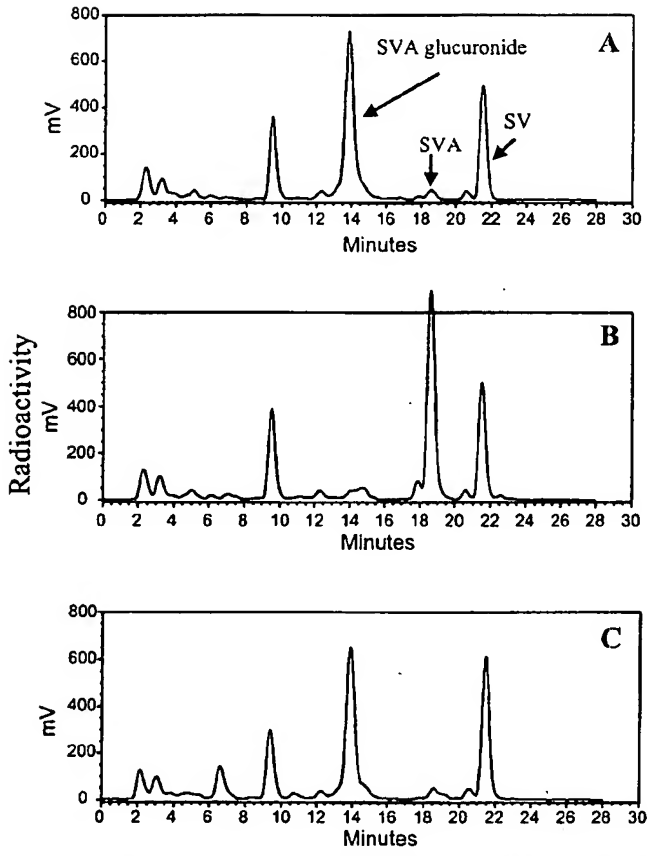

FIG. 8. *Representative HPLC-radioactivity profiles of metabolites of SVA in bile samples collected during the first 2 h postdose, buffered immediately to pH 4.5 without (A) and with (B) treatment with β-glucuronidase, and in bile samples adjusted to pH 7 (C).*

TABLE 3

Recovery of SVA metabolites and total radioactivity in bile collected during 0 to 10 h after administration of [^{14}C]SVA (1.2 mg/kg i.v.) to dogs

Subject	Recovery			
	SVA-Glucuronide	SVA	SV	Total Radioactivity
	% of Dose			
1	14.2	1.0	14.7	52.9
3	19.8	0.9	14.9	56.4
3	26.9	0.7	12.8	77.9
Mean	20.3	0.9	14.1	62.4
S.D.	6.4	0.2	1.2	13.5

noteworthy that the acyl glucuronide conjugates of these statins, at physiological pH, preferentially undergo lactonization compared with acyl migration, a process commonly observed for acyl glucuronides of numerous carboxylic acid-containing compounds (Spahn-Langguth, 1992). It was also found that all statin glucuronides were converted to their respective parent acids when treated with β-glucuronidase.

Although two isomeric ether-linked glucuronides of CVA, conjugated by the two hydroxyl groups of the heptenoic side chain, were identified following the administration of CVA to dogs (Boberg et al., 1998), these conjugates were not detected at significant levels under the present liver microsomal incubation conditions to allow definite characterization. Similarly, glucuronide conjugates other than the acyl glucuronide were not formed to any appreciable extent when SVA or AVA was incubated with liver microsomal preparations or when SVA was administered to dogs. In recombinant UGT systems, the acyl glucuronide also was a major metabolite for each statin. Considering that the total glucuronidation (glucuronide + lactone formation) of SVA did not correlate with that of AVA or CVA in the 10 human livers examined in this study, UGTs other than UGT1A1 and 1A3 might also be involved in the glucuronidation of these statins in human liver microsomes. Based on the kinetic studies with human liver microsomes, which showed apparently monophasic characteristics, these responsible UGTs may posses K_m values in a comparable range to those observed in human liver microsomes.

The relevance of the in vitro findings in dog liver microsomes to the in vivo situation was addressed in studies on the glucuronidation of SVA in the dog. Consistent with the in vitro results, the biliary recovery of SVA glucuronide following administration of [^{14}C]SVA to dogs was substantial, accounting for about 20% of an i.v. dose. Indeed, this figure of 20% may underestimate the fraction of the dose converted to the conjugate if hydrolysis or lactonization occurred to regenerate SVA or to form SV, respectively. The present in vitro finding of more efficient glucuronidation in liver microsomes obtained from dogs than rats also is in agreement with our preliminary in vivo studies, which showed higher biliary levels of SVA glucuronide + SV in dogs than in rats following i.v. administration of [^{14}C]SVA (data not shown). Thus, it may be anticipated that the formation of SVA glucuronide following SVA administration probably would be lower in humans than in dogs. In contrast, based on the present in vitro results, it would not be anticipated that marked species differences in the rates of glucuronidation of AVA and CVA would occur in vivo. In this regard, it is important to point out that in dogs, the combined biliary recoveries of CVA glucuronide (~5%) and the corresponding lactone CV (18%) accounted for >20% of the intraduodenal dose (Boberg et al., 1998) and that relatively high levels of CV and lactone metabolites thereof were observed following administration of CVA to humans (Jemal et al., 1999; Kantola et al., 1999). In the case of AVA, the areas under the plasma concentration versus time curves of the lactone (AV) also were high and similar to those of AVA following AVA administration to healthy subjects (Kantola et al., 1998). Unfortunately, published in vivo data are not available to permit a comparison between the rates of AVA glucuronidation and lactonization in animals or between the amounts of CVA and AVA glucuronides and their lactones formed in humans.

The present study suggests that, in addition to the well known P450-mediated oxidation (Wang et al., 1991; Boberg et al., 1997; Prueksaritanont et al., 1997) and β-oxidation processes (Vickers et al., 1990b; Halpin et al., 1993; Boberg et al., 1997; Black et al., 1999; Prueksaritanont et al., 2001), glucuronidation constitutes a common metabolic pathway for statins. Quantitatively, there seem to be differences in the relative contributions of these pathways to the metabolism of different statins in different species. For most statins, β-oxidation has been shown to be a major pathway in rodents (Arai et al., 1988; Vickers et al., 1990a; Halpin et al., 1993; Black et al., 1998; Boberg et al., 1998; Black et al., 1999), whereas in humans, P450-mediated oxidative metabolism has been regarded as a major pathway of biotransformation (Igel et al., 2001). However, based on the findings of the present study, this assumption may not be valid for all statins and is particularly unlikely to hold true in the case of CVA, which is a low-clearance compound in humans (Mück, 2000). In support of the latter point, our preliminary study using human liver microsomes fortified with NADPH (Prueksaritanont et al., 1999) showed that the CL_{int} of CVA oxidative metabolism (~ 10 μl/min/mg of protein) was in a comparable range to the CL_{int} of glucuronidation, whereas that of AVA oxidation (~50 μl/min/mg of protein) (data not shown) was much higher than the value for UDPGA-dependent me-

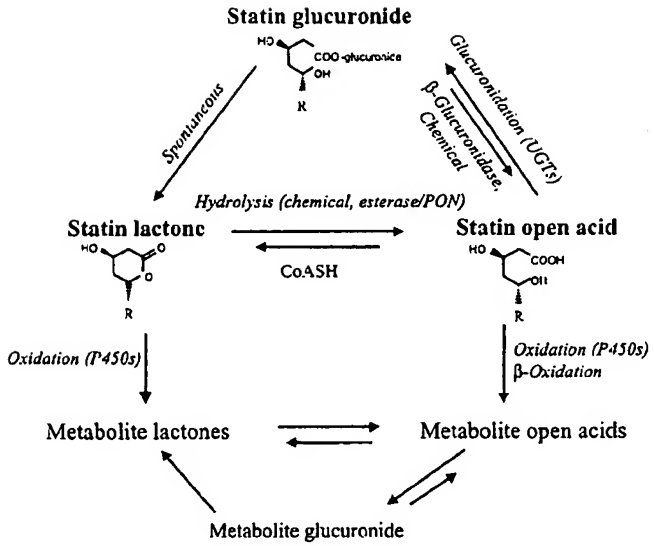

FIG. 9. *Proposed metabolic pathways of statins.*

tabolism (Table 2). In the case of AVA, the value for the CL_{int} under oxidative conditions (in the presence of NADPH) in our study was comparable to that reported in the literature (~80 μl/min/mg; Jacobson et al., 2000).

The present results also suggest that the metabolism of statins is complex, involving acid/lactone interconversion by various pathways, as proposed in Fig. 9. The statin lactones are hydrolyzed to their open acids chemically or enzymatically by esterases or the newly identified paraoxonases (Vickers et al., 1990a; Billecke et al., 2000; Draganov et al., 2000). The statin acids are converted to the corresponding lactones by the acyl glucuronide intermediate, as demonstrated in this study, and by the CoASH-dependent pathway (Prueksaritanont et al., 2001). Both acyl glucuronide and acyl CoA derivatives may revert to the statin acids by hydrolysis. Similar considerations apply to oxidative metabolites of the statins. Indeed, the lactone forms of oxidative metabolites of CVA and glucuronide conjugates of the oxidative metabolites of CVA and AVA have been identified in animals and/or humans following administration of CVA and AVA, respectively (Le Couteur et al., 1996; Boberg et al., 1998; Black et al., 1999). Jacobson et al. (2000) recently hypothesized that most of the hydroxy acid metabolites present in human plasma following AVA administration are converted from metabolites of AV (following lactonization of AVA), which are formed by CYP3A. In the latter study, the mechanism responsible for the lactonization of AVA was thought to be of a chemical nature, and no data on in vivo formation of AV metabolites were provided.

Overall, the present study demonstrates that, in addition to the well known P450-mediated oxidation and β-oxidation processes, glucuronidation also is a common metabolic pathway for the three statins examined. Additionally, this study provides evidence that glucuronidation may play an important role in mediating the lactonization of statins in vivo, and highlights the complexities of statin metabolism associated with hydroxy acid/lactone interconversion. This interconversion process clearly will need to be taken into account in assessing mechanistic aspects of drug-drug interactions involving statins.

Acknowledgments. We thank Drs. A. Jones and C. Raab and Greg Gatto and Nathan Yu for the synthesis and purification of [^{14}C]SVA and also J. Brunner and K. Michel for animal experiments.

References

Arai M, Serizawa N, Terahara A, Tsujita Y, Tanaka M, Masuda H, and Ishikawa S (1988) Pravastatin sodium (CS-514), a novel cholesterol-lowering agent which inhibits HMG-CoA reductase. *Sankyo Kenkyusho Nempo* **40**:1–38.

Billecke S, Draganov D, Counsell R, Stetson P, Watson C, Hsu C, and La Du BN (2000) Human serum paraoxonase (PON1) isozymes Q and R hydrolyze lactones and cyclic carbonate esters. *Drug Metab Dispos* **28**:1335–1342.

Black AE, Hayes RN, Roth BD, Woo P, and Woolf TF (1999) Metabolism and excretion of atorvastatin in rats and dogs. *Drug Metab Dispos* **27**:916–923.

Black AE, Sinz ME, Hayes RN, and Woolf TF (1998) Metabolism and excretion studies in mouse after single and multiple oral doses of the 3-hydroxy-3-methylglutaryl-CoA reductase inhibitor atorvastatin. *Drug Metab Dispos* **26**:755–763.

Boberg M, Angerbauer R, Fey P, Kanhai WK, Karl W, Kern A, Ploschke J, and Radtke M (1997) Metabolism of cerivastatin by human liver microsomes in vitro: characterization of primary metabolic pathways and cytochrome P450 isozymes involved. *Drug Metab Dispos* **25**:321–331.

Boberg M, Angerbauer R, Kanhai WK, Karl W, Kern A, Radtke M, and Steinke W (1998) Biotransformation of cerivastatin in mice, rats, and dogs in vivo. *Drug Metab Dispos* **26**:640–652.

Cheng H, Schwartz MS, Vickers S, Gilbert JD, Amin RD, Depuy B, Liu L, Rogers JD, Pond SD, Duncan CA, et al. (1994) Metabolic disposition of simvastatin in patients with T-tube drainage. *Drug Metab Dispos* **22**:139–142.

Dain JG, Fu E, Gorski J, Nicoletti J, and Scallen TJ (1993) Biotransformation of fluvastatin sodium in humans. *Drug Metab Dispos* **21**:567–572.

Draganov DI, Stetson PL, Watson CE, Billecke SS, and La Du BN (2000) Rabbit serum paraoxonase 3 (PON3) is a high density lipoprotein-associated lactonase and protects low density lipoprotein against oxidation. *J Biol Chem* **275**:33435–33442.

Duggan DE and Vickers S (1990) Physiological disposition of HMG-CoA-reductase inhibitors. *Drug Metab Rev* **22**:333–362.

Everett DW, Chando TJ, Didonato GC, Singhvi SM, Pan HY, and Weinstein SH (1991) Biotransformation of pravastatin sodium in humans. *Drug Metab Dispos* **19**:740–748.

Igel M, Sudhop T, and von Bergmann K (2001) Metabolism and drug interactions of 3-hydroxy-3-methylglutaryl coenzyme A-reductase inhibitors (statins). *Eur J Clin Pharmacol* **57**:357–364.

Jacobson W, Kuhn B, Soldner A, Kirchner G, Sewing K-F, Kollman PA, Benet LZ, and Christians U (2000) Lactonization is the critical first step in the disposition of the 3-hydroxy-3-methylglutaryl-CoA reductase inhibitor atorvastatin. *Drug Metab Dispos* **28**:1369–1378.

Jemal M, Rao S, Salahudeen I, Chen B-C, and Kates R (1999) Quantitation of cerivastatin and its seven acid and lactone biotransformation products in human serum by liquid chromatography-electrospray tandem mass spectrometry. *J Chromatogr B* **736**:19–41.

Halpin RA, Uhm EH, Till AE, Kari PH, Vyas KP, Bunninghake DB, and Duggan DE (1993) Biotransformation of lovastatin V. Species differences in in vivo metabolite profiles of mouse, rat, dog, and human. *Drug Metab Dispos* **21**:1003–1011.

Kantola T, Kivistö KT, and Neuvonen PJ (1998) Effect of itraconazole on cerivastatin pharmacokinetics. *Eur J Clin Pharmacol* **54**:851–855.

Kantola T, Kivistö KT, and Neuvonen PJ (1999) Effect of itraconazole on the pharmacokinetics of atorvastatin. *Clin Pharmacokinet Ther* **64**:58–65.

Le Couteur DG, Martin PT, Braes P, Black A, Hayes R, Woolf T, and Stern R (1996) Metabolism and excretion of [^{14}C]-atorvastatin in patients with T-tube drainage. *Proc Aus Soc Clin Exp Pharmacol Toxicol* **3**:153.

Lindon JC, Nicholson JK, and Wilson ID (2000) Directly coupled HPLC-NMR and HPLC-NMR-MS in pharmaceutical research and development. *J Chromatogr B* **748**:233–258.

Mauro VF (1993) Clinical pharmacokinetics and practical applications of simvastatin. *Clin Pharmacokinet* **24**:195–202.

Mück W (2000) Clinical pharmacokinetics of cerivastatin. *Clin Pharmacokinet* **39**:99–116.

Prueksaritanont T, Gorham LM, Ma B, Liu L, Yu X, Zhao JJ, Slaughter DE, Arison BH, and Vyas KP (1997) In vitro metabolism of simvastatin in humans: identification of metabolizing enzymes and effect of the drug on hepatic P450s. *Drug Metab Dispos* **25**:1191–1199.

Prueksaritanont T, Ma B, Fang X, Subramanian R, Yu J, and Lin JH (2001) β-Oxidation of simvastatin in mouse liver preparations. *Drug Metab Dispos* **29**:1251–1255.

Prueksaritanont T, Ma B, Tang C, Meng Y, Assang C, Lu P, Reider PJ, Lin JH, and Baillie TA (1999) Metabolic interactions between mibefradil and HMG-CoA reductase inhibitors: an in vitro investigation with human liver preparations. *Br J Clin Pharmacol* **47**:291–298.

Spahn-Langguth H (1992) Acyl glucuronides revisited: is the glucuronidation process a toxification as well as a detoxification mechanism? *Drug Metab Rev* **24**:5–48.

Summers MF, Marzilli LG, and Bax A (1986) Complete ^{1}H and ^{13}C assignments of coenzyme B12 through the use of new two-dimensional NMR experiments. *J Am Chem Soc* **108**:4258–4294.

Vickers S, Duncan CA, Chen I-W, Rosegay A, and Duggan DE (1990a) Metabolic disposition studies of simvastatin, a cholesterol-lowering prodrug. *Drug Metab Dispos* **18**:138–145.

Vickers S, Duncan CA, Vyas KP, Kari PH, Arison B, Prakash SR, Ramjit HG, Pitzenberger SM, Stokker G, and Duggan DE (1990b) In vitro and in vivo biotransformation of simvastatin, an inhibitor of HMG-CoA reductase. *Drug Metab Dispos* **18**:476–483.

Wang RW, Kari PH, Lu AYH, Thomas PE, Guengerich FP, and Vyas KP (1991) Biotransformation of lovastatin: IV. Identification of cytochrome P450 3A proteins as the major enzymes responsible for the oxidative metabolism of lovastatin in rat and human liver microsomes. *Arch Biochem Biophys* **290**:355–361.

Table 2

Oral Consumption of *H. rosea* Dried Leaf Powder Lowers Triglyceride Levels in Human Subjects

Subject #	Year 2000	2001	2002	2003	2004	
1	103	----	97	---	78	← **Triglyceride Levels (mg/dL)**
2	124	99	67	48	37	
3	109	98	86	83	69	
4	204	198	187	171	154	

The ages of the subjects used in this study range from 35-60 years. The subjects orally consumed 300 mg dried leaf powder as a supplement three times daily.

The above table represents additional data in 4 human subjects with 5 data points in 3 of the subjects and 3 data points in 1 subject.

0888-8809/05/$15.00/0
Printed in U.S.A.

Molecular Endocrinology 19(6):1593–1605

doi: 10.1210/me.2005-0015

A Peroxisome Proliferator-Activated Receptor α/γ Dual Agonist with a Unique *in Vitro* Profile and Potent Glucose and Lipid Effects in Rodent Models of Type 2 Diabetes and Dyslipidemia

Anne Reifel-Miller, Keith Otto, Eric Hawkins, Robert Barr, William R. Bensch, Chris Bull, Sharon Dana, Kay Klausing, Jose-Alfredo Martin, Ronit Rafaeloff-Phail, Chahrzad Rafizadeh-Montrose, Gary Rhodes, Roger Robey, Isabel Rojo, Deepa Rungta, David Snyder, Kelly Wilbur, Tony Zhang, Richard Zink, Alan Warshawsky, and Joseph T. Brozinick

Endocrinology Division (A.R.-M., K.O., E.H., R.R.-P., K.W., J.T.B.), Lead Optimization Biology (R.B., C.R.-M., R.Z.), Cardiovascular Research (W.R.B., C.B., D.S.), and Medicinal and Developmental Chemistry (J.-A.M., G.R., R.R., I.R., T.Z., A.W.), Lilly Research Laboratories, Indianapolis, Indiana 46285; and Ligand Pharmaceuticals (S.D., K.K., D.R.), San Diego, California 92121

LSN862 is a novel peroxisome proliferator-activated receptor (PPAR)α/γ dual agonist with a unique *in vitro* profile that shows improvements on glucose and lipid levels in rodent models of type 2 diabetes and dyslipidemia. Data from *in vitro* binding, cotransfection, and cofactor recruitment assays characterize LSN862 as a high-affinity PPARγ partial agonist with relatively less but significant PPARα agonist activity. Using these same assays, rosiglitazone was characterized as a high-affinity PPARγ full agonist with no PPARα activity. When administered to Zucker diabetic fatty rats, LSN862 displayed significant glucose and triglyceride lowering and a significantly greater increase in adiponectin levels compared with rosiglitazone. Expression of genes involved in metabolic pathways in the liver and in two fat depots from compound-treated Zucker diabetic fatty rats was evaluated. Only LSN862 significantly elevated mRNA levels of pyruvate dehydrogenase kinase isozyme 4 and bifunctional enzyme in the liver and lipoprotein lipase in both fat depots. In contrast, both LSN862 and rosiglitazone decreased phosphoenol pyruvate carboxykinase in the liver and increased malic enzyme mRNA levels in the fat. In addition, LSN862 was examined in a second rodent model of type 2 diabetes, *db/db* mice. In this study, LSN862 demonstrated statistically better antidiabetic efficacy compared with rosiglitazone with an equivalent side effect profile. LSN862, rosiglitazone, and fenofibrate were each evaluated in the humanized apoA1 transgenic mouse. At the highest dose administered, LSN862 and fenofibrate reduced very low-density lipoprotein cholesterol, whereas, rosiglitazone increased very low-density lipoprotein cholesterol. LSN862, fenofibrate, and rosiglitazone produced maximal increases in high-density lipoprotein cholesterol of 65, 54, and 30%, respectively. These findings show that PPARγ full agonist activity is not necessary to achieve potent and efficacious insulin-sensitizing benefits and demonstrate the therapeutic advantages of a PPARα/γ dual agonist. (*Molecular Endocrinology* 19: 1593–1605, 2005)

BY THE YEAR 2025, more than 300 million individuals worldwide will suffer from type 2 diabetes. This epidemic will be followed closely by a wave of cardiovascular disease, as diabetes is not just a disease characterized by elevated blood glucose levels but is also a serious vascular disease with poor prognosis. One important cardiovascular risk factor in type 2 diabetes is dyslipidemia, which is characterized by decreased high-density lipoprotein cholesterol (HDL-C), elevated very low-density lipoprotein cholesterol (VLDL-C), and an abundance of small, dense low-density lipoprotein cholesterol (LDL-C) (1). Unfortunately, glycemic control with diet, oral hypoglycemic agents, and insulin is often only partially effective in normalizing lipid levels in individuals with type 2 diabetes (2).

Two classes of compounds, the thiazolidinediones (TZDs) and fibrates, were empirically discovered by their abilities to improve insulin sensitivity and lipidemia, respectively, in rodent models. The TZDs reduce both hyperglycemia and the compensatory hyperinsulinemia but exert only marginal effects on plasma lipid parameters in patients with type 2 diabetes (3). In contrast, the fibrates are effective at lowering plasma triglycerides and free fatty acids and increasing favorable HDL-C via increased clearance and decreased synthesis of VLDL-C (4). In addition, fibrates have been shown to improve glycemic control in patients with type 2 diabetes (5, 6).

First Published Online April 14, 2005

***Molecular Endocrinology* is published monthly by The Endocrine Society (http://www.endo-society.org), the foremost professional society serving the endocrine community.**

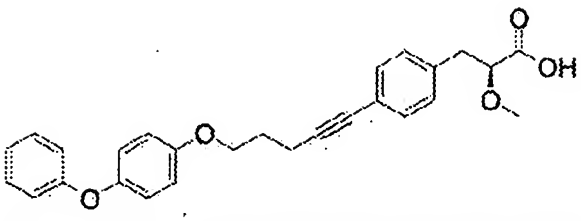

Fig. 1. LSN862: A 2-Methoxydihydrocinnamic Acid-Based PPARα/γ Dual Agonist

The recent discovery that peroxisome proliferator-activated receptor (PPAR)γ and PPARα are the primary targets for TZDs and fibrates, respectively (7, 8), has provided chemists and biologists with the necessary information and tools to apply target-directed approaches to optimize drug candidates. Using this approach, compounds can be identified and studied that have both PPARα and PPARγ agonist properties (PPARα/γ dual agonists), which combine the benefits of a TZD plus a fibrate in a single molecule. Further, compounds with partial agonist *vs.* full agonist activity can be designed and studied for their potential therapeutic benefits.

In the present study, a non-TZD PPAR ligand (Fig. 1) was fully characterized for its PPARγ, PPARα, and PPARδ binding and agonist activity *in vitro* and potential antidiabetic and lipid-altering properties in rodent models of type 2 diabetes and dyslipidemia, respectively.

RESULTS

In Vitro Characterization of LSN862

Competitive binding assays were used to determine the affinity of LSN862 for PPARγ, PPARα, and PPARδ, and standard cotransfection (CTF) assays were used to determine the potency and efficacy of agonist activity. As shown in Table 1, LSN862 is a high-affinity [dissociation constant (K_i) = 7.0 nM], potent (EC_{50} = 239 nM) PPARγ agonist (77% efficacy) with relatively less, but significant affinity (K_i = 770 nM) and agonist activity (EC_{50} = 2622 nM; 35% efficacy) on PPARα. This degree of PPARα affinity is greater than that of two well-studied PPARα agonists, fenofibrate (K_i > 10,000 nM) and WY14,643 (K_i = 9,570 nM) when examined in the same assays (data not shown in table). LSN862 displayed low affinity for PPARδ (K_i = 4123 nM) with no agonist activity detected. The standard PPARγ CTF assay uses a trimeric PPAR response element (PPRE) from the acyl-coenzyme A (CoA) oxidase (AOX) gene. To further explore the PPARγ agonist potential of LSN862, additional CTF assays were performed using trimeric PPREs from promoters of the lipoprotein lipase (LPL) and enoyl-CoA hydratase/3-hydroxyacyl-CoA dehydrogenase (bifunctional enzyme, BIFEZ) genes. In addition, LSN862 was examined in a PPARγ, yeast galactosidase (GAL4) chimeric CTF assay. In all PAPRγ CTF assays, rosiglitazone served as a standard with efficacy set at 100%. Interestingly, LSN862 showed less agonist activity on all PPREs compared with rosiglitazone (Table 2) with PPARγ partial agonist activity demonstrated regardless of the PPRE used in the CTF assay (Fig. 2). These data demonstrate that although LSN862 is a high-affinity ligand for PPARγ, it functions as a PPARγ partial agonist relative to a full agonist like rosiglitazone. LSN862 was also examined for activity on other nuclear hormone receptors. Results from these studies showed that LSN862 is selective for the PPARs with no activity on the retinoic acid receptor, retinoid X receptor, liver X receptor, farnesoid X receptor, and pregnane X receptor (data not shown).

To further characterize LSN862, PPARγ cofactor recruitment assays were performed using the following cofactors: cAMP response element-binding protein (CREB)-binding protein (CBP), peroxisome proliferator-activated receptor γ coactivator-1 (PGC-1), activating signal cointegrator-2 (ASC-2), thyroid hor-

Table 1. PPAR Binding and Cotransfection Profiles for LSN862

Receptor	Binding Assay K_i (nM)		CTF Assay			
			Efficacy (%)[a]		EC_{50} (nM)	
	Mean	SE	Mean	SE	Mean	SE
hPPARγ	7	2	77	4	239	40
hPPARα	770	156	35	2	2622	94
hPPARδ	4123	163	0	0	NC	NC

NC, Not calculated; hPPAR, human PPAR.
[a] Reference compounds: rosiglitazone for PPARγ; LG0070660 for PPARα and PPARδ.

Table 2. Efficacy Values from PPARγ CTF Assays Using Various PPREs

	PPREs					
	LPL		BIFEZ		GAL4	
	Mean	SE	Mean	SE	Mean	SE
LSN862 (% efficacy)	78	5	64	4	62	5
Rosiglitazone (% efficacy)	100		100		100	

Abbreviations: AOX, acyl coA oxidase; ASC-2, activating signal cointegrator-2; BIFEZ, bifunctional enzyme; CBP, cAMP response element-binding protein (CREB)-binding protein; CoA, coenzyme A; CTF assay, cotransfection assay; hApoA1, humanized apolipoprotein A1; HDL-C, high-density lipoprotein cholesterol; LPL, lipoprotein lipase; PDK4, pyruvate dehydrogenase kinase isozyme 4; PEPCK, phosphoenol pyruvate carboxykinase; PGC-1, PPARγ coactivator-1; PPAR, peroxisome proliferator-activated receptor; PPRE, PPAR response element; TRAP, thyroid hormone receptor-activated protein; TZD, thiazolidinedione; UCP, uncoupling protein; VLDL-C, very low-density lipoprotein cholesterol; ZDF rat, Zucker diabetic fatty rat.

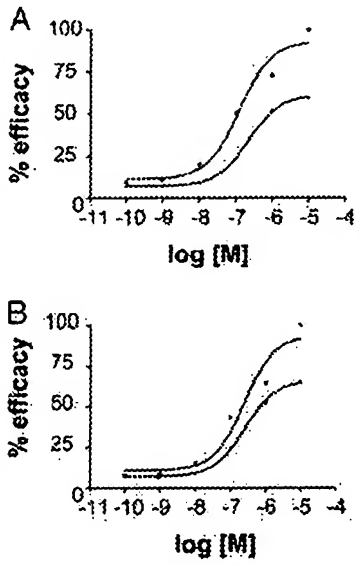

Fig. 2. Representative Dose-Response Curves from CTF Assays

Rosiglitazone (*squares*) and LSN862 (*triangles*) were each examined in full log dilution from 0.1 nM to 10 μM. Dose-response curves from a BIFEZ (A) and AOX (B) CTF assay are shown.

mone receptor-activated protein complex (TRAP220), and the peptide C33. Rosiglitazone served as the standard in these assays, and recruitment of cofactors to PPARγ by rosiglitazone was set at 100%. As seen in Table 3, LSN862 showed a distinct pattern of cofactor recruitment compared with rosiglitazone with equivalent recruitment of ASC-2 and C33, and less recruitment of CBP, PGC-1, and TRAP220. Consistent with the distinct agonist activity of LSN862 seen in the CTF assays, LSN862 does not function as a full PPARγ agonist like rosiglitazone in cofactor recruitment.

Antidiabetic Activity of LSN862

A study in Zucker diabetic fatty (ZDF) rats was done to investigate the antidiabetic properties of LSN862. Before the study described here, the maximally efficacious doses for glucose lowering of LSN862 and rosiglitazone in ZDF rats were determined to be 3.0 and 10.0 mg/kg per day, respectively. In the present study, maximally efficacious doses of LSN862 (3.0 mg/kg per day) and rosiglitazone (10 mg/kg per day) along with an equivalent dose of rosiglitazone (3.0 mg/kg per day) were each administered to ZDF rats for 7 d. Plasma glucose, triglycerides, and adiponectin levels were determined before the study began (d −1) and at the end of the study (d 7). Rosiglitazone decreased glucose and triglyceride levels at both doses examined, with LSN862 at 3.0 mg/kg per day achieving the same degree of efficacy as rosiglitazone at 10.0 mg/kg per day on both glucose and triglyceride lowering (Fig. 3, A and B). Adiponectin levels increased as expected and appear to reflect the glucose-lowering abilities of LSN862 and rosiglitazone; although, interestingly, the adiponectin elevation for LSN862 at 3.0 mg/kg per day was significantly greater than the equally efficacious dose of rosiglitazone (10 mg/kg per day, Fig. 3C).

Because mouse models of type 2 diabetes are often used to explore the side effect profile of PPAR ligands, LSN862 was also evaluated in *db/db* mice. LSN862 and rosiglitazone were each administered orally to *db/db* mice at 30 mg/kg per day for 7 d. LSN862 produced a statistically greater decrease in glucose levels ($P = 0.003$), a trend for better triglyceride lowering ($P = 0.065$), and equivalent body weight gain ($P = 0.875$) compared with rosiglitazone (Fig. 4, A–C). These data suggest that at equivalent glucose lowering, less weight gain would be seen after LSN862 administration.

In Vivo Molecular Activity of LSN862

To gain an understanding of the antidiabetic mechanism of LSN862, expression of candidate genes involved in metabolic pathways in the liver and two fat depots (visceral and epididymal) were investigated. The tissue samples used for these studies were procured from the ZDF rat study described above. Administration of equally efficacious doses of LSN862 (3.0 mg/kg per day) and rosiglitazone (10.0 mg/kg per day) led to a similar decrease in expression of phosphoenol pyruvate carboxykinase (PEPCK) in the liver (Fig. 5A), the enzyme responsible for the rate-limiting step in the gluconeogenesis pathway. In contrast, regulation of pyruvate dehydrogenase kinase isozyme 4 (PDK4) and BIFEZ in the liver by LSN862 and rosiglitazone was very different compared with that seen for PEPCK. A statistically significant decrease in PDK4 expression was produced with rosiglitazone, whereas a large increase in expression of PDK4 was seen with LSN862 (Fig. 5B). A similar pattern was seen for regulated expression of BIFEZ in the liver (Fig. 5C).

Table 3. Efficacy Values for Recruitment of Cofactors to PPARγ

	Cofactors									
	CBP		PGC-1		TRAP		ASC-2		C33	
	Mean	SE	Mean	SE	Mean	SE	Mean	SE	Mean	SE
LSN862 (% efficacy)	56	5	66	14	75	5	106	3	97	3
Rosiglitazone (% efficacy)	100		100		100		100		100	

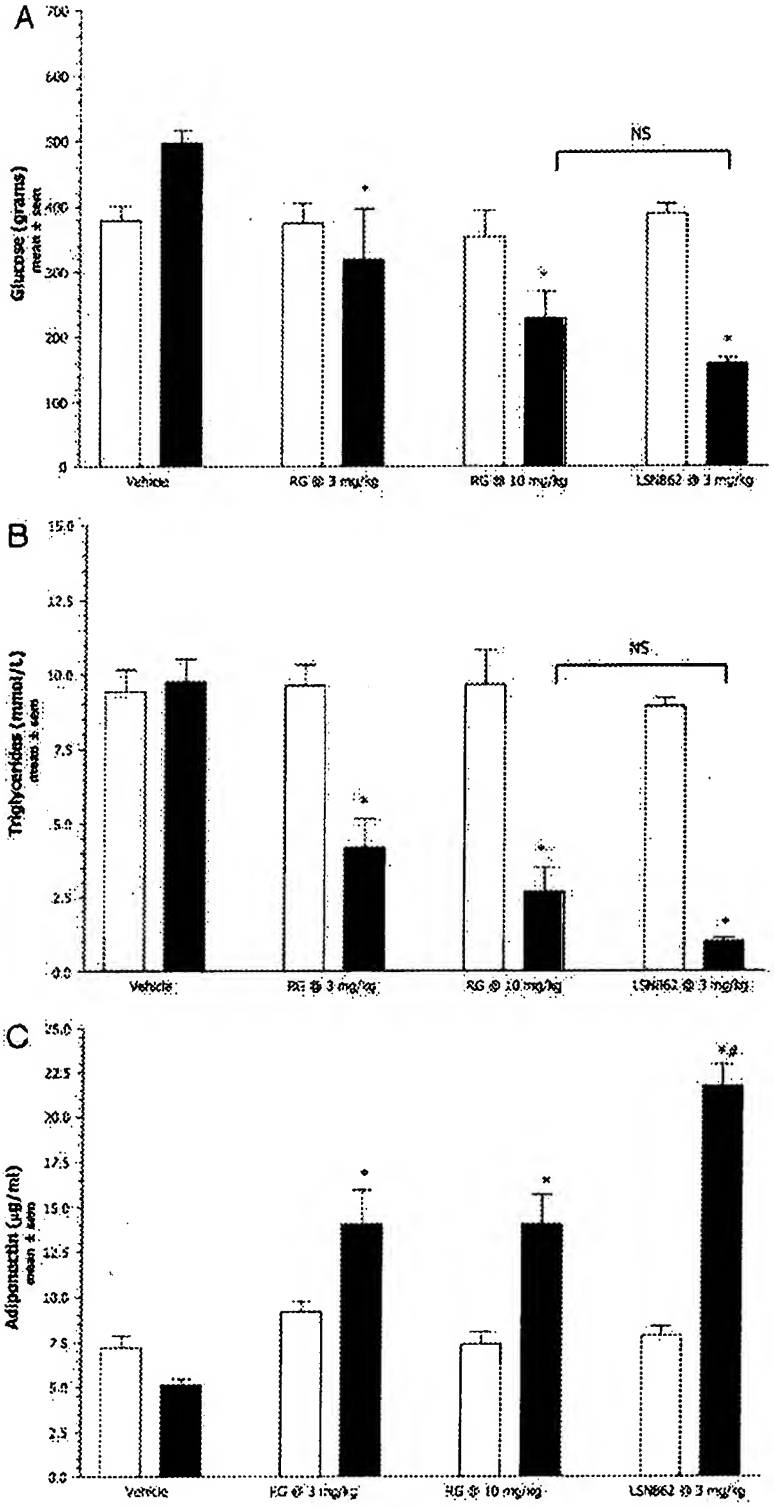

Fig. 3. Plasma Glucose, Triglyceride, and Adiponectin Levels in ZDF Rats after Administration of LSN862 or Rosiglitazone (RG)

LSN862 (3.0 mg/kg) or rosiglitazone (RG, 3.0 and 10.0 mg/kg) were administered to ZDF rats for 7 d. Blood samples were collected the day before the study started, d −1 (□) and on d 7 (■). Plasma samples were analyzed for glucose (A), triglyceride (B), or adiponectin (C) 1 h after the last dose. *, $P < 0.05$ from vehicle group; #, $P < 0.05$ from RG (10 mg/kg per day). NS, Not significantly different (NS ≥ 0.05).

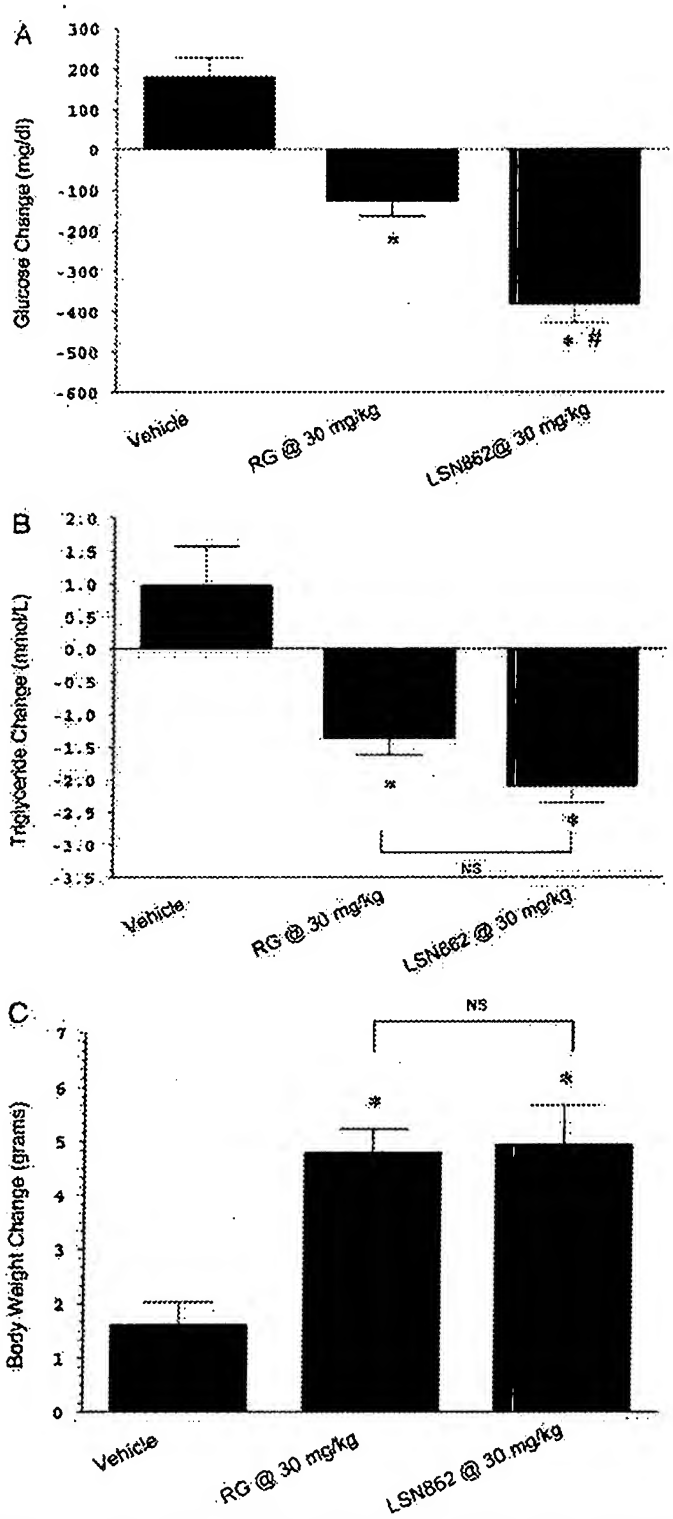

Fig. 4. Changes in Plasma Glucose, Triglycerides, and Body Weight in *db/db* Mice after Administration of LSN862 or Rosiglitazone (RG)

LSN862 (30 mg/kg) or rosiglitazone (30 mg/kg) were each administered to *db/db* mice once daily for 7 d. Blood samples were collected the day before the study started, d −1, and 1 h after the last dose on d 7. Changes in plasma glucose (A) and triglyceride (B) levels from d −1 to d 7 were determined. Body weight gain (C) was determined by subtracting the weight of each mouse on d 1 from its weight on d 7. *, $P < 0.05$ from vehicle group; #, $P < 0.05$ from RG. NS, Not significantly different (NS ≥ 0.05).

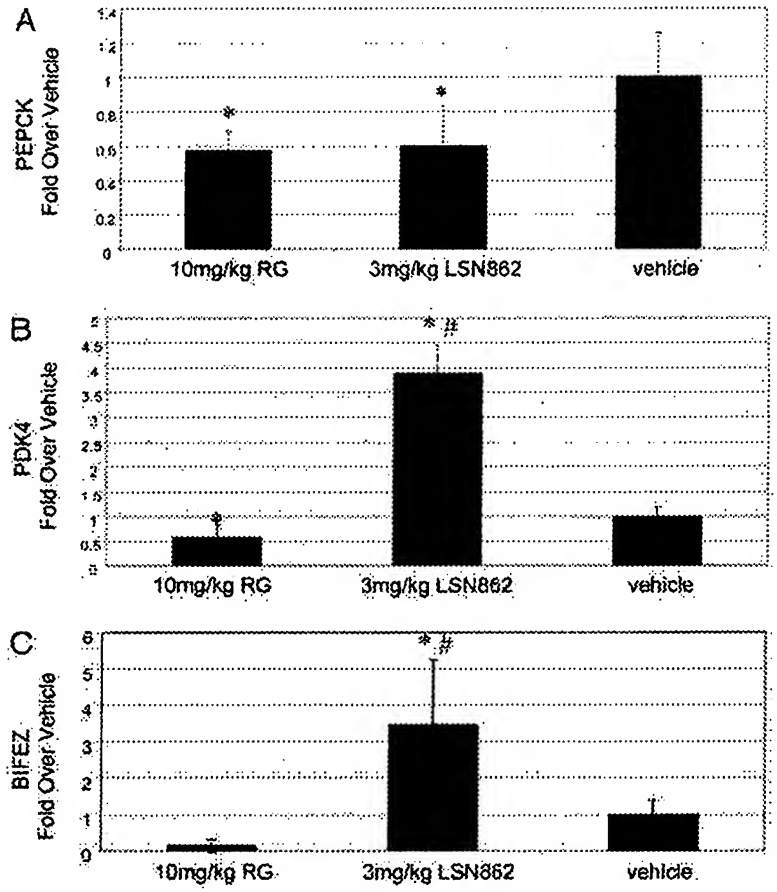

Fig. 5. Regulation of Liver PEPCK (A), PDK4 (B), and BIFEZ (C) Gene Expression

Liver samples from ZDF rats administered an equally efficacious dose of LSN862 (3.0 mg/kg per day) or rosiglitazone (RG, 10.0 mg/kg per day) were used for analysis of PDK4, PEPCK, and BIFEZ mRNA levels. mRNA was extracted from the liver samples, cDNA was synthesized, and RT-PCR was performed as described in *Materials and Methods*. *, $P < 0.05$ from vehicle group; #, $P < 0.05$ from RG (10 mg/kg per day).

Administration of LSN862 led to a significant increase in BIFEZ expression. A trend toward lowered BIFEZ expression was seen with rosiglitazone administration, although this finding was not statistically significant. The differences in LSN862- *vs.* rosiglitazone-regulated expression of PDK4 and BIFEZ are most likely due to the PPARα activity of LSN862.

Changes in expression of adiponectin, malic enzyme, uncoupling protein 1 (UCP-1), glycerol kinase, and LPL were investigated in visceral and epididymal fat. As seen in Fig. 6A, administration of LSN862 (3.0 mg/kg per day) or rosiglitazone (10 mg/kg per day) for 7 d led to a large increase in both malic enzyme and UCP-1 expression and a smaller, although still statistically significant, increase in adiponectin and glycerol kinase expression in visceral fat. Only LSN862 administration led to a statistically significant increase in LPL expression in visceral fat. Gene expression results from the epididymal fat depot were similar to those seen in visceral fat after LSN862 administration, whereas rosiglitazone produced a statistically significant increase in the expression of only malic enzyme (Fig. 6B). Although UCP-1 expression was increased in epididymal fat after rosiglitazone and LSN862 administration, a fold-induction could not be calculated due to the extremely low levels of expression in the vehicle control samples. Interestingly, transcription of only glycerol kinase was statistically different between LSN862 *vs.* rosiglitazone administration.

Effect of LSN862 on Lipid Levels

To determine the effect, if any, of LSN862 on modulating lipid levels, a study in humanized apolipoprotein A1 (hApoA1) transgenic mice was performed. LSN862 (0.3, 1.0, 3.0, 10, 30, and 100 mg/kg per day), rosiglitazone (0.3, 1.0, 3.0, 10, 30, and 100 mg/kg per day), and fenofibrate (100 mg/kg per day) were each administered to hApoA1 mice for 7 d. VLDL-C and HDL-C were determined using blood samples collected 3 h after the last dose. As shown in Table 4, administration of LSN862 led to a decrease in VLDL-C and a dose-dependent increase in HDL-C reaching a 65% increase at the 100 mg/kg per day dose. In contrast,

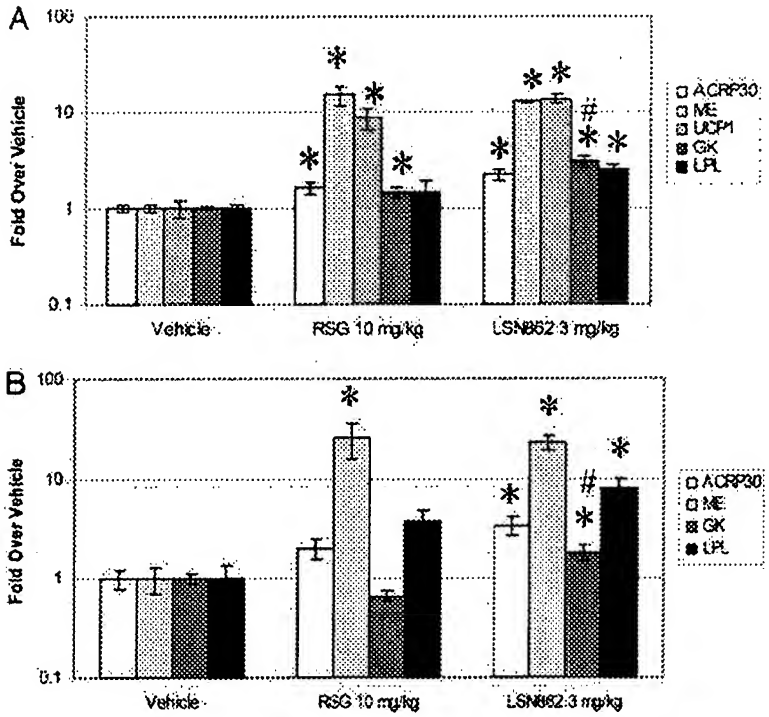

Fig. 6. Regulation of Adiponectin, Malic Enzyme, UCP-1, Glycerol Kinase, and LPL Gene Expression in Visceral (A) and Epididymal (B) Fat

Fat samples from ZDF rats administered an equally efficacious dose of LSN862 (3.0 mg/kg per day) or rosiglitazone (RG, 10.0 mg/kg per day) were used for analysis of adiponectin (ACRP30, □), malic enzyme (ME, *light gray square*, UCP-1 (UCP1, *medium gray square*), glycerol kinase (GK, *dark gray square*) and LPL (■) mRNA levels. mRNA was extracted from the fat samples, cDNA was synthesized, and RT-PCR was performed as described in *Materials and Methods*. *, $P < 0.05$ from vehicle group; #, $P < 0.05$ from RG (10 mg/kg per day).

fenofibrate administration produced a 5% decrease in VLDL-C and a 54% increase in HDL-C. Rosiglitazone administration led to variable VLDL-C levels and modest increases in HDL-C with the greatest increase produced at the 3.0 mg/kg per day dose. These data demonstrate that LSN862 administration led to improvements in the lipid profile of a rodent model of dyslipidemia, which likely reflect the PPARα activity of this compound.

DISCUSSION

In the current report, we describe a new non-TZD PPAR ligand, LSN862, and show that it has a unique *in vitro* profile and potent antidiabetic and lipid-altering effects when tested *in vivo*. LSN862 is not a traditional PPARγ agonist with a TZD structure.

Results from our *in vitro* studies show that LSN862 has a unique profile compared with the well-characterized PPARγ agonist rosiglitazone. LSN862 binds to PPARγ with high affinity and to PPARα with lower affinity. Using standard CTF assays, LSN862 demonstrated PPARγ agonist activity with weaker but significant PPARα agonist activity. Very low affinity was shown for PPARδ, and no PPARδ agonist activity was detected. By examining LSN862 in PPARγ CTF assays using a variety of PPREs and in cofactor recruitment assays with PPARγ and five different cofactors, a broader, more detailed *in vitro* profile was revealed. Results from these studies show that LSN862 has a distinct pattern of activity compared with rosiglitazone functioning as a PPARγ partial agonist in CTF assays with differential agonist activity (partial and full agonist activity) displayed in cofactor recruitment assays. Although it would be easy to speculate that the CTF and cofactor data are related, *i.e.* lower agonist activity on the BIFEZ PPRE may be due to the inability to recruit CBP, the data have not been compiled to make this type of correlation. The PPARγ partial agonist activity of LSN862 may become a distinct advantage for this compound because a number of studies have shown that PPARγ partial agonists including selective PPAR modulators have improved side effect profiles compared with full agonists (9–14). These reports are consistent with our findings in *db/db* mice, which demonstrate that LSN862 has better antidiabetic efficacy with the same weight gain and suggest that at equivalent glucose-lowering doses, LSN862 administration would lead to less weight gain compared with rosigli-

Table 4. Summary of VLDL-C and HDL-C Values from hApoA1 Mice

Group		VLDL	% Change	HDL	% Change
Compound	Dose (mg/kg per day)	(mg/dl)	from Control	(mg/dl)	from Control
Control	0	30		217	
Feno	100	29	−5	333	54
LSN862	0.3	29	−5	240	11
LSN862	1	26	−13	246	13
LSN862	3	29	−5	281	30
LSN862	10	27	−11	313	44
LSN862	30	28	−7	318	47
LSN862	100	25	−18	357	65
Rosiglitazone	0.3	32	5	241	11
Rosiglitazone	1	30	0	246	14
Rosiglitazone	3	32	4	282	30
Rosiglitazone	10	29	−3	240	11
Rosiglitazone	30	33	9	245	13
Rosiglitazone	100	42	37	270	25

Feno, Fenofibrate.

tazone. Although others have reported on the development of a PPARγ partial agonist for the treatment of type 2 diabetes (12, 14), this is the first report to describe a compound with PPARγ partial agonist plus PPARα activities.

Although the PPARα affinity and agonist activity of LSN862 appears weak compared with its PPARγ activity, the affinity of LSN862 for PPARα is greater than that of the well-characterized PPARα agonists, fenofibrate and WY14,643. In addition, beneficial *in vivo* effects were seen, which are most likely due to the PPARα activity of LSN862. These PPARα-mediated contributions will be discussed below.

LSN862 functions as a potent and efficacious antidiabetic agent. In ZDF rats and *db/db* mice, rodent models of type 2 diabetes, LSN862 normalized glucose and triglyceride levels. Some of the antidiabetic activity of LSN862 may be due to its PPARα activity. Recent findings have shown that activation of PPARα leads to improved whole-body and muscle insulin resistance and hyperinsulinemia in various animal models of type 2 diabetes and insulin resistance (15–19). In addition, other investigators have shown that treatment with a PPARα/γ dual agonist results in reduced circulating insulin and improved insulin sensitivity to a greater extent than treatment with rosiglitazone (20), although, the underlying mechanisms responsible for this enhanced antidiabetic activity remain unclear.

Adiponectin levels were elevated after both LSN862 and rosiglitazone administration, although the levels were statistically higher with LSN862 administration at an equally efficacious dose. The greater adiponectin response is not due to the additional PPARα activity of LSN862, as we have examined the adiponectin promoter in CTF assays and have shown that it is not activated by PPARα agonists (Gillespie G., unpublished observations). It is possible that the additional adiponectin effect is due to the PPARγ partial agonist activity of LSN862; however, very little is known at this time regarding the mechanism for PPARγ-induced adiponectin expression. Regardless, the substantial increase in adiponectin could give LSN862 unique advantages according to recent reports describing adiponectin's antiinflammatory (21) and antidiabetic effects without increasing body weight (22–24).

Expression of candidate genes in liver and fat were investigated to gain a better understanding of the molecular mechanisms underlying the therapeutic activity of LSN862. In the liver, LSN862 and rosiglitazone both reduced expression of PEPCK, the enzyme responsible for the rate-limiting step in gluconeogenesis. These findings are consistent with those of others who have reported that PPARγ agonists decrease PEPCK mRNA levels in streptozotocin-treated rats (25) and rodent models of type 2 diabetes (20, 26). The decrease in PEPCK expression suggests a molecular explanation for the findings that PPARγ agonists reduce hepatic glucose output (27, 28). The decrease in PEPCK expression may not be a direct effect of LSN862 but rather a secondary effect due to the increase in insulin sensitivity or elevated adiponectin levels (22).

Interestingly, LSN862 increased expression of PDK4 approximately 4-fold in the liver, whereas rosiglitazone decreased the expression of this enzyme. PDK (of which there are four isozymes) and pyruvate dehydrogenase phosphatase (of which there are two isozymes) control the flux of pyruvate through the pyruvate dehydrogenase complex (29–33). Up-regulation of PDK4 inactivates the pyruvate dehydrogenase complex, which blocks pyruvate oxidation and conserves lactate and alanine for gluconeogenesis; in

contrast, a down-regulation of PDK4 allows complete oxidative decarboxylation of pyruvate to reduced nicotinamide adenine dinucleotide, acetyl-CoA, and CO_2 in oxidative tissue or to the synthesis of lipids in lipogenic tissues. PPARα agonists have been shown to increase the expression of PDK4 in heart, kidney, skeletal muscle, and liver (34). Thus, elevation of PDK4 expression in the liver by LSN862 is most likely due to the PPARα agonist activity of this compound. Treatment with LSN862 also increased the expression of BIFEZ, the enzyme that catalyzes the second step in the β-oxidation pathway of fatty acid metabolism (35), whereas rosiglitazone administration did not statistically affect expression of this enzyme. These data indicate that LSN862, like the PPARα activating fibrates, stimulates peroxisomal fatty acid oxidation.

Because PPARγ is expressed at high levels in most fat depots, expression of genes was evaluated in visceral and epididymal fat from the ZDF rat study described above. Malic enzyme and UCP-1 mRNA levels were increased by LSN862 and rosiglitazone in epididymal and visceral fat depots. Due to the extremely low levels of UCP-1 expression in epididymal fat from the vehicle-treated animals, the fold-induction of this gene could not be accurately calculated for either compound. UCPs are small intramembranous mitochondrial proteins that are expressed in a tissue-selective manner and play key roles in thermogenesis (36, 37). UCP-1 is present primarily in brown adipose tissue (38, 39), whereas UCP-3 is expressed in brown fat and skeletal muscle (40, 41). UCP-2 is found in most tissues (42, 43). The thermogenic role of UCP-1 has been shown definitively by many gain- and loss-of-function experiments (44–46). Interestingly, overexpression of PGC-1 in cultured white fat cells, 3T3-F422A, has been shown to increase UCP-1 mRNA levels (47), suggesting that LSN862 and rosiglitazone might increase the expression of UCP-1 in visceral and epididymal fat depots, at least in part, through recruitment of PGC-1.

Consistent with our findings are those by Way *et al.* (26), who show that administration of GW1929, a non-TZD PPARγ-selective agonist, to ZDF rats for 7 d increased malic enzyme mRNA levels in white and brown adipose tissues. Because malic enzyme is required for fatty acid synthesis and storage, our data are consistent with the hypothesis mentioned above that at least some of the efficacy of PPARγ ligands on insulin sensitization is via increased disposal of free fatty acids.

LSN862, but not rosiglitazone, administration led to a statistically significant increase in glycerol kinase expression in epididymal fat, whereas both compounds increased expression of glycerol kinase in visceral fat. Importantly, the increase in transcription due to LSN862 administration is statistically greater than that after rosiglitazone administration in both fat depots. Glycerol kinase stimulates glycerol incorporation into triglycerides and thus reduces free fatty acid secretion from adipocytes. Elevated free fatty acids in the circulation are known to be associated with insulin resistance (48, 49), and thus reducing levels of circulating free fatty acids would lead to greater insulin sensitivity. Therefore, the greater elevation of glycerol kinase expression due to LSN862 compared with rosiglitazone administration could play a role in the trend toward better glucose- and triglyceride-lowering by LSN862 in the ZDF rat study. Guan *et al.* (50) write eloquently about TZDs stimulating a "futile" fuel cycle resulting from enhanced expression of glycerol kinase in adipocytes. In their study, ZDF rats were administered rosiglitazone at 4.0 mg/kg per day for 10 d, and a statistical increase of approximately 2.5-fold was seen in glycerol kinase mRNA from epididymal fat analyzed by Northern blotting. The discrepancy in the results presented here and those reported by Guan *et al.*, could be due to the administered dose of rosiglitazone, duration of the study, and/or methods used to quantitative mRNA levels.

Increased expression of LPL in adipose tissue may explain some of the triglyceride-lowering activities of LSN862 and rosiglitazone, as LPL is a key player in triglyceride catabolism (51). Only LSN862 significantly increased LPL mRNA in both visceral and epididymal fat; however, a trend for enhanced LPL expression was seen with rosiglitazone in both fat depots. Although not statistically significant, LSN862-treated rats displayed a greater reduction in triglyceride levels compared with rosiglitazone-treated animals. This enhanced efficacy may reflect both the greater LPL expression and the additional PPARα activity of LSN862, as PPARα agonists are known to decrease liver apolipoprotein C-III transcription (52).

Emerging data suggest that visceral and sc adipose tissue have distinct physiological functions and contribute to obesity and type 2 diabetes to different extents (53). In the studies shown here, similar gene expression profiles were seen in epididymal and visceral fat depots from rats administered LSN862. In contrast, rosiglitazone administration led to a more robust response in visceral fat compared with epididymal fat. Interestingly, both compounds caused significant changes in the metabolic profiles of the treated animals, suggesting that visceral fat may play a greater role in contributing to the overall metabolic homeostasis of this rodent model of type 2 diabetes.

LSN862 was administered to hApoA1 mice to investigate the lipid-altering properties of this compound. These mice were selected for the study based on findings that human and mouse apolipoprotein A1 (ApoA1), the major protein constituent of HDL-C, are regulated in opposite directions by PPARα agonists, with mouse ApoA1 decreased and human ApoA1 increased after administration of PPARα agonists (54). Administration of LSN862 led to a modest decrease in VLDL-C and a dose-dependent increase in HDL-C, with neither response showing dose dependency. The effect of LSN862 on HDL-C was similar to that seen with an equivalent dose of fenofibrate. In contrast, rosiglitazone showed modest alterations in both

VLDL-C and HDL-C. These data are consistent with the *in vitro* data, which showed that only LSN862 had significant affinity for PPARα. Other investigators have also reported that a small amount of PPARα activity measured by *in vitro* binding and CTF assays can have surprising effects on lipid levels *in vivo* (55). Therefore, the improved lipid profile of LSN862 is most likely due to its additional PPARα agonist activity.

In conclusion, LSN862 is a new PPARα/γ dual agonist with a unique *in vitro* profile. Based on its potent antidiabetic activity, beneficial effects on lipid levels, potential for less body weight gain, and unique gene regulation profile, LSN862 may be an improved therapeutic agent for the treatment of type 2 diabetes and associated dyslipidemia. In addition, the data presented here demonstrate that PPARγ full agonist activity, as seen with rosiglitazone *in vitro*, is not necessary to achieve potent and efficacious antidiabetic benefits *in vivo*.

MATERIALS AND METHODS

Competitive Displacement Binding Assays

Binding assays were performed using scintillation proximity assay technology, PPAR receptors, and corresponding radiolabeled ligands. PPARα, PPARδ, and PPARγ along with their heterodimeric partner, retinoid X receptor α, were each produced using a baculovirus expression system. Biotinylated oligonucleotides containing PPREs were used to couple the corresponding receptor dimers to yttrium silicate streptavidin-coated scintillation proximity assay beads. PPARγ- and PPARα/δ-specific ligands were labeled with tritium and used in the appropriate corresponding assays. The K_i values for each competing compound were calculated after deduction of nonspecific binding (measured in the presence of 10 μM unlabeled ligand). Compounds were evaluated using an 11-point dose-response curve with concentrations ranging from 0.169 nM to 10 μM. Reported values represent means from three separate experiments.

CTF Assays

PPARγ, PPARα, or PPARδ were constitutively expressed using plasmids containing the cytomegalovirus promoter. Reporter plasmids for the PPARγ CTF assays contained PPREs from the following genes: AOX, LPL, or BIFEZ plus the thymidine kinase (TK) promoter upstream of the luciferase reporter cDNA. A PPARγ GAL4 chimeric system was also used. For PPARα and PPARδ, a GAL4 chimeric system was the standard CTF assay performed. All assays were done in CV-1 cells. Compounds were tested in full-log dilution, from 0.1 nM to 10 μM in duplicate. Percent efficacy was determined relative to reference molecules with the efficacy value reflecting the greatest amount of agonist activity achieved in the CTF assay for each compound. The reference compounds were rosiglitazone (PPARγ assays) and LG0070660 (PPARα and PPARδ assays). EC_{50} values were determined by computer fit to a concentration-response curve. An EC_{50} value was not calculated if the efficacy for the compound was less than 20%. Reported values represent means from three to 10 separate experiments. CTF assays for additional nuclear hormone receptors (retinoid X receptor, retinoic acid receptor, liver X receptor, farnesoid X receptor, pregnane X receptor) were performed as described above using appropriate nuclear receptors and corresponding reference ligands.

Cofactor Recruitment Assays

A mammalian two-hybrid assay system in CTF format was done in CV-1 cells. The following plasmids were used: a mammalian expression vector encoding a fusion of the GAL4 DNA-binding domain with the PPARγ ligand-binding domain; a mammalian expression vector encoding a fusion of the VP16 transactivation domain with the nuclear receptor interaction domain of the respective coactivators: CBP, PGC-1, ASC-2, TRAP220, and the peptide C33; and a reporter plasmid (multimerized GAL4 binding sites/minimal TK promoter driving a luciferase cDNA). Cells were transfected in batch format and treated with compound (full-log dilution from 0.1 nM to 10 μM) or vehicle for 24 h. Subsequently, the cells were lysed and luciferase activity was measured. Luciferase activity serves as the endpoint for interaction between coactivator and receptor. The data are presented as percent efficacy relative to rosiglitazone. Reported values represent means from three separate experiments.

RNA Quantitation

Liver mRNA was isolated using a FastTrack 2.0 kit from Invitrogen (Carlsbad, CA), and adipose mRNA was isolated using guanidine isothiocyanate/phenol/chloroform extraction. Isolated mRNA was first treated with DNase using a DNA-free kit from Ambion, Inc. (Austin, TX) and then 2.5 μg of DNase-treated mRNA was used for cDNA synthesis. Primer and probe sets for each gene of interest were designed using Primer Express 1.5 from Applied Biosystems (Foster City, CA). Each cDNA sample was analyzed in triplicate per gene in a 96-well plate using an ABI Prism 7700 Sequence Detector (Applied Biosystems). Results were averaged and normalized to 36B4 expression. Samples from each group of animals ($n = 5$) were averaged and compared with the vehicle group. Data are presented as mean standard error of the mean for each group. After taking the base 10 logarithm of the normalized expression results, group differences were assessed by ANOVA with pairwise contrasts examined using Fisher's protected least significant difference, where the significance level for the overall ANOVA was $P < 0.05$.

ZDF Rat Studies

Male ZDF rats were obtained from Genetic Models, Inc., (Indianapolis, IN) at 6 wk of age. After a 2-wk acclimation period, rats were prebled and assigned to four groups (five animals per group; vehicle, LSN862 at 3.0 mg/kg per day; rosiglitazone at 3.0 or 10.0 mg/kg per day) based on starting plasma glucose levels and body weight (d −1). Rats were administered compound daily by oral gavage between 0830 and 0930 h for 7 d. The dosing vehicle was 1% (wt/vol) carboxymethylcellulose, 0.25% Tween 80. Blood samples were obtained 1 h postdose on d 7 from the tail vein of conscious animals by gentle massage after tail snip. Blood was collected in EDTA tubes and kept chilled on ice. After centrifugation of blood samples, plasma was used for measurements of glucose, adiponectin, and triglyceride levels. Statistical significance was determined by one-way ANOVA. When statistical significance was detected with this method, group differences were determined by Neuman-Keuls *post hoc* analyses. Samples of liver and fat (visceral and epididymal) were removed on d 7, 6 h after the final dose of compound. Principles of laboratory animal care (NIH publication no. 85–23, revised 1985) were followed, and the use of animals was in accordance with the local animal ethics committee at Lilly Research Laboratories.

Db/db Mouse Studies

db/db Mice (5 wk of age) were purchased from Jackson Laboratories (Bar Harbor, ME). After a 2-wk acclimation period, the mice were prebled and assigned to three groups (vehicle, rosiglitazone, and LSN862; five animals per group) based on starting plasma glucose and body weight. The dosing vehicle for all studies was 1% (wt/vol) carboxymethylcellulose, 0.25% Tween 80. Compound was administered once daily by oral gavage between 0830 and 0930 h at a dose of 30 mg/kg for 7 d. Plasma was collected 1 h after compound administration on the last day of the study for measurement of plasma glucose and triglyceride levels. Statistical significance was determined by one-way ANOVA. When statistical significance was detected with this method, group differences were determined by Neuman-Keuls *post hoc* analyses. Principles of laboratory animal care (NIH publication no. 85–23, revised 1985) were followed, and the use of animals was in accordance with the local animal ethics committee at Lilly Research Laboratories.

Homozygous Human ApoA-1 Transgenic Mouse Studies

hApoA1 transgenic mice (56) were purchased from Jackson Laboratories. After a 2-wk acclimation period, the mice were assigned (based on weight) to individual groups with five animals per group. The mice were administered compound daily by oral gavage between 0600 and 0700 h for 7 d. Fenofibrate was administered at 100 mg/kg per day, whereas LSN862 and rosiglitazone were each given at 0.3, 1.0, 3.0, 10, 30, and 100 mg/kg per day. The dosing vehicle was 1% (wt/vol) carboxymethylcellulose, 0.25% Tween-80 with control animals receiving dosing vehicle only. Blood was collected by heart draw for analysis 3 h after the final dose. Principles of laboratory animal care (NIH publication no. 85–23, revised 1985) were followed, and the use of animals was in accordance with the local animal ethics committee at Lilly Research Laboratories.

Determination of VLDL-C and HDL-C

Lipoproteins were separated by fast protein liquid chromatography, and cholesterol was quantitated with an in-line detection system based on that described by Kieft *et al.* (57). Briefly, 35-μl plasma samples/50-μl pooled sample was applied to a Superose 6 HR 10/30 size exclusion column (Amersham Pharmacia Biotech, Piscataway, NJ) and eluted with PBS, pH 7.4 (diluted 1:10), containing 5 mM EDTA, at 0.5 ml/min. Cholesterol reagent from Roche Diagnostics (Indianapolis, IN) at 0.16 ml/min was mixed with the column effluent through a T connection; the mixture was then passed through a 15 m × 0.5 mm knitted tubing reactor (Aura Industries, New York, NY) immersed in a 37 C water bath. The colored product produced in the presence of cholesterol was monitored in the flow stream at 505 nm, and the analog voltage from the monitor was converted to a digital signal for collection and analysis. The change in voltage corresponding to change in cholesterol concentration was plotted *vs.* time, and the area under the curve corresponding to the elution of VLDL-C and HDL-C was calculated using Turbochrome (version 4.12F12) software from PerkinElmer (Norwalk, CT).

Acknowledgments

Received January 10, 2005. Accepted April 5, 2005.

Address all correspondence and requests for reprints to: Anne Reifel-Miller, Ph.D., Building 98/C/2331, Endocrinology Division, Lilly Research Laboratories, Indianapolis, Indiana 46285. E-mail: a.r.miller@lilly.com.

No grants or fellowships supported the writing or work described in this paper.

REFERENCES

1. Taskinen MR 2001 Diabetic dyslipidemia. Atherosclr Suppl 3:47–51
2. Garber AJ, Karlsson FO 2001 Treatment of dyslipidemia in diabetes. Endocrinol Metab Clin North Am 30: 999–1010
3. Aronoff S, Rosenblatt S, Braithwaite S, Egan JW, Mathisen AL, Schneider RL 2000 Pioglitazone hydrochloride monotherapy improves glycemic control in the treatment of patients with type 2 diabetes: a 6-month randomized placebo-controlled dose-response study. Diabetes Care 23:1605–1611
4. Staels B, Dallongeville J, Auwerx J, Schoonjans K, Leitersdorf E, Fruchart JC 1998 Mechanism of action of fibrates on lipid and lipoprotein metabolism. Circulation 98:2088–2093
5. Jones IR, Swai A, Taylor R, Miller M, Laker MR, Algerti KG 1990 Lowering of plasma glucose concentrations with bezafibrate in patients with moderately controlled NIDDM. Diabetes Care 13:855–863
6. Kobayashi M, Shigeta Y, Hirata Y, Omori Y, Sakamoto N, Nambu S, Baba S 1988 Improvement of glucose tolerance in NIDDM by clofibrate. Randomized double-blind study. Diabetes Care 11:495–499
7. Issemann I, Green S 1990 Activation of a member of the steroid hormone receptor superfamily by peroxisome proliferators. Nature 347:645–650
8. Lehmann JM, Moore LB, Smith-Oliver TA, Wilkison WO, Wilson TM, Kliewer SA 1995 An antidiabetic thiazolidinedione is a high affinity ligand for peroxisome proliferator-activated receptor γ (PPARγ). J Biol Chem 270: 12953–12956
9. Rocchi S, Picard F, Vamecq J, Gelman L, Potier N, Zeyer D, Dubuquoy L, Bac P, Champy M-F, Plunket KD, Leesnitzer LM, Blanchard SG, Desreumaux P, Moras D, Renaud J-P, Auwerx J 2001 A unique PPARγ ligand with potent insulin-sensitizing yet weak adipogenic activity. Mol Cell 8:737–747
10. Berger JP, Petro AE, Macnaul KL 2003 Distinct properties and advantages of a novel PPARγ selective modulator. Mol Endocrinol 17:662–676
11. Shimaya A, Kurosaki E, Nakano R, Hirayama R, Shibasaki M, Shikama H 2000 The novel hypoglycemic agent YM440 normalizes hyperglycemia without changing body fat weight in diabetic db/db mice. Metabolism 49:411–417
12. Chakrabarti R, Vikramadithyan R, Misra P, Suresh J, Rajagopalan R 2003 Balaglitazone, a quinazalone analogue of thiazolidinedione shows excellent antidiabetic and hypolipidemic potential with less adipogenic activity. Diabetes 52(Suppl 1):601P (Abstract)
13. Kawai T, Takei I, Oguma Y 1999 Effects of troglitazone on fat distribution in the treatment of male type 2 diabetes. Metabolism 48:1102–1107
14. Wulff E, Pedersen K, Sauerberg P 2003 Balaglitazone a new partial PPARγ agonist has a better cardiovascular safety profile and glycemic control compared with the full PPARγ agonist rosiglitazone. Diabetes 52(Suppl 1):594P (Abstract)
15. Guerre-Millo M, Gervois P, Raspe E 2000 Peroxisome proliferator-activated receptor α activators improve insulin sensitivity and reduce adiposity. J Biol Chem 275: 16638–16642
16. Nagai Y, Nishio Y, Nakamura T, Maegawa H, Kikkawa R, Kashiwagi A 2002 Amelioration of high fructose-induced

metabolic derangements by activation of PPARα. Am J Physiol Endocrinol Metab 282:E1180–E1190
17. Winegar DA, Brown PJ, Wilkison WO, Lewis MC, Ott, RJ, Tong WQ, Brown HR, Lehmann JM, Kliewer SA, Plunket KD, Way JM, Bodkin NL, Hansen BC 2001 Effects of fenofibrate on lipid parameters in obese rhesus monkeys. J Lipid Res 42:1543–1551
18. Ye J-M, Doyal PJ, Iglesias MA, Watson DG, Cooney GJ, Kraegen EW 2001 Peroxisome proliferator-activated receptor (PPAR)-α activation lowers muscle lipids and improves insulin sensitivity in high fat-fed rats: comparison with PPAR-γ activation. Diabetes 50:411–417
19. Aasum E, Belke DD, Severson DL, Riemersma RA, Cooper M, Andressen M, Larsen TS 2002 Cardiac function and metabolism in type 2 diabetic mice after treatment with BM17.0744, a novel ppar-α activator. Am J Physiol Heart Circ Physiol 283:H949–H957
20. Brand CL, Sturis J, Gotfredsen CF, Fleckner J, Fledelius C, Hansen BF, Andersen B, Ye J-M, Sauerberg P, Wassermann K 2003 Dual PPARα/γ activation provides enhanced improvement of insulin sensitivity and glycemic control in ZDF rats. Am J Physiol Endocrinol Metab 284: E841–E854
21. Ouchi N, Kihara S, Arita Y, Okamoto Y, Maeda K, Kuriyama H, Hotta K, Nishida M, Takahashi M, Muraguchi M, Ohmoto Y, Nakamura T, Yamashita S, Funahashi T, Matsuzawa Y 2000 Adiponectin, an adipocyte-derived plasma protein, inhibits endothelial NF-κB signaling through a camp-dependent pathway. Circulation 102: 1296–1301
22. Combs TP, Berg AH, Obici S, Scherer PE, Rossetti L 2001 Endogenous glucose production is inhibited by the adipose-derived protein Acrp30. J Clin Invest 108: 1875–1881
23. Fruebis J, Tsao T-S, Javorschi S 2001 Proteolytic cleavage product of 30 kDa adipocyte complement-related protein increases fatty acid oxidation in muscle and causes weight loss in mice. Proc Natl Acad Sci USA 98:2005–2010
24. Yamauchi T, Kamon J, Waki H 2001 The fat derived hormone adiponectin reverses insulin resistance associated with both lipoatrophy and obesity. Nat Med 7:941–946
25. Hofmann C, Lorenz K, Williams D, Palazuk BJ, Colca JR 1995 Insulin sensitization in diabetic rat liver by an antihyperglycemic agent. Metabolism 44:384–389
26. Way JM, Harrington WW, Brown KK, Gottschalk WK, Sundseth SS, Mansfield TA, Ramachandrán RK, Willson TM, Kliewer SA 2001 Comprehensive messenger ribonucleic acid profiling reveals that peroxisome proliferator-activated receptor γ activation has coordinate effects on gene expression in multiple insulin-sensitive tissues. Endocrinology 142:1269–1277
27. Day C 1999 Thiazolidinediones: a new class of antidiabetic drugs. Diabet Med 16:179–192
28. Reginato MJ, Lazar MA 1999 Mechanisms by which thiazolidinediones enhance insulin action. Trends Endocrinol Metab 10:9–13
29. Popov KM, Kedishvili NY, Zhao Y, Shimomura Y, Crabb DW, Harris RA 1993 Primary structure of pyruvate dehydrogenase kinase establishes a new family of eukaryotic protein kinases. J Biol Chem 268:26602–26606
30. Popov KM, Kedishvili NY, Zhao Y, Gudi R, Harris RA 1994 Molecular cloning of the p445 subunit of pyruvate dehydrogenase kinase. J Biol Chem 269:29720–29724
31. Rowles J, Scherer SW, Xi T 1996 Cloning and characterization of PDK4 on 7q21.3 encoding a fourth pyruvate dehydrogenase kinase isoenzyme in humans. J Biol Chem 271:22376–22398
32. Lawson JE, Niu XD, Browning KS, Trong HL, Yan J, Reed LJ 1993 Molecular cloning and expression of the catalytic subunit of bovine pyruvate dehydrogenase phosphatase and sequence similarity with protein phosphatase 2C. Biochemistry 32:8987–8993
33. Huang B, Gudi R, Wu P, Harris RA, Hamilton J, Popov KM 1998 Isoenzymes of pyruvate dehydrogenase phosphatase. DNA-derived amino acid sequences, expression, and regulation. J Biol Chem 273:17680–17688
34. Wu P, Peters JM, Harris RA 2001 Adaptive increase in pyruvate dehydrogenase kinase 4 during starvation is mediated by peroxisome proliferator-activated receptor α. Biochem Biophys Res Comm 287:391–396
35. Agnihotri G, Liu H-W 2003 Enoyl-CoA hydratase: reaction, mechanism, and inhibition. Bioorg Med Chem 11: 9–20
36. Flier JS, Lowell BB 1997 Obesity research springs a protein leak. Nat Genet 15:223–224
37. Ricquier D, Bouillaud, F 1997 The mitochondrial uncoupling protein: structural and genetic studies. Prog Nucleic Acid Res Mol Biol 56:83–108
38. Jacobsson A, Stadler U, Glotzer MA, Kozak LP 1985 Mitochondrial uncoupling protein from mouse brown fat. Molecular cloning and genetic mapping, and mRNA expression. J Biol Chem 260:16250–16254
39. Bouillaud F, Weissenbach J, Ricquier D 1986 Complete cDNA-derived amino acid sequence of rat brown fat uncoupling protein. J Biol Chem 261:1487–1490
40. Boss O, Samec S, Paoloni-Giacobino A, Rossier C, Dulloo A, Seydoux J, Muzzin P, Giacobino J-P 1997 Uncoupling protein-3: a new member of the mitochondrial carrier family with tissue-specific expression. FEBS Lett 408:39–42
41. Vidal-Puig A, Solanes G, Grujic D, Flier JS, Lowell BB 1997 UCP3: an uncoupling protein homologue expressed preferentially and abundantly in skeletal muscle and brown adipose tissue. Biochem Biophys Res Commun 235:79–82
42. Fleury C, Neverova M, Collins S, Raimbault S, Champigny O, Levi-Meyrueis C, Bouillaud F, Seldin MF, Surwit RS, Ricquier D, Warden CH 1997 Uncoupling protein-2: a novel gene linked to obesity and hyperinsulinemia. Nat Genet 15:269–272
43. Gimeno RE, Dembski M, Weeng X 1997 Cloning and characterization of an uncoupling protein homolog: a potential molecular mediator of human thermogenesis. Diabetes 46:900–906
44. Lowell BB, Susulic VS, Hamann A, Lawitts JA, Himms-Hagen J, Boyer BB, Kozak LP, Flier JS 1993 Development of obesity in transgenic mice after genetic ablation of brown adipose tissue. Nature 366:740–742
45. Kopecky J, Clarke G, Enerback S, Spiegelman B, Kozak LP 1995 Expression of the mitochondrial uncoupling protein gene from the aP2 gene promoter prevents genetic obesity. J Clin Invest 96:2914–2923
46. Enerback S, Jacobsson A, Simpson EM, Guerra C, Yamashita H, Harper M-E, Kozak LP 1997 Mice lacking mitochondrial uncoupling protein are cold-sensitive but not obese. Nature 387:90–94
47. Wu Z, Puigserver P, Andersson U 1999 Mechanisms controlling mitochondrial biogenesis and respiration through the thermogenic coactivator PGC-1. Cell 98: 115–124
48. Boden G 2001 Pathogenesis of type 2 diabetes and insulin resistance. Endocrinol Metab Clin North Am 30: 801–815
49. Roden M, Stingl H, Chandramouli V 2000 Effects of free fatty acid elevation on postabsorptive endogenous glucose production and gluconeogenesis in humans. Diabetes 49:701–707
50. Guan H-P, Li Y, Jensen MV, Newgard CB, Steppan CM, Lazar MA 2002 A futile metabolic cycle activated in adipocytes by antidiabetic agents. Nat Med 8:1122–1126
51. Goldberg I 1996 Lipoprotein lipase and lipolysis: central roles in lipoprotein metabolism and atherogenesis. J Lipid Res 37:693–707

52. Lefebvre AM, Peinado-Onsurbe J, Leitersdorf I, Briggs MR, Paterniti JR, Fruchart JC, Fievet C, Auwerx J, Staels B 1997 Regulation of lipoprotein metabolism by thiazolidinediones occurs through a distinct but complementary mechanism relative to fibrates. Arterioscler Thromb Vasc Biol 17:1756–1764
53. Wajchenberg GL, Biannella-Neto D, Da Silva ME, Santos RF 2002 Depot-specific hormonal characteristics of subcutaneous and visceral adipose tissue and their relation to the metabolic syndrome. Horm Metab Res 34: 616–621
54. Berthou L, Duverger N, Emmanuel F, Langouet S, Auwerx J, Guillouzo A, Fruchart JC, Rubin E, Denefle P, Staels B, Branellec D 1996 Opposite regulation of human versus mouse apolipoprotein A-I by fibrates in human apolipoprotein A-I transgenic mice. J Clin Invest 97: 2408–2416
55. Wilson GG, Abou-Donia M, Frith L, Patel J, Fiedorek FT 2000 Monotherapy with GI262570, a tyrosine-based non-thiazolidinedione PPARγ agonist significantly reduces triglyceride and increases HDL-C concentrations in patients with type 2 diabetes mellitus. Diabetes 49(Suppl 1):158OR (Abstract)
56. Rubin EM, Ishida BY, Clift SM, Krauss RM 1991 Expression of human apolipoprotein A-I in transgenic mice results in reduced plasma levels of murine apolipoprotein A-I and the appearance of two new high density lipoprotein size subclasses. Proc Natl Acad Sci USA 88: 434–438
57. Kieft KA, Bocan TMA, Krause BR 1991 Rapid on-line determination of cholesterol distribution among plasma lipoproteins after high-performance gel filtration chromatography. J Lipid Res 32:859–866

Molecular Endocrinology **is published monthly by The Endocrine Society (http://www.endo-society.org), the foremost professional society serving the endocrine community.**

Available online at www.sciencedirect.com
ScienceDirect
European Journal of Pharmacology 551 (2006) 80–86
ejp
www.elsevier.com/locate/ejphar

Anti-hyperlipidemic properties of CM108 (a flavone derivative) in vitro and in vivo

Lei Guo *, Wei-Rong Hu, Ji-Hong Lian, Wei Ji, Ting Deng, Ming Qian, Bang-Qiang Gong

State Key Laboratory of Bioreactor Engineering, East China University of Science and Technology, Shanghai 200237, China

Received 24 April 2006; received in revised form 22 August 2006; accepted 28 August 2006
Available online 6 September 2006

Abstract

Peroxisome proliferator-activated receptors (PPARs) and liver X receptor α are ligand-activated transcription factors that belong to nuclear receptors superfamily and are involved in the regulation of lipid metabolism. PPAR, especially PPAR-α, PPAR-γ agonists and liver X receptor α agonists can regulate the expression or biosynthesis of some factors involved in the formation and function of HDL, such as apolipoprotein (apo) A-I and ATP binding cassette transporter A1 (ABCA1). It is well known that HDL plays an important role in the treatment of hyperlipidemia as the carrier of reverse cholesterol transport. In the present study, the anti-hyperlipidemic properties of CM108, a derivative of flavone, 9-Hydroxy-2-mercapto-6-phenyl-2-thioxo-1,3,5-trioxa-2λ^5-phospha-cyclopenta[*b*]naphthalen-8-one, were studied. Through the transactivation assays of in vitro study, it was discovered that CM108 could activate PPAR-α PPAR-γ and liver X receptor α at 40–150 μg/ml, which subsequently resulted in activating ABCA1 promoter and enhancing apoA-I and apoA-II production, whereas reducing apoC-III production significantly. Furthermore, after in vivo study that the hyperlipidemic rats were treated with CM108 for 4 weeks, a significant increase was found in HDL cholesterol levels (26.7%, $P<0.05$) and a significant decrease was also noticed in triglyceride levels (26.3%, $P<0.01$) at 100 mg/kg CM108 group compared with that of control animals. Meanwhile, the atherogenicity index, represented by total cholesterol/HDL ratio, was significantly reduced ($P<0.01$). In conclusion, CM108 can effectively elevate HDL levels and lower triglyceride levels in hyperlipidemic rats maybe by regulating a series of genes, receptors and proteins related to HDL.

Keywords: High-density lipoprotein (HDL); Peroxisome proliferator-activated receptors (PPARs); Liver X receptor α; Apolipoprotein A-I (apoA-I); ATP binding cassette transporter A1 (ABCA1)

1. Introduction

Numerous epidemiological studies have demonstrated an inverse relationship between high-density lipoprotein (HDL) cholesterol levels and cardiovascular diseases. Low plasma HDL cholesterol is an independent risk factor for cardiovascular disease (Gotto, 2001; Assmann et al., 1996). In fact, a 1% increase of HDL cholesterol levels is associated with a 2–3% decrease in cardiovascular morbidity and mortality (Gordon et al., 1981; Forte and McCall, 1994). An important mechanism underlying this protective effect is the role of HDL in the removal of excess cholesterol from peripheral tissues (including the arterial wall) to the liver. This process named as reverse cholesterol transport is often invoked to explain the anti-atherogenic effect of HDL. But in addition, HDL is also suggested to ameliorate endothelial function (Uittenbogaard et al., 2000; Yuhanna et al., 2001) and to have anti-oxidative, anti-inflammatory, anti-coagulant, anti-aggregatory properties (Van Lenten et al., 2001; Nofer et al., 2002).

With increasing evidence that HDL plays an important role in cholesterol reverse transport and cholesterol clearance, it has been concluded that compounds which could accelerate the reverse cholesterol transport process may be beneficial in reducing cardiovascular disease (Patrick and Alan, 2004).

PPAR-α and liver X receptor α are ligand-activated transcription factors that belong to the nuclear receptor superfamily. The PPAR-α and liver X receptor α agonists are believed to have atheroprotective effects (Joyce and David, 2002; Daniel et al., 2004). We established the cell-based PPAR-α and liver X receptor α agonists screening system to identify compounds that can activate PPAR-α and liver X receptor α gene

* Corresponding author. Tel./fax: +86 21 6424 3923.
E-mail address: giet77@sohu.com (L. Guo).

0014-2999/$ - see front matter © 2006 Elsevier B.V. All rights reserved.
doi:10.1016/j.ejphar.2006.08.048

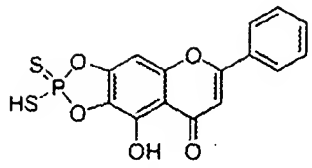

Fig. 1. Chemical structure of CM108.

expression simultaneously. A derivative of flavone, 9-Hydroxy-2-mercapto-6-phenyl-2-thioxo-1,3,5-trioxa-2λ^5-phospha-cyclopenta[*b*]naphthalen-8-one (CM108, Fig. 1), represents the above character. In the present study, the anti-hyperlipidemic action of CM108 was examined through in vitro and in vivo assays. The results gave potent proof that CM108 could exhibit a comprehensive regulation of the genes, receptors and proteins related to reveres cholesterol transport carried by HDL, which allowed CM108 to increase HDL cholesterol levels and lower triglyceride levels simultaneously.

2. Materials and methods

2.1. Materials

CM108 was synthesized by Comman Pharmaceutical Co. Ltd (Shanghai, China). Gemfibrozil was purchased from Sigma (ST Louis, USA). For in vitro assay, CM108 was dissolved in dimethylsulfoxide (DMSO). For in vivo assay, CM108 and Gemfibrozil were suspended in 0.5% Tween-80 (Sigma, ST Louis, USA) aqueous solution, and a uniform suspension was obtained by ultrasonication.

2.2. Transcription regulation assays

For PPAR-α, PPAR-γ and liver X receptor α, expression constructs were prepared respectively by inserting the ligand binding domains of human PPAR-α, PPAR-γ and liver X receptor α cDNAs adjacent to the yeast GAL4 transcription factor DNA binding domain in the mammalian expression vector pcDNA3.1 to create pcDNA3.1-GAL4/PPARα, pcDNA3.1-GAL4/PPARγ and pcDNA3.1-GAL4/LXRα. The GAL4-responsive reporter construct, pGL3BN-tk-luciferase, contained five copies of the GAL4 response element was placed adjacent to the thymidine kinase minimal promoter, the luciferase reporter gene and the neomycin resistance gene. For ABCA1 (similarly to Guo et al., 2006), expression construct was prepared by inserting the upstream regulatory sequence in the expression vector pGL3BN to create pGL3BN-ABCA1. For stable transfections, HepG2 cells were seeded at 4×10^5 cells/well in 6-well plates in Dulbecco's modified Eagle's medium (DMEM, high glucose) containing 10% fetal calf serum (PAA, Pasching, Austria) at 37 °C and incubated overnight. Transfections were performed with LipofectAMINE (Invitrogen, Carlsbad, CA) according to the manufacturer's protocol. For PPAR-α, PPAR-γ and liver X receptor α, transfection mixes contained 2 μg of GAL4/PPARα or GAL4/PPARγ or GAL4/LXRα expression vectors and reporter vector *p*GL3BN-tk-luc in a ratio of 5:1; for ABCA1, transfection substance contained 2 μg of *p*GL3BN-

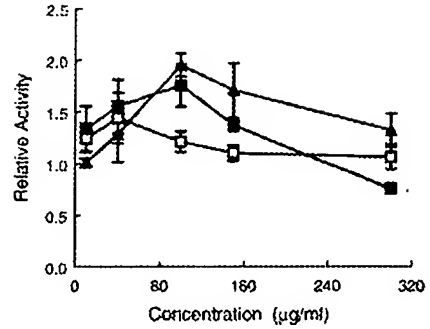

Fig. 2. CM108 is active on PPAR-α, PPAR-γ and liver X receptor α in transactivation assays. Transactivation assays were performed using chimeric receptors as described under "Materials and methods". Data shown are mean and S.D. for triplicate wells. Relative activities are derived from "CM108 reading/DMSO reading". □ Represents PPAR-α, ■ represents PPAR-γ, ▲ represents liver X receptor α.

ABCA1. Twenty-four hours after transfection, cell culture media were replaced by fresh media containing Geneticin (G418, Invitrogen, Carlsbad, CA) at final concentration of 800 mg/l. Monoclones were selected by limited dilution in the presence of G418 to generate stable cell lines. Compounds were characterized by incubation with transfected stable cells for 24 h across a range of concentrations in DMEM (high glucose). Cell lysates were prepared from washed cells using cell lysis buffer (Promega, WI, USA). Luciferase activity in cell extracts was measured using TD2020 Luminometer (Turner Designs, CA) in luciferase assay buffer (Promega, WI, USA). The Luminometer reading was corrected by the absorbance (*A*) value measured from MQX200 (Bio-Tek Inc., USA) at 570 nm.

2.3. Protein regulation assays

Compounds were characterized by incubation with HepG2 cells for 24 h across a range of concentrations in DMEM (high glucose). Cell supernatants were collected and measured. In the enzyme-linked immunosorbent assay (Sambrook and Russell, 2001), cell supernatants were coated on 96-well plates

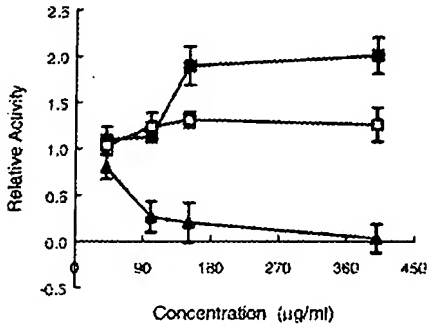

Fig. 3. CM108 increases apoA-I, apoA-II production and decreases apoC-III production in HepG2 Cells. HepG2 Cells were incubated with various concentrations of CM108 for 24 h, and then the levels of apoA-I, apoA-II and apoC-III protein were measured as described under "Materials and methods". Data are the means of triplicate wells, and the *error bars* indicate the range of triplicates. Relative activities are derived from "CM108 reading/DMSO reading". ■ Represents apoA-I, □ represents apoA-II and ▲ represents apoC-III.

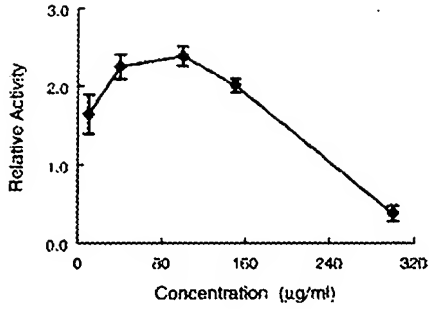

Fig. 4. Effect of CM108 on ABCA1 promoter expression. Transactivation assay was performed and described under "Materials and methods". Data shown are mean and S.D. for triplicate wells, relative activities are derived from "CM108 reading/DMSO reading".

(Corning, USA) (50 μl/well) overnight at 4 °C. Subsequent procedures were performed at room temperature. After being washed with 0.01 M phosphate-buffered saline (pH 7.4) containing 0.05% Tween-20 and 0.9% NaCl (PBST), the plates were incubated for 1 h with 5% skim milk in PBS. After washed with PBST for six times, the plates were incubated at a 1:1000 dilutions of goat anti-human apoA-I or apoA-II or apoC-III (Academy Bio-Medical, Houston, USA) (50 μl/well) and incubated for 1 h. After washed with PBST for another six times, the plates were incubated with horseradish peroxidase-conjugated anti-goat IgG (Jackson ImmunoResearch Laboratories, West Grove, USA) (50 μl/well) at a 1:1000 dilution for 1 h. After six washes, the plates were incubated with *o*-phenylenediamine (100 μl/well) for 30 min. After terminating the reaction by adding 2 M H_2SO_4 (50 μl/well), the absorbance at 492 nm was measured by MQX200 (Bio-Tek Inc., USA).

2.4. Animals and experimental design

Male Sprague–Dawley rats (4–6 weeks old) were purchased from Shanghai experimental animal center, China. The rats were housed in an environmentally controlled room at (22±2 °C), relative humidity at (60±10%) and 12 h light/dark cycle (light period: 6:00–18:00). Diets and tap water were provided *ad libitum*. After 1-week acclimation, the initial lipids profile of all rats were measured, and then sixty rats began to be fed with high cholesterol diet (normal diet supplemented with 0.5% cholesterol, 0.5% cholic acid and 5.5% olive oil) for 1 week. Animals were bled for measurement of lipids profile and fifty rats were ascertained as the successful model rats. Then the fifty model rats were randomly divided into 5 groups of 10 animals per group. After that, high cholesterol diets were replaced by normal diets. The low, middle and high dose groups of model rats, named CM108 groups, were administrated orally with CM108 at a dosage of 30 mg/kg, 60 mg/kg and 100 mg/kg respectively. The rats named Gemfibrozil group were administrated orally with Gemfibrozil (100 mg/kg), and the control group rats were only administrated with the dosing vehicle. After 4 weeks of treatment, animals were bled for measurement of lipids profile and liver was obtained for weight measurement. Body weight was recorded at the times indicated. During the feeding period, care and treatment of rats were in compliance with the Guide for the Care and Use of Laboratory Animals and local institutional guidelines.

2.5. Measurement of blood lipids and lipoproteins

After the bloods were put at room temperature for 1 h, serum was separated by centrifugation at 1500 ×*g* for 15 min. The levels of serum total cholesterol, HDL cholesterol, and triglyceride were measured by enzymatic methods (Roche, USA) with an automatic analyzer (7170, Hitachi, Japan). Low-density lipoprotein (LDL) cholesterol levels were calculated by the Friedewald formula.

2.6. Statistical analysis

The results were reported as the mean±S.D. of *n* observations. For the in vitro studies, *n* represents the number of 3

Table 1
Baseline characteristics (initial and before treatment)

	Control	CM108			Gemfibrozil
		30 mg/kg	60 mg/kg	100 mg/kg	100 mg/kg
Initial					
Total cholesterol, mmol/L	1.83±0.19	1.89±0.23	1.65±0.33	1.81±0.31	1.70±0.28
Triglyceride, mmol/L	0.68±0.16	0.68±0.15	0.62±0.18	0.72±0.25	0.68±0.15
HDL, mmol/L	1.31±0.23	1.39±0.34	1.23±0.27	1.25±0.20	1.20±0.22
LDL, mmol/L	0.24±0.17	0.18±0.20	0.14±0.18	0.24±0.24	0.20±0.24
Total cholesterol/HDL ratio	1.42±0.17	1.39±0.22	1.35±0.15	1.47±0.26	1.44±0.20
LDL/HDL ratio	0.24±0.14	0.15±0.16	0.12±0.13	0.21±0.23	0.18±0.22
Before treatment					
Total cholesterol, mmol/L	3.84±0.33[b]	3.96±0.34[b]	4.03±0.44[b]	4.31±0.35[b]	3.95±0.54[b]
Triglyceride, mmol/L	1.20±0.44[b]	1.35±0.45[b]	1.36±0.46[b]	1.60±0.52[b]	1.48±0.42[b]
HDL, mmol/L	1.37±0.12	1.42±0.14	1.37±0.16	1.39±0.13	1.41±0.15
LDL, mmol/L	1.62±1.19[b]	1.93±0.23[b]	2.04±0.32[b]	2.20±0.40[b]	1.87±0.45[b]
Total cholesterol/HDL ratio	2.81±0.29[b]	2.80±0.21[b]	2.97±0.42[b]	3.12±0.32[b]	2.82±0.42[b]
LDL/HDL ratio	1.18±0.89[b]	1.37±0.21[b]	1.51±0.31[b]	1.59±0.35[b]	1.33±0.33[b]

Values are given as mean±S.D., $n=10$. Before treatment values are equal to the measured values for rats 1 week after fed on high-cholesterol diet.
[a]$P<0.05$, [b]$P<0.01$: before treatment vs. initial (of each dose group).

Table 2
Absolute changes in lipids and lipoproteins according to the dose of CM108 after 4 weeks of treatment

	Control	CM108			Gemfibrozil
		30 mg/kg	60 mg/kg	100 mg/kg	100 mg/kg
Total cholesterol, mmol/L	−0.75±1.02	−0.97±0.72	−1.06±1.09	−1.39±0.71	−1.15±0.85
Triglyceride, mmol/L	−0.45±0.37	−0.64±0.47	−0.62±0.37	−0.98±0.41[a]	−0.90±0.44
HDL, mmol/L	−0.12±0.18	0.02±0.34	0.04±0.27	0.25±0.28[b]	0.20±0.33[b]
LDL, mmol/L	−0.14±1.67	−0.70±0.86	−0.82±0.95	−1.20±0.83	−0.94±0.69
Total cholesterol/HDL ratio	−0.38±0.51	−0.63±0.67	−0.83±0.66	−1.30±0.55[b]	−1.03±0.59[b]
LDL/HDL ratio	−0.04±1.20	−0.42±0.68	−0.62±0.62	−0.94±0.59	−0.72±0.47

Values are given as mean± S.D., $n=10$.
[a]$P<0.05$, [b]$P<0.01$: each dose group vs. control group.

parallel experiments performed. For the in vivo studies, n represents the number of animals studied. Differences between the experimental and control group were determined by the Student's t-test and P values less than 0.05 were considered to be significant.

3. Results

3.1. Transcription regulation effects of CM108 on PPAR-α, PPAR-γ and liver X receptor α

CM108 was identified as a PPAR-α agonist during the compounds' screening. The structure of CM108 is shown in Fig. 1. With the treatment of CM108, PPAR-α level was enhanced by 11–44% at 40–150 μg/ml in the transactivation assay, and the maximal activation was achieved 44% at 40 μg/ml. Furthermore, CM108 was identified as an agonist of both liver X receptor α and PPAR-γ, and their activation percentages achieved with CM108 were 37–76% and 29–95% at 40–150 μg/ml and the maximal activation percentages achieved was 76% and 95% at 100 μg/ml respectively, the results are shown in Fig. 2. CM108 was, therefore, found to be active in similar transactivation assays for the nuclear receptors PPAR-α, PPAR-γ and liver X receptor α.

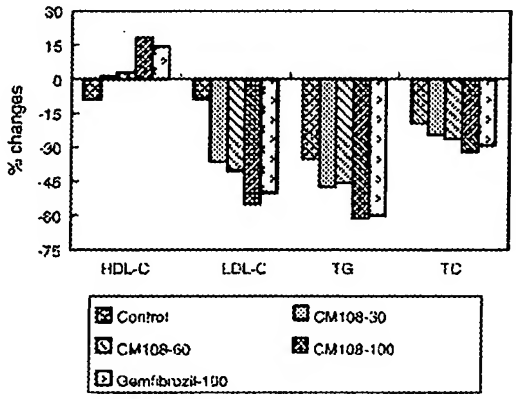

Fig. 5. Percentage changes of HDL cholesterol, LDL cholesterol, triglyceride, and total cholesterol from baseline after 4 weeks of treatment. HDL-C: HDL cholesterol; LDL-C: LDL cholesterol; TG: triglyceride; TC: total cholesterol.

3.2. Effects of CM108 on apoA-I, apoA-II and apoC-III production

In the protein regulation assays, the effects of CM108 were tested on apoA-I, apoA-II and apoC-III production. As shown in Fig. 3, CM108 was shown a dose-dependently curve for apoA-I, apoA-II and apoC-III in the tested concentrations respectively. CM108 enhanced apoA-I and apoA-II production by 90% and 31% at 150 μg/ml, whereas CM108 reduced apoC-III production by 80% at the same concentration.

3.3. Effect of CM108 on ABCA1 expression

Meanwhile, we identified the effect of CM108 on ABCA1 expression in the similar transactivation assay, the Fig. 4 showed that CM108 is effective on ABCA1 expression at 10–150 μg/ml and the maximal activation percentage achieved with CM108 was 2–2.38-fold higher than that of the control at 40–150 μg/ml.

3.4. Effects of CM108 on lipids and lipoproteins

To clarify the hypolipidemic properties of CM108 in vivo, we further investigated the effects of CM108 on the lipid profiles in hyperlipidemic rats by feeding them with high-cholesterol diet. In vitro results indicated that the activation

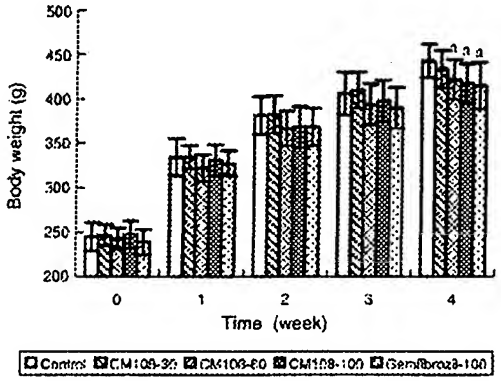

Fig. 6. Change in the mean body weight of rats before and after 4 weeks treatment. Data are shown mean±S.D., $n=10$. [a]$P<0.05$ vs. control group.

percentage of CM108 on PPAR-α at 60 μg/ml was almost equal to that of Gemfibrozil at 100 μg/ml (data not shown), thus, here we used 100 mg/kg Gemfibrozil as the positive control and 30, 60, 100 mg/kg as doses of CM108 (Nagao et al., 1998). Besides, Table 1 described the lipids and lipoproteins baseline of initial level and before treatment with CM108 level. Here, the initial lipids and lipoproteins baseline referred to the measured basic level for rats before they were fed with high-cholesterol diet. The baseline before treatment with CM108 referred to the measured level for rats 1 week after fed on high-cholesterol diet. Compared with the corresponding initial groups, it was clear to observe the results that the different measured levels of before-treatment groups were significantly increased such as the total cholesterol, triglyceride, LDL cholesterol, total cholesterol/HDL ratio and LDL/HDL ratio ($P<0.01$).

Table 2 provides the changes in these parameters after 4 weeks of treatment, and the percentage changes are illustrated in Fig. 5. In the rat groups treated with active drug, a dose-dependent increase in HDL cholesterol was observed which reached a significant increase (26.7%, $P<0.05$) at 100 mg/kg CM108 after 4 weeks of treatment. Moreover, a decrease was recorded of triglyceride levels in all groups, reaching statistical significance at 100 mg/kg CM108 group (26.3%, $P<0.01$). Total cholesterol and LDL cholesterol levels were not significantly changed as statistics indicated in all 3 doses groups. The atherogenicity index, represented by total cholesterol/HDL ratio, was greatly reduced in 100 mg/kg CM108 group ($P<0.01$) compared with the control group.

3.5. Effect of CM108 on body weight and the ratio of liver/body weight

Every group showed increased body weight throughout the experimental period. But the increase in the 60 mg/kg, 100 mg/kg CM108 groups and Gemfibrozil group were lower than the increase in the control group, and there were significant differences ($P<0.05$) compared 60 mg/kg, 100 mg/kg CM108 groups and Gemfibrozil group with the control group at the 4th week of treatment, respectively (Fig. 6). Furthermore, CM108 didn't increase the ratio of liver/body weight compared with the control group at the end of the experiments (data not shown).

4. Discussion

HDL as the carrier of reverse cholesterol transport renders it anti-atherogenic. This process includes three steps: Firstly, the expression and secretion of apoA-I, the major structural apolipoprotein of HDL lipoprotein, from the liver. Secondly lipid-poor or lipid-free apoA-I can subsequently act as an acceptor for ABC transporters (ABCA1 and ABCG1)-mediated efflux of cholesterol and phospholipids from macrophages, which results in the formation of HDL. Finally, HDL cholesterol can be taken up by the liver and secreted into the bile (Patrick and Alan, 2004). The results of this study suggested that CM108 compound is not only a potent enhancer of HDL in vitro but also acts as a hypolipidemic agent in vivo.

PPARs are ligand-activated transcription factors that belong to the nuclear receptors superfamily and consist of the three members PPAR-α, PPAR-γ and PPAR-δ. These proteins contain a central DNA-binding domain consisting of a zinc-finger module and a large ligand-binding domain with a lipophilic core that binds specific small lipid molecules. After ligands binding, nuclear receptors undergo a conformational change. This change promotes their interaction with co-activator proteins, which therefore facilitates transcription of cognate target genes. Each of them controls a distinct network of target genes. A common feature is their involvement in fatty-acid metabolism (Joel et al., 2005).

PPAR-α is expressed highly in organs with a high rate of fatty-acid catabolism, such as brown adipose tissue, liver, kidney and heart (Kersten, 2002). The clinical importance of fibrates as PPAR-α agonists has been identified for its decreasing plasma triglyceride levels and increasing HDL cholesterol levels. The former action of decreasing plasma triglyceride levels is mediated by increasing lipid uptake, activation and catabolism through the transcriptional modulation of numerous genes that control these processes (Daniel et al., 2004). Moreover, the metabolism of triglyceride-rich lipoproteins is strongly affected (Schoonjans et al., 1996). The induction of enzymes involved in the β-oxidation pathway in the liver resulted in the distinctively reduced secretion of very low-density lipoproteins (VLDL) particles by the liver. Additionally, PPAR-α activators decrease plasma triglyceride-rich lipoproteins levels by increasing the activity of the enzyme lipoprotein lipase (LPL) (Daniel et al., 2004). PPAR-α agonists directly increase transcriptional activity of the LPL gene promoter (Schoonjans et al., 1996) and indirectly reduce the levels of apoC-III, an inhibitor of LPL activity (Staels et al., 1995). The latter action of increasing HDL cholesterol levels is partly mediated by increasing hepatic production of apoA-I (Vu-Dac et al., 1998) and apoA-II (Vu-Dac et al., 1995), which are the two major components of HDL. Similarly, in this study, we found that CM108 could activate PPAR-α in the transactivation assay in vitro. All the research findings corroborated our conclusion that CM108 was shown a dose-dependently curve for biosynthesis of apoA-I, apoA-II and apoC-III respectively, CM108 enhanced apoA-I and apoA-II production, whereas CM108 reduced apoC-III production at the same concentration in vitro.

PPAR-γ, another member of the PPAR family, is most highly expressed in adipose tissue and has been shown to be essential for adipocyte differentiation and normal glucose metabolism (Spiegelman and Flier, 2001). Recent evidence indicates that in vivo PPAR-γ activators protect against atherosclerosis but do not up-regulate ABCA1. By contrast, they induced macrophage ABCG1 and cholesterol efflux to HDL, indicating that this might be a key mechanism of protection by this class of drugs (Li et al., 2004). Several studies report that activation of both PPAR-α and PPAR-γ can inhibit NF-κB signaling and suppress the secretion of various pro-inflammatory cytokines in vitro, and therefore PPAR-α, PPAR-γ activators decreased

atherosclerosis, whereas PPAR-δ activators did not in vivo (Moore et al., 2001; Chakrabarti et al., 2004; Li et al., 2004). In this study, CM108 was found that it could significantly activate PPAR-γ, maybe CM108 can exert its potential partly through inducing macrophage ABCG1 expression and cholesterol efflux to HDL or inhibiting the inflammation.

Liver X receptors are also ligand-activated transcription factors that belong to the family of nuclear receptors. Two isoforms, liver X receptor α and β, have been identified and have described as crucial regulators of genes involved in lipid metabolism and homeostasis (Chawla et al., 2001). Liver X receptor α is highly expressed in the liver, kidney, macrophages and intestine, whereas liver X receptor β is detectable in nearly every tissue (Joyce and David, 2002). In macrophages, liver X receptor agonists activate ABCA1, ABCG1 and ABCG4 expressions, which subsequently promote reverse cholesterol transport (Wang et al., 2004). In liver, liver X receptor target genes (ABCG5 and ABCG8) involved in cholesterol secretion into the bile, free cholesterol is either secreted directly into bile through the dual transporters ABCG5 and ABCG8 or catabolized by CYP7A1 into bile acids. Bile acids also stimulate their own transport into bile by increasing the expression of the bile salt efflux pump (ABCB11) (Joyce and David, 2002). Treatment with GW3965, a synthetic agonist of liver X receptor, has been shown to inhibit the development of atherosclerosis in mice (Joseph et al., 2002). In this study, similar to its effect on PPAR-α and PPAR-γ, CM108 can serve as an agonist for liver X receptor α and subsequently activate ABCA1 gene expression in vitro.

Furthermore, we established rat model of hyperlipidemia by feeding the rats on high-cholesterol diet and used this animal model to assess the in vivo hypolipidemic action of CM108. We observed that 100 mg/kg CM108 significantly increase HDL cholesterol levels and decrease triglyceride levels, the atherogenicity index, represented by total cholesterol/HDL ratio, was significantly reduced in 100 mg/kg CM108 group compared with the control group. Meanwhile, there were significant differences in body weight comparing 100 mg/kg CM108 group to control group, however, CM108 didn't increase the ratio of liver/body weight compared with control group after treatment.

Certainly, because the interaction patterns between drugs and nuclear receptors are varying within different species and the human hyperlipidemia syndrome exhibits its distinctive complexity, further research and in-depth studies should be taken out to ascertain whether CM108 could be applied to human.

In conclusion, the present data suggest that compound CM108 is an effective enhancer of HDL levels in vitro. Moreover, CM108 acts as a HDL-elevating and triglyceride-lowering agent in hyperlipidemic rats which maybe caused by the regulation of a series of genes, receptors and proteins related to HDL.

Acknowledgements

We appreciate G.-J. Zhang, L.-M. Wang and J.-X. Cao for their excellent technical assistance.

References

Assmann, G., Schulte, H., von Eckardstein, A., Huang, Y., 1996. High-density lipoprotein cholesterol as a predictor of coronary heart disease risk. The PROCAM experience and pathophysiological implications for reverse cholesterol transport. Atherosclerosis 124, 11–20 (Suppl.).

Chakrabarti, R., Misra, P., Vikramadithyan, R.K., Premkumar, M., Hiriyan, J., Datla, S.R., Damarla, R.K., Suresh, J., Rajagopalan, R., 2004. Antidiabetic and hypolipidemic potential of DRF 2519—a dual activator of PPAR-α and PPAR-γ. Eur. J. Pharmacol. 491, 195–206.

Chawla, A., Repa, J.J., Evans, R.M., Mangelsdorf, D.J., 2001. Nuclear receptors and lipid physiology: opening the X-files. Science 294, 1866–1870.

Daniel, H.R., Min, Li., Haydn, P., Kishor, M.V., 2004. Peroxisome Proliferator-Activated Receptor (PPAR)-α: a Pharmacological target with a promising future. Pharm. Res. 21, 1531–1537.

Forte, T.M., McCall, M.R., 1994. The role of apolipoprotein A-I-containing lipoproteins in atherosclerosis. Curr. Opin. Lipidol. 5, 354–364.

Gordon, T., Kannel, W.B., Castelli, W.P., Dawber, T.R., 1981. Lipoproteins, cardiovascular disease, and death. The Framingham Study. Arch. Intern. Med. 141, 1128–1131.

Gotto Jr., A.M., 2001. Low high-density lipoprotein cholesterol as a risk factor in coronary heart disease: a working group report. Circulation 103, 2213–2218.

Guo, L., Lian, J.H., Ji, W., Hu, W.R., Wu, G.L., Gong, B.Q., 2006. Establishment of a cell-based drug screening system for identifying selective down-regulators of mPGES-1. Inflamm. Res. 55, 114–118.

Nagao, K., Yoshida, S., Nakagiri, H., Sakono, M., Sato, M., Imaizumi, K., 1998. Gemfibrozil reduces non-high-density lipoprotein cholesterol in exogenously hypercholesterolemic (ExHC) rats fed a high-cholesterol diet. Comp. Biochem. Physiol., B 120, 579–586.

Joel, P.B., Taro, E.A., Peter, T.M., 2005. PPARs: therapeutic targets for metabolic disease. Trends Pharmacol. Sci. 26, 244–251.

Joseph, S.B., McKilligin, E., Pei, L., Watson, M.A., Collins, A.R., Laffitte, B.A., Chen, M., Noh, G., Goodman, J., Hagger, G.N., Tran, J., Tippin, T.K., Wang, X., Lusis, A.J., Hsueh, W.A., Law, R.E., Collins, J.L., Willson, T.M., Tontonoz, P., 2002. Synthetic LXR ligand inhibits the development of atherosclerosis in mice. Proc. Natl. Acad. Sci. U. S. A. 99, 7604–7609.

Joyce, J.R., David, J.M., 2002. The liver X receptor gene team: potential new players in atherosclerosis. Nat. Med. 8, 1243–1248.

Kersten, S., 2002. Peroxisome proliferator activated receptors and obesity. Eur. J. Pharmacol. 440, 223–234.

Li, A.C., Binder, C.J., Gutierrez, A., Brown, K.K., Plotkin, C.R., Pattison, J.W., Valledor, A.F., Davis, R.A., Willson, T.M., Witztum, J.L., Palinski, W., Glass, C.K., 2004. Differential inhibition of macrophage foam cell formation and atherosclerosis in mice by PPARα, β/δ and γ. J. Clin. Invest. 114, 1564–1576.

Moore, K.J., Fitzgerald, M.L., Freeman, M.W., 2001. Peroxisome proliferator-activated receptors in macrophage biology: friend or foe? Curr. Opin. Lipidol. 12, 519–527.

Nofer, J.R., Kehrel, B., Fobker, M., Levkau, B., Assmann, G., von Eckardstein, A., 2002. HDL and arteriosclerosis: beyond reverse cholesterol transport. Atherosclerosis 61, 1–16.

Patrick, L.N., Alan, R.T., 2004. HDL as a target in the treatment of atherosclerotic cardiovascular disease. Nature 4, 193–205.

Sambrook, J., Russell, D.W., 2001. Molecular Cloning: A Laboratory Manual, 3rd ed. Cold Spring Harbor Laboratory Press.

Schoonjans, K., Peinado-Onsurbe, J., Lefebvre, A.M., Heyman, R.A., Briggs, M., Deeb, S., Staels, B., Auwerx, J., 1996. PPARα and PPARγ activators direct a distinct tissue-specific transcriptional response via a PPRE in the lipoprotein lipase gene. EMBO J. 15, 5336–5348.

Spiegelman, B.M., Flier, J.S., 2001. Obesity and the regulation of energy balance. Cell 104, 531–543.

Staels, B., Vu-Dac, N., Kosykh, V.A., Saladin, R., Fruchart, J.C., Dallongeville, J., Auwerx, J., 1995. Fibrates down-regulate apolipoprotein C-III expression independent of induction of peroxisomal acyl co-enzyme A oxidase. J. Clin. Invest. 65, 705–712.

Uittenbogaard, A., Shaul, P.W., Yuhanna, I.S., Blair, A., Smart, E.J., 2000. High density lipoprotein prevents oxidized low density lipoprotein-induced inhibition of endothelial nitricoxide synthase localization and activation in caveolae. J. Biol. Chem. 275, 11278–11283.

Van Lenten, B.J., Navab, M., Shih, D., Fogelman, A.M., Lusis, A.J., 2001. The role of high-density lipoproteins in oxidation and inflammation. Trends Cardiovasc. Med. 11, 155–161.

Vu-Dac, N., Schoonjans, K., Kosykh, V., Dallongeville, J., Fruchart, J.C., Staels, B., Auwerx, J., 1995. Fibrates increase human apolipoprotein A-II expression through activation of the peroxisome proliferator-activated receptor. J. Clin. Invest. 96, 741–750.

Vu-Dac, N., Chopin-Delannoy, S., Gervois, P., Bonnelye, E., Martin, G., Fruchart, J.C., Laudet, V., Staels, B., 1998. The nuclear receptors peroxisome proliferator-activated receptor alpha and Rev-erbalpha mediate the species-specific regulation of apolipoprotein A-I expression by fibrates. J. Biol. Chem. 273, 25713–25720.

Wang, N., Lan, D., Chen, W., Matsuura, F., Tall, A.R., 2004. ATP-binding cassette transporters G1 and G4 mediate cellular cholesterol efflux to high-density lipoproteins. Proc. Natl. Acad. Sci. U. S. A. 101, 9774–9779.

Yuhanna, I.S., Zhu, Y., Cox, B.E., Hahner, L.D., Osborne-Lawrence, S., Lu, P., Marcel, Y.L., Anderson, R.G., Mendelsohn, M.E., Hobbs, H.H., Shaul, P.W., 2001. High-density lipoprotein binding to scavenger receptor-BI activates endothelial nitric oxide synthase. Nat. Med. 7, 853–857.

J Appl Physiol 98: 981–990, 2005.
First published November 12, 2004; doi:10.1152/japplphysiol.01029.2004.

Dexamethasone treatment in the newborn rat: fatty acid profiling of lung, brain, and serum lipids

Eric D. Bruder,[1] Ping C. Lee,[2,3] and Hershel Raff[1,4]

[1]*Endocrine Research Laboratory, St. Luke's Medical Center, Milwaukee;* [2]*Departments of Pediatrics,* [3]*Pharmacology and Toxicology, and* [4]*Medicine, Medical College of Wisconsin, Milwaukee, Wisconsin*

Submitted 16 September 2004; accepted in final form 9 November 2004

Bruder, Eric D., Ping C. Lee, and Hershel Raff. Dexamethasone treatment in the newborn rat: fatty acid profiling of lung, brain, and serum lipids. *J Appl Physiol* 98: 981–990, 2005. First published November 12, 2004; doi:10.1152/japplphysiol.01029.2004.—Dexamethasone is used as treatment for a variety of neonatal syndromes, including respiratory distress. The present study utilized the power of comprehensive lipid profiling to characterize changes in lipid metabolism in the neonatal lung and brain associated with dexamethasone treatment and also determined the interaction of dexamethasone with hypoxia. A 4-day tapering-dose regimen of dexamethasone was administered at 0800 on postnatal *days 3* (0.5 mg/kg), *4* (0.25 mg/kg), *5* (0.125 mg/kg), and *6* (0.05 mg/kg). A subgroup of rats was exposed to hypoxia from birth to 7 days of age. Dexamethasone treatment elicited numerous specific changes in the lipid profile of the normoxic lung, such as increased concentrations of saturated fatty acids in the phosphatidylcholine and cholesterol ester classes. These increases were more profound in the lungs of hypoxic pups. Additional increases in cardiolipin concentrations were also measured in lungs of hypoxic pups treated with dexamethasone. We measured widespread increases in serum lipids after dexamethasone treatment, but the effects were not equivalent between normoxic and hypoxic pups. Dexamethasone treatment in hypoxic pups increased 20:4n6 and 22:6n3 concentrations in the free fatty acid class of the brain. Our results suggest that dexamethasone treatment in neonates elicits specific changes in lung lipid metabolism associated with surfactant production, independent of changes in serum lipids. These findings illustrate the benefits of dexamethasone on lung function but also raise the potential for negative effects due to hyperlipidemia and subtle changes in brain lipid metabolism.

hypoxia; glucocorticoid therapy; neonate

INHALED AND SYSTEMIC GLUCOCORTICOIDS have been widely used to treat syndromes of perinatal distress, many of which have an inflammatory component requiring pharmacological therapy (3, 7, 23, 25, 53). Dexamethasone, a highly potent glucocorticoid, has been the treatment of choice for neonates who are hypoxic due to cardiopulmonary conditions such as bronchopulmonary dysplasia (2, 13, 33, 46, 50). A major motivation for this therapy is the promotion of surfactant production and lung maturation and to induce closure of the ductus arteriosus (6, 34, 43, 45, 47). Dexamethasone decreases the duration of ventilatory support and lowers the incidence of chronic lung disease (13, 23, 33, 50).

Dexamethasone therapy, however, may lead to unfavorable long-term sequelae, including decreases in neuromotor and cognitive function (4, 15, 30, 36, 37, 55), and may also lead to left ventricular abnormalities and metabolic dysfunction (5, 14, 17, 24). A report of lipid intolerance in infants treated with dexamethasone highlights this potential for long-term metabolic dysfunction (2). It is for these reasons that the use of dexamethasone in neonates is decreasing (39) and that its use as a primary defense against the development of chronic lung disease is now being questioned (4). However, some of the short-term benefits of dexamethasone may outweigh the long-term risks (33).

The pathophysiology of and adaptation to neonatal hypoxia has been a subject of intense investigation (18–20, 31, 35, 41, 49). We have recently shown that hypoxia induces specific alterations in the lipid and fatty acid profiles of the adrenal gland and liver (8, 9). These studies have greatly benefited from the power of comprehensive lipid profiling, through which it is possible to analyze the concentrations of specific fatty acid metabolites in distinct lipid classes (51, 52). This method also allows the evaluation of the metabolic interaction of dexamethasone and hypoxia in the neonate (9).

The goal of the present study was to assess changes in lipid metabolism in the lung and brain associated with dexamethasone treatment, utilizing comprehensive lipid profiling. Furthermore, we used our model of neonatal hypoxia as a classic perturbation for which dexamethasone is used as treatment. We hypothesize that dexamethasone-induced changes in lung and brain lipid composition occur independently of changes in serum lipids. Our specific aims were to *1*) analyze the effects of dexamethasone on the comprehensive lipid profile of the lung, *2*) analyze the effects of hypoxia on lung lipid composition, *3*) examine the effects of dexamethasone on the hypoxic lung, and *4*) assess the effects of dexamethasone and/or hypoxia on the lipid composition of the brain and serum.

METHODS

Animal treatment. All experimentation was approved by the Institutional Animal Care and Use Committees of the Medical College of Wisconsin and St. Luke's/Aurora Sinai Medical Center. Timed pregnant Sprague-Dawley rats (Harlan Sprague Dawley, Indianapolis, IN; $n = 8$) were obtained at 14 days gestation and maintained on a standard sodium diet (Richmond Standard 5001, Brentwood, MO) and water ad libitum in a controlled environment (lights on, 0600–1800). Parturition usually occurred on the afternoon of gestational *day 22*, during which time rats were kept under observation. After litters were completely delivered, litter size was equalized by cross fostering, and the dam and pups (~13 per litter; mixed sexes) were immediately exposed to normobaric hypoxia (12% O_2) or kept in room air as control (21% O_2), as described previously (40, 41). We have previously shown that this exposure leads to arterial Po_2 levels in

Address for reprint requests and other correspondence: H. Raff, Endocrinology, St. Luke's Physician's Office Bldg., 2801 W. KK River Pkwy., Suite 245, Milwaukee, WI 53215 (E-mail: hraff@mcw.edu).

The costs of publication of this article were defrayed in part by the payment of page charges. The article must therefore be hereby marked "*advertisement*" in accordance with 18 U.S.C. Section 1734 solely to indicate this fact.

adults of ~50–55 Torr with sustained hypocapnia and alkalosis (40, 42).

Lactating dams were maintained with their litters for 7 days in a hypoxic or normoxic environment (49). Dexamethasone phosphate (Sigma, St. Louis, MO) was administered subcutaneously in a tapering regimen to normoxic and hypoxic pups at 0800 as follows: postnatal *days 3* (0.5 mg/kg), *4* (0.25 mg/kg), *5* (0.125 mg/kg), and *6* (0.05 mg/kg) (15). Control pups were injected with saline. Pups were weighed on each day of injection. At 0800 on postnatal *day 7*, dams were removed from the chambers. Pups were quickly decapitated, and lung and brain tissue were quickly washed to remove any remaining blood and immediately snap frozen in liquid N_2 ($n = 4$ pups/treatment group). Blood from each pup was immediately centrifuged for 5 s at room temperature, and the serum was quickly frozen on dry ice. Serum from two additional pups from the same treatment group was sequentially added to the previously frozen sample (on dry ice) to pool the serum from three pups ($n = 4$ pooled samples/treatment group). Samples were obtained from pups from four normoxic (with or without dexamethasone) and four hypoxic (with or without dexamethasone) litters.

Lipid profiling. A comprehensive assessment of lung, brain, and serum lipid profiles was performed (Lipomics Technologies, West Sacramento, CA). Brain and lung tissue (50 mg) and serum (200 μl) lipids were extracted in the presence of internal standards by the method of Folch et al. using chloroform:methanol (2:1 vol/vol) (16). Individual lipid classes from each extract were separated by preparative thin-layer chromatography, as described previously (51, 52). Authentic lipid class standards were spotted on the two outside lanes of the thin-layer chromatography plate to enable localization of the sample lipid classes. Lipid fractions were scraped from the plate and transesterified in 3 N methanolic-HCl in a sealed vial under a N_2 atmosphere at 100°C for 45 min. The resulting fatty acid methyl esters were extracted with hexane containing 0.05% butylated hydroxytoluene and prepared for gas chromatography by sealing the extracts under N_2. Fatty acid methyl esters were separated and quantified by capillary gas chromatography using a gas chromatograph (Hewlett-Packard model 6890, Wilmington, DE) equipped with a 30-m DB-225MS capillary column (J & W Scientific, Folsom, CA) and a flame-ionization detector, as described previously (51, 52). Intra-assay coefficients of variation were as follows: cholesterol ester (CE; 2.0%), diglyceride (DG; 5.5%), free fatty acid (FFA; 3.5%), lysophosphatidylcholine (LPC; 12.2%), phosphatidylcholine (PC; 5.0%), sphingomyelin (SM; 11.4%), phosphatidylethanolamine (PE; 13.0%), and triglyceride (TG; 0.4%). Assay sensitivity was set at 0.1 μmol/g because concentrations below this value increased the analytic variability to >20%.

Statistical analyses. Fatty acid/lipid profile data obtained were quantitative (nmol fatty acid/g of tissue or serum). Significance of differences between vehicle-treated and dexamethasone-treated samples, normoxic and hypoxic samples, or a combination of the two interventions were assessed by unpaired Student's *t*-tests ($P < 0.05$). This statistical approach has been validated for this type of metabo-

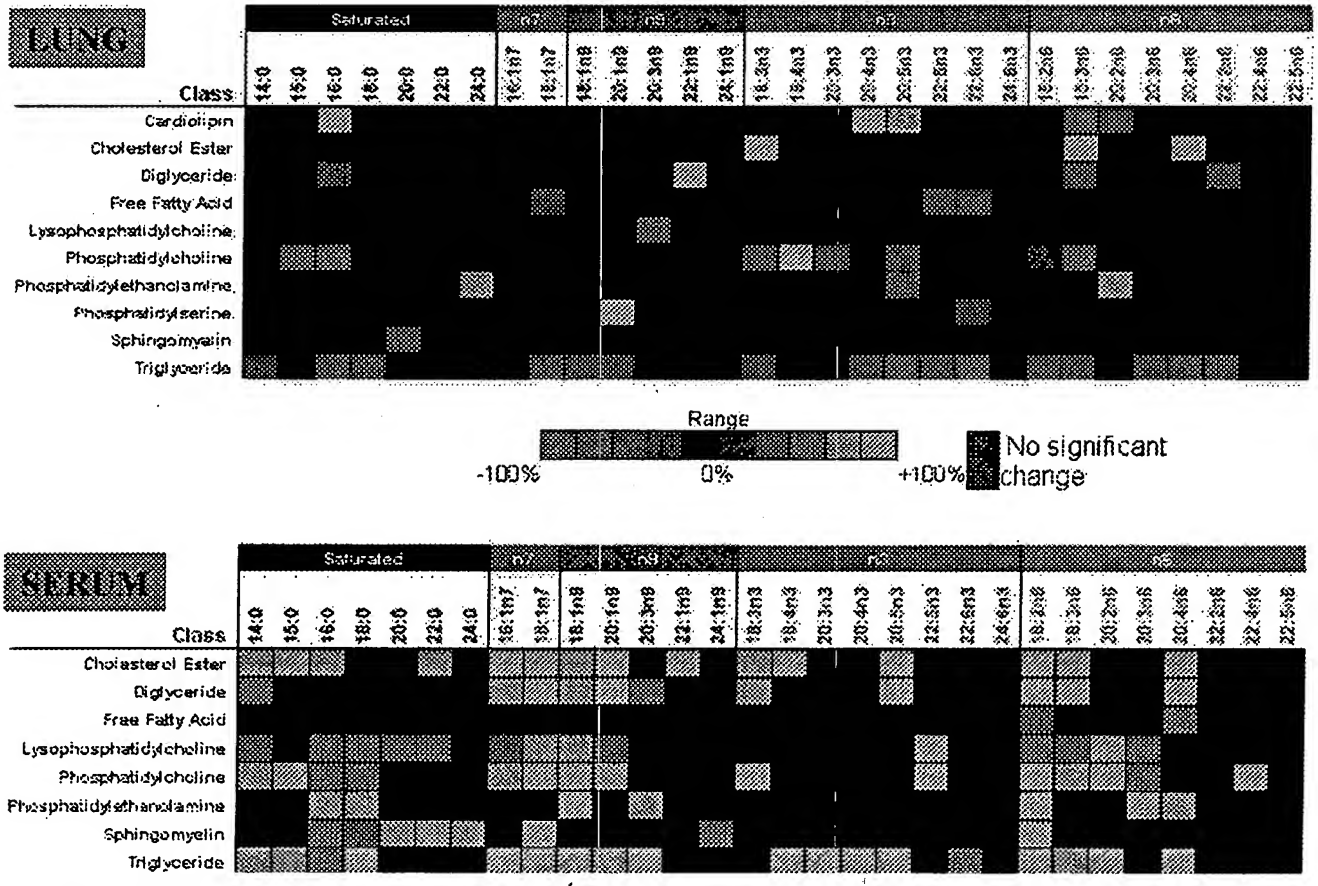

Fig. 1. Effects of dexamethasone treatment on the concentrations of individual fatty acid metabolites in lung tissue (*top*) and serum (*bottom*) of neonatal rats. Heat map showing individual fatty acid metabolite concentrations, as they appear in each lipid class, in lung tissue and serum of normoxic 7-day-old rats treated with a tapering dose regimen of dexamethasone ($n = 4$ rats/treatment). Quantitative data were used to calculate the percent increase (green squares) or decrease (red squares) of each measurement from the vehicle-treated control. Significance of differences was analyzed by *t*-test, with colors denoting $P < 0.05$. Differences not meeting $P < 0.05$ are shown in black. Cardiolipin and phosphatidylserine were only measured in the lung.

lomic analysis (51, 52). Quantitative data were visualized using the Lipomics Surveyor software system. The system creates a "heat map" graph for significant differences between samples. The heat map displays statistically significant increases from control values as green or yellow squares and statistically significant decreases as red or blue squares. The brightness of each individual square denotes the magnitude of the difference, as displayed with each of the heat maps. Differences not meeting $P < 0.05$ are shown in black. Data not presented in heat map form are expressed as means ± SE, and significance of differences was assessed by two-way ANOVA and Student-Newman-Keuls method for multiple comparisons ($P < 0.05$). Fatty acid ratios were calculated from individual sample measurements. The mean ratio, across all lipid classes, from each replicated treatment ($n = 4$ per group) was treated as one datum. Lipid class ratios were calculated from individual sample measurements, and the mean ratio from each replicated treatment ($n = 4$ per group) was treated as one datum.

RESULTS

Dexamethasone: effects on normoxic lung and serum lipid profiles. The effects of dexamethasone treatment per se on the lung and serum lipid profiles in normoxic pups are shown in Fig. 1. The column headers indicate fatty acid metabolites as they appear in each distinct lipid class (rows). First, notice the greater number of significant changes in the serum profile compared with that of the lung. Dexamethasone decreased the concentration of a number of fatty acid metabolites in the TG class ($P < 0.05$) of the lung. Treatment with dexamethasone increased the concentrations of several fatty acids in the PC class (e.g., 16:0, 18:3n3, 20:5n3, and 18:2n6), the cardiolipin (CL) class (e.g., 16:0 and 20:5n3), and the CE class (e.g., 18:3n3 and 20:4n6) ($P < 0.05$) of the lung. Dexamethasone also elicited a number of specific changes in the remaining lipid classes of the lung, including DG, FFA, LPC, PE, phosphatidylserine (PS) and SM. Dexamethasone caused widespread increases in fatty acid concentrations in the serum of normoxic pups, with increases in at least three fatty acids in all lipid classes ($P < 0.05$) except FFA. Major fatty acid metabolites, such as 16:0, 18:0, 16:1n7, 18:1n9, 18:2n6, and 20:4n6, were increased in several lipid classes of the serum, including the CE, DG, LPC, PC, PE, and SM classes ($P < 0.05$). The concentration of 18:2n6 was increased in every lipid class analyzed ($P < 0.05$). Dexamethasone treatment had the fewest effects on the n3 fatty acids (across all classes). Differences not meeting $P < 0.05$ are shown in black.

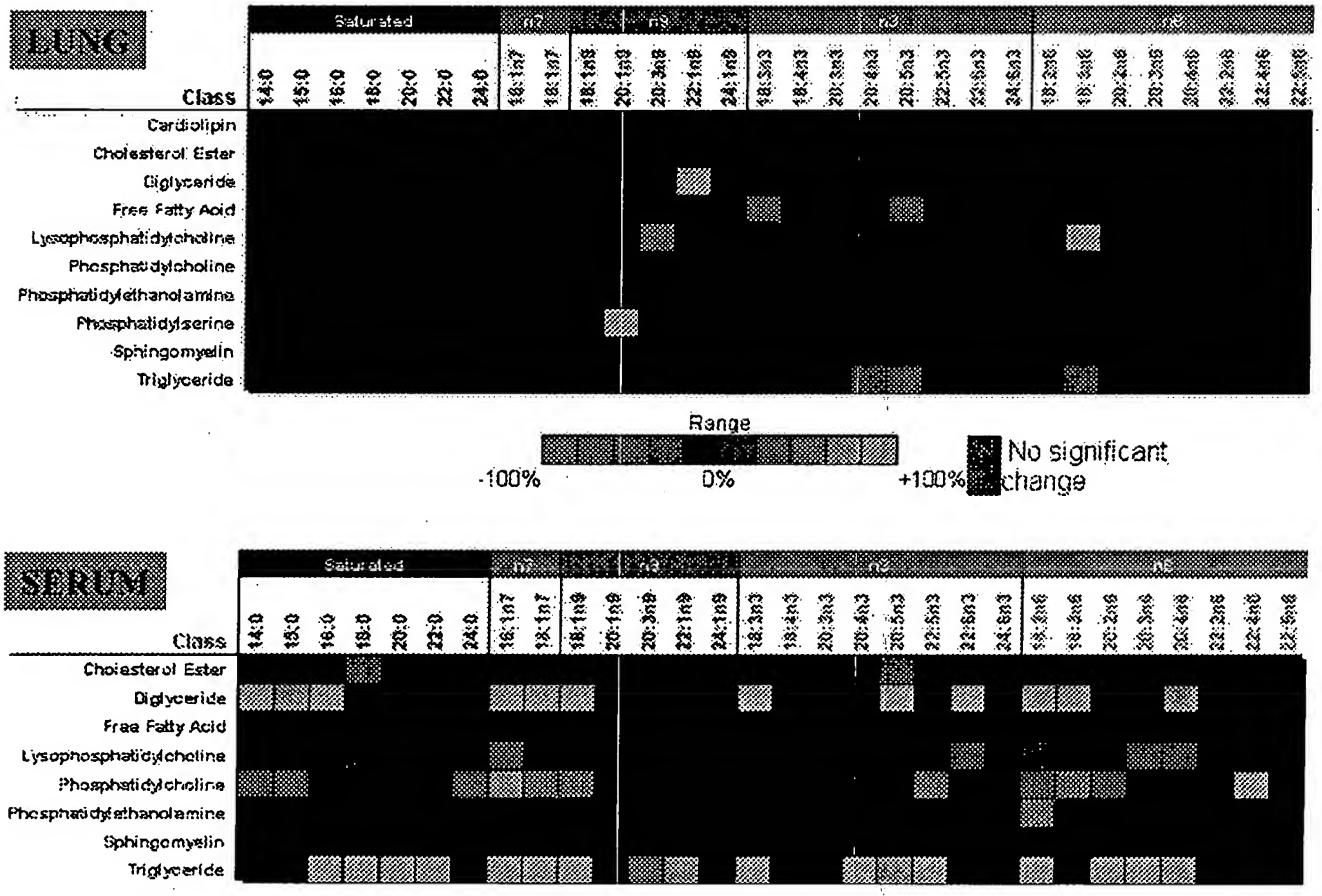

Fig. 2. Effects of hypoxia from birth on the concentrations of individual fatty acid metabolites in lung tissue (*top*) and serum (*bottom*) of neonatal rats. Heat map showing individual fatty acid metabolite concentrations, as they appear in each lipid class, in lung tissue and serum of 7-day-old rats exposed to hypoxia from birth ($n = 4$ rats/treatment). Quantitative data were used to calculate the percent increase (green squares) or decrease (red squares) of each measurement from the normoxic control. Significance of differences was analyzed by *t*-test, with colors denoting $P < 0.05$. Differences not meeting $P < 0.05$ are shown in black. Cardiolipin and phosphatidylserine were only measured in the lung.

Hypoxia: effects on lung and serum lipid profiles. Figure 2 depicts the effects of hypoxia per se on lipid profiles in lung tissue and serum. Again note the abundance of changes in the serum profile compared with the lung; hypoxia had minimal effects on the lipid profile of the neonatal lung. The concentration of 20:5n3 was decreased in the FFA and TG classes, whereas the concentration of 18:3n3 was decreased only in the FFA class in the lung ($P < 0.05$). In the serum, hypoxia caused significant increases in most major fatty acid metabolites of the TG class, encompassing all fatty acid families measured ($P < 0.05$). Several metabolites in the DG class of serum were increased by hypoxia (e.g., 16:0, 16:1n7, 18:1n9, 22:6n3, and 20:4n6) ($P < 0.05$). Hypoxia also increased the concentrations of several fatty acids in the PC class (e.g., 14:0, 16:1n7, 18:1n9, and 18:2n6) ($P < 0.05$). Decreases in fatty acid concentrations in the serum of hypoxic pups were measured in the CE class (e.g., 16:0, 20:5n3, and 20:4n6) and the LPC class (e.g., 18:0, 22:6n3, 18:2n6, and 20:4n6) ($P < 0.05$).

Dexamethasone: effects on hypoxic lung and serum lipid profiles. The effects of dexamethasone on the lipid profiles of lung tissue and serum of hypoxic pups compared with vehicle-treated hypoxic pups are depicted in Fig. 3. Although hypoxia by itself had little effect, dexamethasone treatment in hypoxic pups had profound effects on the lung lipid profile. Dexamethasone elicited increases in many of the fatty acid metabolites in the CL class (e.g., 16:0, 18:0, 18:1n9, 22:6n3, and 18:2n6) in addition to those in the PC class (e.g., 16:0, 18:3n3, 22:6n3, and 20:4n6) ($P < 0.05$). The lungs of hypoxic pups treated with dexamethasone also exhibited decreases in the TG class (e.g., 16:0, 18:1n9, 20:5n3, and 20:4n6) ($P < 0.05$). Other isolated changes were measured in the CE, FFA, PE, PS, and SM classes (all $P < 0.05$). Treatment of hypoxic pups with dexamethasone increased the serum concentration of numerous metabolites in the CE class (e.g., 16:0, 16:1n7, 18:1n9, 20:5n3, and 20:4n6) and elicited various increases in the LPC, PC, and SM classes ($P < 0.05$). Dexamethasone treatment in hypoxic pups also decreased the concentrations of various fatty acid metabolites in the TG, DG, PC, and PE classes (all $P < 0.05$).

Dexamethasone: effects on major fatty acids in the normoxic and hypoxic lung. Figure 4 depicts the effects of dexamethasone on the concentrations of major fatty acid metabolites, across all lipid classes, in lung tissue of normoxic and hypoxic pups. Dexamethasone elicited a decrease in the concentration of 18:1n9 in normoxic ($P < 0.02$) and hypoxic ($P < 0.05$) lung

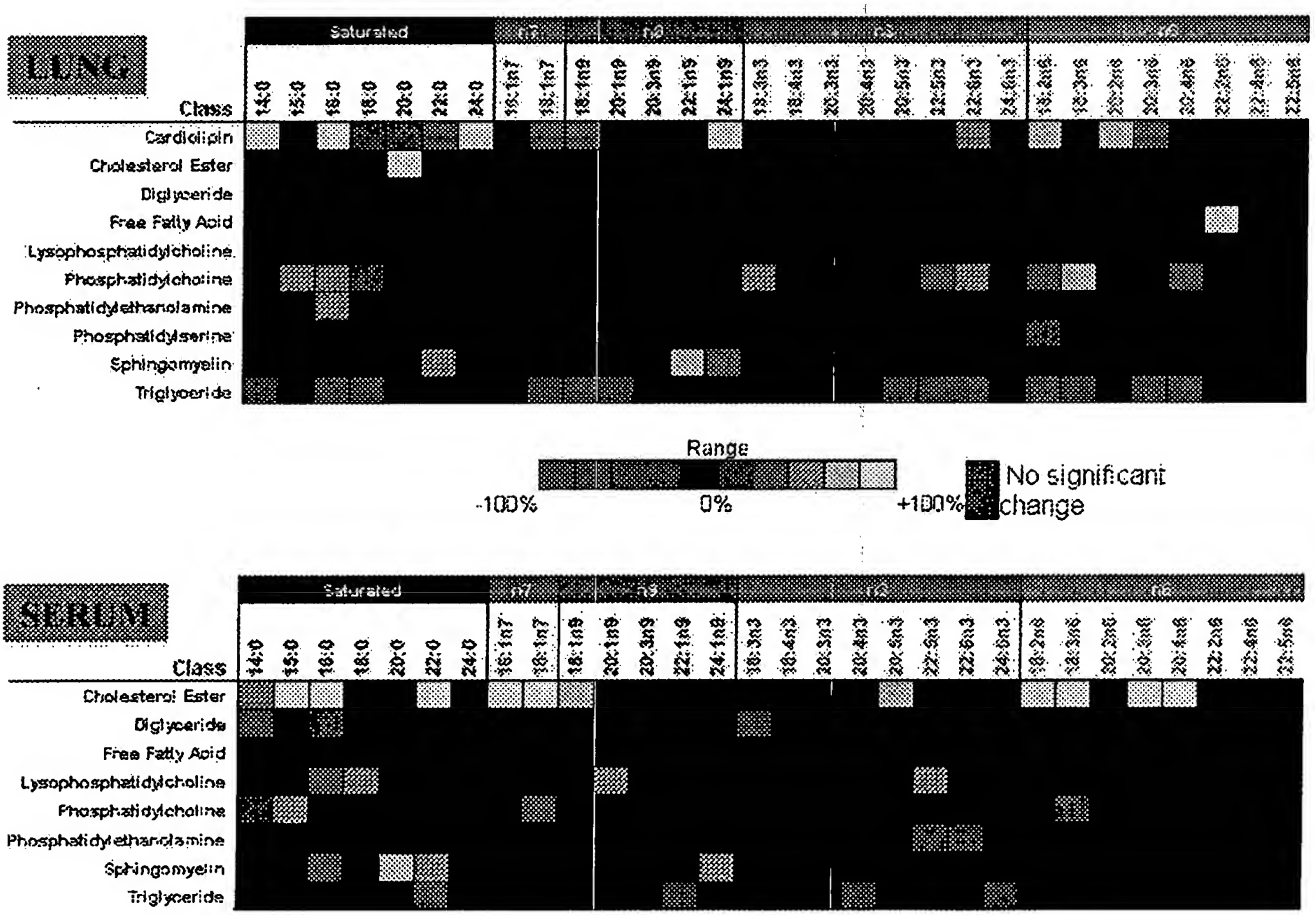

Fig. 3. Effects of dexamethasone treatment on the concentrations of individual fatty acid metabolites in lung tissue (*top*) and serum (*bottom*) of neonatal rats exposed to hypoxia from birth. Heat map showing individual fatty acid metabolite concentrations, as they appear in each lipid class, in lung tissue and serum of 7-day-old rats exposed to hypoxia from birth and treated with a tapering dose regimen of dexamethasone ($n = 4$ rats/treatment). Quantitative data were used to calculate the percent increase (yellow squares) or decrease (blue squares) of each measurement from the vehicle-treated hypoxic samples. Significance of differences was analyzed by *t*-test, with colors denoting $P < 0.05$. Differences not meeting $P < 0.05$ are shown in black. Cardiolipin and phosphatidylserine were only measured in the lung.

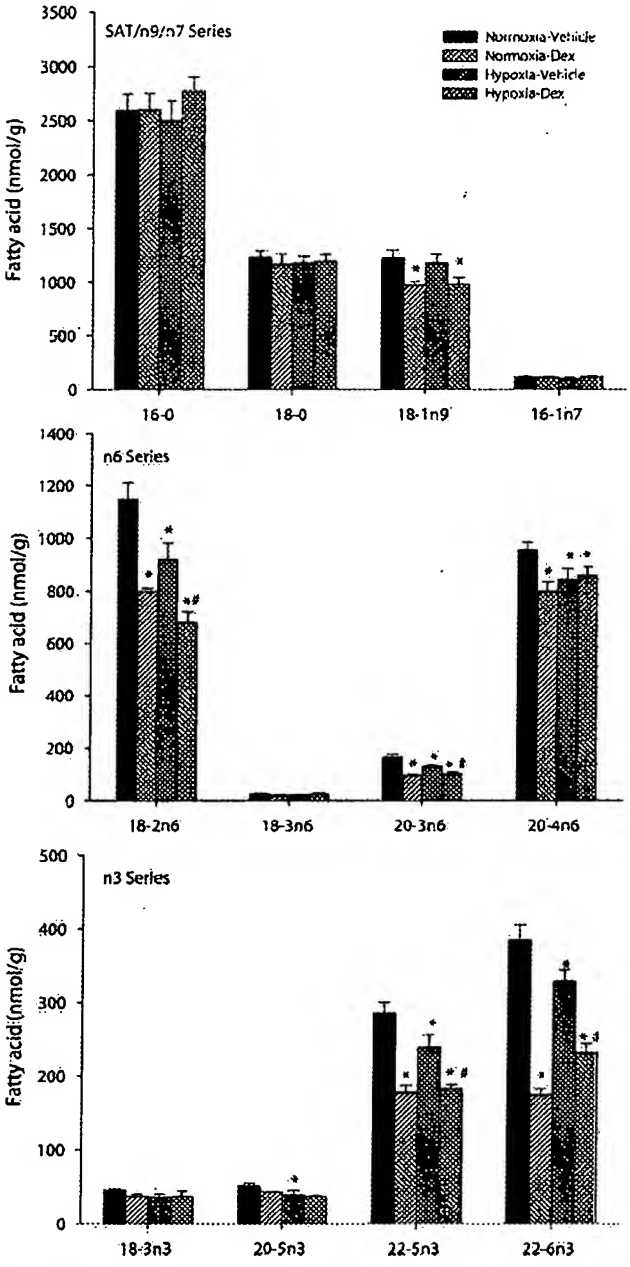

Fig. 4. Effects of dexamethasone treatment on the concentrations of specific fatty acid metabolites in lung tissue of normoxic and hypoxic neonatal rats. *Top*: concentrations of metabolites belonging to the saturated and n9 families. Note that 16:1n9 was not assessed in the lipid profile. *Middle*: metabolites of the n6 family. *Bottom*: metabolites of the n3 family. Fatty acid concentrations were obtained by lipid profiling (n = 4 rats/treatment). The concentration of each metabolite is the mean concentration across all lipid classes measured. *Significant difference from normoxia-vehicle ($P < 0.05$). #Significant difference from hypoxia-vehicle ($P < 0.05$).

tissue when compared with normoxic pups treated with vehicle. Hypoxia had no effect on 16:0, 18:0, 18:1n9, or 16:1n7 in the lung ($P > 0.05$). Figure 4, *middle*, shows four major fatty acids belonging to the n6 series. Lung tissue of normoxic pups treated with dexamethasone had decreased concentrations of 18:2n6 ($P < 0.001$), 20:3n6 ($P < 0.001$), and 20:4n6 ($P < 0.008$). Hypoxia by itself caused significant decreases in 18:2n6 ($P < 0.008$), 20:3n6 ($P < 0.006$), and 20:4n6 ($P < 0.04$). Dexamethasone treatment in hypoxic pups resulted in further decreases in 18:2n6 ($P < 0.006$) and 20:3n6 ($P < 0.01$) in lung tissue compared with hypoxic pups treated with vehicle. The concentrations of four major n3 fatty acids are depicted in Fig. 4, *bottom*. Dexamethasone decreased the concentrations of 22:5n3 ($P < 0.001$) and 22:6n3 ($P < 0.001$) in lung tissue of normoxic pups. Hypoxia also caused decreases in the concentrations of 22:5n3 ($P < 0.02$) and 22:6n3 ($P < 0.02$), as well as in the concentration of 20:5n3 ($P < 0.05$). Dexamethasone treatment in hypoxic pups further decreased the concentrations of 22:5n3 ($P < 0.009$) and 22:6n3 ($P < 0.001$).

Dexamethasone: effects on normoxic and hypoxic lung and serum lipid classes. Table 1 summarizes the interaction of dexamethasone treatment with hypoxia on lipid class concentrations in lung tissue and serum. The lungs of normoxic pups treated with dexamethasone showed increases in CE and PC ($P < 0.02$), as well as a large decrease in TG ($P < 0.001$). Hypoxia by itself had no effect on any of the measured lipid classes in the lung ($P > 0.05$). Dexamethasone treatment in hypoxic pups increased the concentrations of PC and CL ($P < 0.001$) in the lung but decreased the TG concentration more than twofold ($P < 0.001$) compared with hypoxic pups treated with vehicle. Nearly all serum phospholipid classes measured were increased by dexamethasone treatment in normoxic pups. These include increases in LPC ($P < 0.001$), PE ($P < 0.001$), PC ($P < 0.001$), and SM ($P < 0.005$). Dexamethasone also caused increases in the serum concentrations of TG ($P < 0.008$) and CE ($P < 0.001$) in normoxic pups. Hypoxia alone caused increases in the serum concentrations of DG and TG ($P < 0.001$). Dexamethasone treatment in hypoxic pups caused increases in serum CE ($P < 0.001$), LPC ($P < 0.004$), and SM ($P < 0.05$) concentrations and decreases in DG ($P < 0.02$) and TG ($P < 0.03$) compared with hypoxic pups treated with vehicle.

Dexamethasone: effects on normoxic and hypoxic PC- and TG-associated fatty acids in the lung. Table 2 highlights the effects of dexamethasone on specific fatty acid concentrations in the PC and TG classes of normoxic and hypoxic lung tissue. In the PC class of normoxic lung tissue, dexamethasone increased the concentrations of 16:0 ($P < 0.005$), 18:2n6 ($P < 0.02$), and 20:5n3 ($P < 0.04$) and also increased the total concentration of saturated fatty acids ($P < 0.02$) in this lipid class. Hypoxia alone had no significant effects on any fatty acid concentrations in the PC class ($P > 0.05$). However, dexamethasone treatment in hypoxic pups increased the concentrations of 14:0 ($P < 0.03$), 16:0 ($P < 0.001$), 16:1n7 ($P < 0.02$), total saturated fatty acids ($P < 0.001$), 18:2n6 ($P < 0.003$), and 20:5n3 ($P < 0.02$) in the PC class. In the TG class of normoxic lung tissue, dexamethasone decreased the concentrations of 14:0 ($P < 0.02$), 16:0 ($P < 0.001$), total saturated fatty acids ($P < 0.001$), 18:2n6 ($P < 0.001$), and 20:5n3 ($P < 0.001$). Hypoxia by itself decreased the concentrations of 18:2n6 ($P < 0.01$) and 20:5n3 ($P < 0.001$) in the TG class. Treatment with dexamethasone elicited significant decreases in the concentrations of 14:0 ($P < 0.01$), 16:0 ($P < 0.001$), total saturated fatty acids ($P < 0.001$), 18:2n6 ($P < 0.001$), and 20:5n3 ($P < 0.003$) in the TG class of hypoxic lung tissue compared with hypoxic pups treated with vehicle.

Table 1. *Effects of dexamethasone and/or hypoxia on lipid class concentrations in lung and serum of neonatal rats*

Lipid Class	Normoxia-Vehicle	Normoxia-Dex	Hypoxia-Vehicle	Hypoxia-Dex
Lung, nmol/g				
CE	2,491±176	3,643±377*	2,535±303	2,665±241
TG	10,459±830	4,094±186*	8,374±953	3,411±493*†
PC	9,901±401	12,464±781*	10,252±638	14,445±745*†
CL	1,358±85	1,697±111	1,426±113	2,121±143*†
Serum, nmol/g				
CE	1,918±39	3,531±44*	1,664±81	3,059±132*†
DG	110±6	159±15	235±28*	159±19†
TG	3,155±205	5,782±424*	9,043±1810*	5,673±313*†
LPC	527±19	729±5*	463±5	574±39†
PE	952±36	1,402±27*	983±37	1,080±63
PC	3,767±160	5,964±373*	4,212±171	4,566±384
SM	305±28	439±19*	287±13	374±40†

Values are means ± SE. CE, cholesterol ester; DG, diglyceride; TG, triglyceride; LPC, lysophosphatidylcholine; PE, phosphatidylethanolamine; PC, phosphatidylcholine; SM, sphingomyelin; CL, cardiolipin. DG, LPC, PE, and SM concentrations in lung tissue were not affected by dexamethasone (Dex) or hypoxia. CL concentrations were not measured in serum. *Significant difference from Normoxia-Vehicle; $P < 0.05$ ($n = 4$). †Significant difference from Hypoxia-Vehicle: $P < 0.05$.

Dexamethasone: effects on lipid and fatty acid ratios in the normoxic and hypoxic lung. Table 3 shows the effects of dexamethasone on lipid and fatty acid ratios in lung tissue. In normoxic pups, dexamethasone decreased the TG-to-FFA ($P < 0.005$) and TG-to-PC ($P < 0.001$) ratios and also increased the CL-to-DG ($P < 0.03$) and CE-to-FFA ($P < 0.02$) ratios. Dexamethasone increased the saturated-to-unsaturated fatty acid ratio within the CL ($P < 0.02$) and PC ($P < 0.003$) classes of normoxic lung tissue. The only significant effect of hypoxia was to decrease the TG-to-PC ($P < 0.04$) ratio. Treatment of hypoxic pups with dexamethasone, compared with hypoxic pups treated with vehicle, elicited decreases in the TG-to-FFA ($P < 0.02$) and TG-to-PC ($P < 0.001$) ratios. Dexamethasone also increased the ratios of CL to DG ($P < 0.002$), 16:0 to 18:0 (an indicator of elongase activity; $P < 0.05$), and 18:3n3 to 20:5n3 (an indicator of Δ5 and Δ6 desaturase activity; $P < 0.04$) in hypoxic lung tissue. The ratio of saturated to unsaturated fatty acids in the CL ($P < 0.001$) and PC ($P < 0.004$) classes was also increased by dexamethasone. The 18:0-to-18:1n9 (an indicator of Δ9 desaturase activity) and 18:2n6-to-20:4n6 (an indicator of Δ5 and Δ6 desaturase activity) ratios were not significantly affected by dexamethasone or hypoxia ($P > 0.05$; data not shown).

Dexamethasone: effects on the normoxic and hypoxic lipid profile of the brain. The effects of dexamethasone on the brain lipid profile of normoxic and hypoxic pups are shown in Table 4. Dexamethasone treatment in normoxic pups elicited increases in FFA (e.g., 14:0 and 20:4n6), PE (20:2n6), and PS (20:2n6) classes ($P < 0.05$). Hypoxia alone increased the concentration of 20:2n6 in the PE class, increased 22:5n3 and 20:3n6 in the TG class, and decreased the concentration of 18:1n7 in the PS class ($P < 0.05$). Dexamethasone treatment in hypoxic pups elicited increases in DG (18:1n7), FFA (e.g. 22:6n3 and 20:4n6), PC (20:2n6), PE (18:1n7 and 20:3n9), and PS (20:3n9 and 20:3n6) ($P < 0.05$). The brains of hypoxic pups treated with dexamethasone also had decreased concentrations of 20:3n9 in the TG class ($P < 0.05$).

DISCUSSION

The use of comprehensive lipid profiling has led to the development of a highly detailed metabolic characterization of

Table 2. *Effects of dexamethasone and/or hypoxia on fatty acid concentrations in the phosphatidylcholine and triglyceride fractions of lungs from neonatal rats*

Fatty Acid	Normoxia-Vehicle	Normoxia-Dex	Hypoxia-Vehicle	Hypoxia-Dex
Phosphatidylcholine				
14:0	1,433±129	1,786±259	1,711±136	2,519±286*†
16:0	8,728±485	12,775±781*	9,430±728	14,787±1,145*†
Total saturated	11,926±571	16,332±1150*	12,848±915	19,332±1,382*†
16:1n7	283±29	370±17	290±28	408±43*†
18:2n6	1,638±76	1,953±99*	1,594±52	2,024±85*†
20:5n3	80±7	107±5*	86±9	116±9*†
Triglyceride				
14:0	900±95	547±51*	783±112	417±69*†
16:0	8,684±629	3,068±148*	6,955±971	2,466±483*†
Total saturated	11,910±892	4,775±256*	9,894±1,307	4,192±654*†
16:1n7	451±53	303±46	282±82	264±98
18:2n6	6,040±491	2,231±89*	4,463±448*	1,440±300*†
20:5n3	239±18	84±5*	141±22*	57±12*†

Values are means ± SE; $n = 4$. "Total saturated" signifies the mean concentration of saturated fatty acids for that particular lipid class, calculated from the individual values for 14:0, 15:0, 16:0, 18:0, 20:0, 22:0, and 24:0. *Significant difference from Normoxia-Vehicle; $P < 0.05$. †Significant difference from Hypoxia-Vehicle: $P < 0.05$.

Table 3. *Effects of dexamethasone and/or hypoxia on lipid class ratios, fatty acid ratios within lipid classes, and fatty acid ratios across lipid classes in lungs from neonatal rats*

Ratio	Normoxia-Vehicle	Normoxia-Dex	Hypoxia-Vehicle	Hypoxia-Dex
Lipid class ratio,				
TG/FFA	1.52±0.24	0.75±0.08*	1.22±0.15	0.60±0.10*†
CL/DG	0.82±0.06	1.30±0.05*	0.97±0.04	1.71±0.25*†
CE/FFA	0.36±0.05	0.62±0.07*	0.38±0.06	0.47±0.05
TG/PC	1.06±0.09	0.33±0.02*	0.82±0.10*	0.24±0.04*†
Fatty acid ratio within lipid classes				
Sat/Unsat-CL	0.70±0.01	0.81±0.02*	0.75±0.02	0.92±0.05*†
Sat/Unsat-PC	1.62±0.08	2.15±0.05*	1.82±0.05	2.32±0.17*†
Fatty acid ratio across lipid classes				
16:0/18:0	2.14±0.06	2.37±0.05	2.19±0.08	2.44±0.11*†
18:2n6/20:4n6	1.22±0.07	1.42±0.08	1.15±0.04	1.08±0.05
18:3n3/20:5n3	0.63±0.03	0.81±0.07	0.79±0.08	1.20±0.22*†

Values are means ± SE; $n = 4$. FFA, free fatty acid; Sat, mean concentration of all saturated fatty acids; Unsat, mean concentration of all unsaturated fatty acids. *Significant difference from Normoxia-Vehicle; $P < 0.05$. †Significant difference from Hypoxia-Vehicle; $P < 0.05$.

tissues affected by an intervention or disease process (8, 9, 51, 52). The present study utilized this robust technology to examine the effects of dexamethasone treatment on lipid metabolism in normoxic and hypoxic neonates. The results extended previous findings in the lung with a broader and more detailed analysis of lipid composition (6, 43, 45, 47). We measured unique changes in serum lipid profiles as a result of dexamethasone treatment and/or hypoxia, the most notable being the differential effects dexamethasone had on serum TG concentrations between normoxic and hypoxic pups. We also demonstrated specific and direct actions of dexamethasone on the lung, independent of changes in serum. Finally, the subtle changes in fatty acid composition in the brain with dexamethasone may have affected development of the central nervous system.

Effects of dexamethasone on the lipid profile of the normoxic lung. Previous studies have demonstrated that dexamethasone promotes lung maturation through the stimulation of surfactant production (6, 33, 47, 50). This action of dexamethasone can be divided into at least two mechanisms: *1*) to promote the production of surfactant-associated proteins (45) and *2*) to increase the activity of choline-phosphate cytidylyltransferase, the enzyme responsible for the synthesis of PC (43). The concentration of lung PC was increased in our study, and we also found an increase in the concentration of saturated fatty acids associated with PC. Although the present analysis did not measure distinct molecular species, the observed effect of dexamethasone is likely due to increased incorporation of 16:0 into PC (6). Interestingly, dexamethasone also increased the concentration of 18:2n6 and 20:5n3 in the PC class of the lung while decreasing the total concentrations of these fatty acids across lipid classes. This is a novel finding and could play a role in lung pathology, since a previous study found that increased PC concentrations of 18:2n6 and 20:5n3 induce detrimental changes in lung function (6, 47, 53).

Table 4. *Significant effects of dexamethasone and hypoxia on fatty acid concentrations of brain lipid classes*

Lipid Class	Fatty Acid	Dex vs. Vehicle Normoxia	Dex vs. Vehicle Hypoxia	Hypoxia vs. Normoxia Vehicle
DG	18:1n7	ns	ns	+32%
FFA	14:0	+75%	ns	ns
	20:3n6	+116%	ns	+170%
	20:4n6	+74%	ns	+119%
	18:1n7	+117%	ns	+57%
	22:6n3	ns	ns	+121%
PC	20:2n6	ns	ns	+24%
PE	20:2n6	+52%	+38%	ns
	20:3n9	ns	ns	+46%
	18:1n7	ns	ns	+21%
PS	20:2n6	+32%	ns	ns
	20:3n6	ns	ns	+36%
	20:3n9	ns	ns	+46%
	18:1n7	ns	−43%	ns
TG	20:3n6	ns	+286%	ns
	20:3n9	ns	ns	−92%
	22:5n3	ns	+582%	ns

All values were considered significant ($P < 0.05$), except ns (not significant; $P > 0.05$). +, increased; −, decreased.

Dexamethasone treatment in the normoxic neonate also led to increased concentrations of CE in the lung. Surfactant lipids are composed of PC and CE species as well as anionic phospholipids (48). It has been shown that the dexamethasone-induced increase in surfactant CE is most likely due to increased delivery of very-low-density lipoprotein CE to type II pneumocytes (21). Decreases in the ratios of lung TG to FFA and TG to PC, along with an increase in the ratio of CE to FFA, suggest that dexamethasone acts by stimulating the transfer of fatty acids from the TG class to the CE and PC classes. Another novel finding was that dexamethasone increased the CL-to-DG ratio, suggesting that dexamethasone stimulates the synthesis of CL, a product of DG metabolism. We also measured an increase in the saturation of CL-associated fatty acids. CL is associated with mitochondrial functions such as proton trapping, apoptosis, and oxidative metabolism (22, 26, 28). The implications of the relationship of these findings to lung function are likely to be significant and deserve further attention.

Effects of dexamethasone on the lipid profile of the hypoxic lung. Hypoxia alone had few effects on the lipid profile of the lung and had no significant effect on any single lipid class. The effects of hypoxia were subtle and only evident on the total concentrations of specific fatty acid metabolites as they occurred across lipid classes. In fact, hypoxia decreased the concentrations of only polyunsaturated fatty acids (e.g., 18:2n6, 20:4n6, 20:5n3, and 22:6n3) throughout the lung. Fatty acids of this type may actually be detrimental to the action of surfactant in lung function (6, 47, 54); their decreased concentrations may represent an inherent mechanism by which the

hypoxic neonate alters lipid metabolism in an attempt to adapt to the environment. Hypoxia only tended to increase the concentration of PC and the saturation of PC-associated fatty acids and tended to decrease the concentration of lung TG, which could also be part of an adaptive response.

The pulmonary benefits of dexamethasone treatment in hypoxic neonates have been extensively studied (7, 13, 23, 46). Our results indicate that many of the effects of dexamethasone measured in the normoxic lung were qualitatively similar to those found in the hypoxic lung. Moreover, these effects were often more pronounced in the hypoxic lung and highlight the benefits of dexamethasone treatment in neonatal respiratory distress. Dexamethasone increased the concentration of PC and CL in the hypoxic lung and further decreased the concentration of TG (compared with vehicle-treated hypoxic pups). In the PC fraction of the hypoxic lung, dexamethasone increased the concentrations of numerous fatty acid metabolites (e.g., 16:0, 16:1n7, and 18:2n6). Perhaps the most notable change in the dexamethasone-treated hypoxic lung was the increased concentration and saturation of CL. As stated above, CL has been implicated in a variety of mitochondrial functions and is a key component of the inner mitochondrial membrane (26, 28). Increased mitochondrial CL concentrations could confer advantages at the cellular level by increasing the efficiency of oxidative phosphorylation under nonoptimal conditions, such as hypoxia (22, 28). Our findings suggest another possible beneficial effect of dexamethasone treatment in the lungs of hypoxic neonates.

Effects of dexamethasone on the serum lipid profile. Treatment of normoxic pups with dexamethasone resulted in global increases in serum lipids. We have previously reported increased serum concentrations of TG and total cholesterol after dexamethasone treatment (9). The present results extend the characterization of serum lipids and fatty acids affected by dexamethasone. Another study, which examined the effects of dexamethasone on serum lipids in neonates with bronchopulmonary dysplasia, measured increases in plasma TG and FFA (2). Interestingly, the FFA class was the least affected in our study. The dexamethasone-induced increases in serum TG and CE are likely due to the stimulation of very-low-density lipoprotein synthesis and secretion by the liver (38), which may have contributed to changes in CE concentrations in the lung (21). Dexamethasone also induced increases in serum PC concentrations, which may have contributed to the increase in lung PC. However, the twofold-greater concentration of PC in the lung (compared with the serum) suggests a direct effect on the lung itself, as described previously (6, 43, 45, 47).

We and others have previously shown that hypoxia in neonates leads to increased serum TG concentrations (9, 12, 18, 20, 29). Hypoxia may modulate the function of enzymes associated with TG synthesis and degradation (12, 38). The only significant effect of hypoxia on serum lipids, besides increased TG, was an increase in DG. A small component of the increase in DG could be explained by changes in dietary intake (10), since our experimental approach requires hypoxic exposure of the dam. Dexamethasone treatment in hypoxic pups did not mimic the effects observed in serum of normoxic pups. The concentrations of CE, LPC, and SM were increased by dexamethasone in serum from normoxic and hypoxic pups. Dexamethasone decreased the concentration of serum TG in the hypoxic pups (compared with vehicle-treated hypoxic pups), an effect opposite of that found in normoxic pups. This finding is at variance with previous results from our laboratory, which found serum TG in the hypoxic pup to be further increased by dexamethasone (9). This discrepancy between studies is likely the result of sample handling and/or assay methodology; the previous study utilized a colorimetric assay to measure TG (9).

Effects of dexamethasone on brain lipid profile. Hypoxia by itself also had a minimal effect on brain lipids. This study, to our knowledge, is the first to provide a highly detailed profile of brain lipid and fatty acid concentrations after dexamethasone treatment in neonates. It is now generally accepted that neonatal dexamethasone treatment is detrimental to neurodevelopment and brain function in the long term (4, 15, 30, 36, 37, 55). The exact mechanisms through which this dysfunction develops remain uncertain. A recent study (32) found that neurite growth is dependent on increased internalization of 20:4n6 and 22:6n3, which are eventually incorporated into phospholipids. These two fatty acids have also been implicated in the proper development of the visual system (27). Although we did not detect increased concentrations of these two fatty acids in any phospholipid class, we did measure an increase in 20:4n6 in the FFA class of dexamethasone-treated normoxic pups. Likewise, hypoxic pups treated with dexamethasone had increased concentrations of 20:4n6, as well as 22:6n3, in the FFA class. The significance of these findings and how they may relate to future neural dysfunction remain unclear. Because we analyzed the brain as a whole, we could not evaluate potential changes in lipid composition in specific nuclei or brain regions.

Summary and perspectives. Dexamethasone is used to treat neonatal lung disease, which is often due to bronchopulmonary dysplasia or other inflammatory processes (2, 13, 33, 46, 50). These syndromes are often the result of premature birth. In the United States, ~12% of live births annually are preterm, providing a large population of potential candidates for dexamethasone treatment (1). The benefits of dexamethasone use in treating lung disease of prematurity are well characterized, and the main function of this treatment is to promote the production of surfactant (6, 43, 45, 47). Our results extend these findings and offer additional insight into the beneficial role dexamethasone treatment has on lung function. As with any animal model, caution must be taken when extrapolating results to human pathophysiology. For example, alveolarization of the rat lung occurs postnatally, and surfactant phospholipid metabolism differs from species to species (11, 44). Dexamethasone therapy has been shown to decrease the time sick infants require ventilation, but its overall effects on morbidity and mortality remain a point of argument (4, 39).

Although the use of dexamethasone for the treatment of neonatal illness is on the decline, there are still situations in which the benefits of treatment far outweigh the short- and long-term risks (33). A number of recent studies have shown that dexamethasone use in the neonate leads to neurological dysfunction later in life (4, 15, 30, 36, 37, 55). It is now a general consensus that, when required, the dose of dexamethasone should be reduced to the smallest effective dose (4, 42, 50). Our results indicate that the detrimental effects of dexamethasone on brain function likely do not involve short-term changes in lipid metabolism. This suggests a more subtle effect

on neurodevelopment and helps to explain why these developmental defects often do not present until adolescence (36, 55).

ACKNOWLEDGMENTS

The authors thank Barbara M. Jankowski and Peter J. Homar for expert technical assistance.

GRANTS

This study was supported in part by National Institute of Diabetes and Digestive and Kidney Diseases Grant DK-54685 to H. Raff and St. Luke's Medical Center/Aurora Health Care.

REFERENCES

1. **American College of Obstetrics and Gynecology Practice Bulletin.** Management of preterm labor. *Int J Gynecol Obstet* 82: 127–135, 2003.
2. **Amin SB, Sinkin RA, McDermott MP, and Kendig JW.** Lipid intolerance in neonates receiving dexamethasone for bronchopulmonary dysplasia. *Arch Pediatr Adolesc Med* 153: 795–800, 1999.
3. **Banks BA, Stouffer N, Cnaan A, Ning Y, Merrill JD, Ballard RA, and Ballard PL.** North American Thyrotropin-Releasing Hormone Trial Collaborators. Association of plasma cortisol and chronic lung disease in preterm infants. *Pediatrics* 107: 494–498, 2001.
4. **Baud O.** Postnatal steroid treatment and brain development. *Arch Dis Child Fetal Neonatal Ed* 89: F96–F100, 2004.
5. **Bensky AS, Kothadia JM, and Covitz W.** Cardiac effects of dexamethasone in very low birth weight infants. *Pediatrics* 97: 818–821, 1996.
6. **Bernhard W, Hoffmann S, Dobrowsky H, Rau GA, Kamlage A, Kappler M, Haitsma JJ, Freihorst J, von der Hardt H, and Poets CF.** Phosphatidylcholine molecular species in lung surfactant: composition in relation to respiratory rate and lung development. *Am J Respir Cell Mol Biol* 25: 725–731, 2001.
7. **Bolt RJ, van Weissenbruch MM, Lafeber HN, and Delemarre-van de Waal HA.** Glucocorticoids and lung development in the fetus and preterm infant. *Pediatr Pulmonol* 32: 76–91, 2001.
8. **Bruder ED, Lee PC, and Raff H.** Metabolomic analysis of adrenal lipids during hypoxia in the neonatal rat: implications in steroidogenesis. *Am J Physiol Endocrinol Metab* 286: E697–E703, 2004.
9. **Bruder ED, Lee PC, and Raff H.** Metabolic consequences of hypoxia from birth and dexamethasone treatment in the neonatal rat: comprehensive hepatic lipid and fatty acid profiling. *Endocrinology* 145: 5364–5372, 2004.
10. **Bruder ED, Lee PC, and Raff H.** Lipid and fatty acid profiles in the brain, liver, and stomach contents of neonatal rats: effects of hypoxia. *Am J Physiol Endocrinol Metab* 288: E314–E320, 2005.
11. **Burri PH.** The postnatal growth of the rat lung. 3. Morphology. *Anat Rec* 180: 77–98, 1974.
12. **Chiodi H and Whitmore S.** Lipid metabolism in suckling rat with fatty liver induced by hypoxia. *Experientia* 30: 463–465, 1974.
13. **Collaborative Dexamethasone Trial Group.** Dexamethasone therapy in neonatal chronic lung disease: an international placebo-controlled trial. *Pediatrics* 88: 421–427, 1991.
14. **De Vries WB, Van der Leij FR, Bakker JM, Kamphuis PJGH, Van Oosterhout MFM, Schipper MEI, Smid GB, Bartelds B, and Van Bel F.** Alterations in adult rat heart after neonatal dexamethasone therapy. *Pediatr Res* 52: 900–906, 2002.
15. **Flagel SB, Vazquez DM, Watson SJ, and Neal CR.** Effects of tapering neonatal dexamethasone on rat growth, neurodevelopment, and stress response. *Am J Physiol Regul Integr Comp Physiol* 282: R55–R63, 2002.
16. **Folch J, Lees M, and Sloane-Stanley GH.** A simple method for the isolation and purification of total lipids from animal tissues. *J Biol Chem* 226: 497–509, 1957.
17. **Ford LR, Willi SM, Hollis BW, and Wright NM.** Suppression and recovery of the neonatal hypothalamic-pituitary-adrenal axis after prolonged dexamethasone therapy. *J Pediatr* 131: 722–726, 1997.
18. **Frankel L and Stevenson DK.** Metabolic emergencies of the newborn: hypoxemia and hypoglycemia. *Compr Ther* 13: 14–19, 1987.
19. **Friedman AH and Fahey JT.** The transition from fetal to neonatal circulation: normal responses and implications for infants with heart disease. *Semin Perinatol* 17: 106–121, 1993.
20. **Grongnet JF.** Metabolic consequences of induced hypoxia in newborn lambs. *Ann Rech Vet* 15: 17–28, 1984.
21. **Guthmann F, Harrach-Ruprecht B, Looman AC, Stevens PA, Robenek H, and Rustow B.** Interaction of lipoproteins with type II pneumocytes in vitro: morphological studies, uptake kinetics and secretion rate of cholesterol. *Eur J Cell Biol* 74: 197–207, 1997.
22. **Haines TH and Dencher NA.** Cardiolipin: a proton trap for oxidative phosphorylation. *FEBS Lett* 528: 35–39, 2002.
23. **Halliday HL.** Postnatal steroids and chronic lung disease in the newborn. *Paediatr Respir Rev* 5: S245–S248, 2004.
24. **He J, Varma A, Weissfeld LA, and Devaskar SU.** Postnatal glucocorticoid exposure alters the adult phenotype. *Am J Physiol Regul Integr Comp Physiol* 287: R198–R208, 2004.
25. **Huysman MWA, Hokken-Koelega ACS, De Ridder MAJ, and Sauer PJJ.** Adrenal function in sick very preterm infants. *Pediatr Res* 48: 629–633, 2000.
26. **Iverson SL and Orrenius S.** The cardiolipin-cytochrome c interaction and the mitochondrial regulation of apoptosis. *Arch Biochem Biophys* 423: 37–46, 2004.
27. **Jensen CL and Heird WC.** Lipids with an emphasis on long-chain polyunsaturated fatty acids. *Clin Perinatol* 29: 261–281, 2002.
28. **Koshkin V and Greenberg ML.** Oxidative phosphorylation in cardiolipin-lacking yeast mitochondria. *Biochem J* 347: 687–691, 2000.
29. **Lee PC, Jelinek B, Struve M, Bruder ED, and Raff H.** Effect of neonatal hypoxia on the development of hepatic lipase in the rat. *Am J Physiol Regul Integr Comp Physiol* 279: R1341–R1347, 2000.
30. **LeFlore JL, Salhab WA, Broyles RS, and Engle WD.** Association of antenatal and postnatal dexamethasone exposure with outcomes in extremely low birth weight neonates. *Pediatrics* 110: 275–279, 2002.
31. **Low JA, Froese AB, Galbraith RS, Smith JT, Sauerberi EE, and Derrick EJ.** The association between preterm newborn hypotension and hypoxemia and outcome during the first year. *Acta Paediatr* 82: 433–437, 1993.
32. **Marszalek JR, Kitidis C, Dararutana A, and Lodish HF.** Acyl-CoA synthetase 2 overexpression enhances fatty acid internalization and neurite growth. *J Biol Chem* 279: 23882–23891, 2004.
33. **McEvoy C, Bowling S, Williamson K, McGaw P, and Durand M.** Randomized, double-blinded trial of low-dose dexamethasone: II. Functional residual capacity and pulmonary outcome in very low birth weight infants at risk for bronchopulmonary dysplasia. *Pediatr Pulmonol* 38: 55–63, 2004.
34. **Momma K, Nakanishi T, and Imamura S.** Inhibition of in vivo constriction of fetal ductus arteriosus by endothelin receptor blockade in rats. *Pediatr Res* 53: 479–485, 2003
35. **Mortola JP.** How newborn mammals cope with hypoxia. *Respir Physiol* 116: 95–103, 1999.
36. **Murphy BP, Inder TE, Huppi PS, Warfield S, Zientara GP, Kikinis R, Jolesz FA, and Volpe JJ.** Impaired cerebral cortical gray matter growth after treatment with dexamethasone for neonatal chronic lung disease. *Pediatrics* 107: 217–221, 2001.
37. **Neal CR, Weidemann G, Kabbaj M, and Vazquez DM.** Effect of neonatal dexamethasone exposure on growth and neurological development in the adult rat. *Am J Physiol Regul Integr Comp Physiol* 287: R375–R385, 2004.
38. **Plonne D, Schulze HP, Kahlert U, Meltke K, Seidolt H, Bennett AJ, Cartwright IJ, Higgins JA, Till U, and Dargel R.** Postnatal development of hepatocellular apolipoprotein B assembly and secretion in the rat. *J Lipid Res* 42: 1865–1878, 2001.
39. **Raff H.** Neonatal dexamethasone therapy: short and long-term consequences. *Trends Endocrinol Metab* 15: 351–352, 2004.
40. **Raff H and Chadwick CJ.** Aldosterone responses to ACTH during hypoxia in conscious rats. *Clin Exp Pharmacol Physiol* 13:827–830, 1986.
41. **Raff H, Jankowski BM, Bruder ED, Engeland WC, and Oaks MK.** The effect of hypoxia from birth on the regulation of aldosterone in the 7-day-old rat plasma hormones, steroidogenesis in vitro and steroidogenic enzyme mRNA. *Endocrinology* 140: 3147–3153, 1999.
42. **Raff H, Sandri RB, and Segerson TP.** Renin, ACTH, and adrenocortical function during hypoxia and hemorrhage in conscious rats. *Am J Physiol Regul Integr Comp Physiol* 250: R240–R244, 1986.
43. **Rooney SA, Smart DA, Weinhold PA, and Feldman DA.** Dexamethasone increases the activity but not the amount of choline-phosphate cytidylyltransferase in fetal rat lung. *Biochim Biophys Acta* 1044: 385–389, 1990.
44. **Shelley SA, Pagica JE, and Balis JU.** Lung surfactant phospholipids in different animal species. *Lipids* 19: 857–862, 1984.

45. **Shimizu H, Miyamura K, and Kuroki Y.** Appearance of surfactant proteins, SP-A and SP-B, in developing rat lung and the effects of in vivo dexamethasone treatment. *Biochim Biophys Acta* 1081: 53–60, 1991.
46. **Sinkin RA, Dweck HS, Horgan MJ, Gallaher KJ, Cox C, Maniscalco WM, Chess PR, D'Angio CT, Guillet R, Kendig JW, Ryan RM, and Phelps DL.** Early dexamethasone—attempting to prevent chronic lung disease. *Pediatrics* 105: 542–548, 2000.
47. **Sullivan LC and Orgeig S.** Dexamethasone and epinephrine stimulate surfactant secretion in type II cells of embryonic chickens. *Am J Physiol Regul Integr Comp Physiol* 281: R770–R777, 2001.
48. **Takamoto DY, Lipp MM, von Nahmen A, Lee KYC, Waring AJ, and Zasadzinksi JA.** Interaction of lung surfactant proteins with anionic phospholipids. *Biophys J* 81: 153–169, 2001.
49. **Thomas T and Marshall JM.** A study on rats of the effects of chronic hypoxia from birth on respiratory and cardiovascular responses evoked by acute hypoxia. *J Physiol* 487: 513–525, 1995.
50. **Vermont Oxford Network Steroid Study Group.** Early postnatal dexamethasone therapy for the prevention of chronic lung disease. *Pediatrics* 108: 741–748, 2001.
51. **Watkins SM, Lin TY, Davis RM, Ching JR, DePeters GM, Halpern GM, Walzem RI, and German JB.** Unique phospholipid metabolism in mouse heart in response to dietary docosahexaenoic or α-linolenic acids. *Lipids* 36: 247–254, 2001.
52. **Watkins SM, Reifsnyder PR, Pan H, German JB, and Leiter EH.** Lipid metabolome-wide effects of the PPAR-gamma agonist rosiglitazone. *J Lipid Res* 43: 1809–1817, 2002.
53. **Watterberg KL, Scott SM, Backstrom C, Gifford KL, and Cook KL.** Links between early adrenal function and respiratory outcome in preterm infants: airway inflammation and patent ductus arteriosus. *Pediatrics* 105: 320–324, 2000.
54. **Wolfe RR, Martini WZ, Irtun O, Hawkins HK, and Barrow RE.** Dietary fat composition alters pulmonary function in pigs. *Nutrition* 18: 647–653, 2002.
55. **Yeh TF, Lin YJ, Lin HC, Huang CC, Hsieh WS, Lin CH, and Tsai CH.** Outcomes at school age after postnatal dexamethasone therapy for lung disease of prematurity. *N Engl J Med* 350: 1304–1313, 2004.

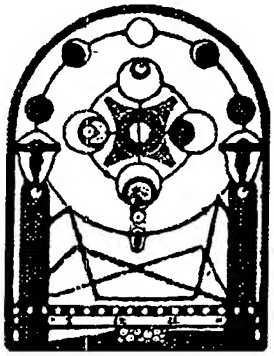

Arteriosclerosis, Thrombosis, and Vascular Biology

JOURNAL OF THE AMERICAN HEART ASSOCIATION

American Heart Association®

Learn and Live℠

Dexamethasone-induced suppression of aortic atherosclerosis in cholesterol-fed rabbits. Possible mechanisms

K Asai, C Funaki, T Hayashi, K Yamada, M Naito, M Kuzuya, F Yoshida, N Yoshimine and F Kuzuya

Arterioscler. Thromb. Vasc. Biol. 1993;13;892-899

Arteriosclerosis, Thrombosis, and Vascular Biology is published by the American Heart Association. 7272 Greenville Avenue, Dallas, TX 72514

 Print ISSN: 1079-5642. Online ISSN: 1524-4636

Dexamethasone-Induced Suppression of Aortic Atherosclerosis in Cholesterol-Fed Rabbits

Possible Mechanisms

Kanichi Asai, Chiaki Funaki, Toshio Hayashi, Kazuyoshi Yamada, Michitaka Naito, Masafumi Kuzuya, Futoshi Yoshida, Noboru Yoshimine, and Fumio Kuzuya

We investigated the mechanisms by which corticosteroids affect atherosclerosis. Male New Zealand White rabbits were injected with 0.125 mg dexamethasone ($n=10$) or vehicle (control group, $n=10$). Both groups were fed a 1% cholesterol diet for 8 weeks. Although the dexamethasone-treated animals exhibited a greater degree of hyperlipidemia, they exhibited significantly less atherosclerotic plaque of the aortic surface than control animals (7.8% versus 47.2%). Immunofluorescence study of the aortic plaque specimens showed that dexamethasone administration reduced both macrophages and T lymphocytes. In vitro, dexamethasone suppressed the proliferation and differentiation of U937 cells and inhibited uptake and degradation of β-very low density lipoproteins by mouse peritoneal macrophages. These findings suggest that dexamethasone suppresses the development of atherosclerosis in the aorta of rabbits by inhibiting recruitment and proliferation of macrophages and the formation of foam cells in plaques. (*Arteriosclerosis and Thrombosis* 1993;13:892–899)

KEY WORDS • dexamethasone • atherosclerosis • macrophages • rabbits • pathogenesis

Atherosclerotic plaque is characterized by intimal cell proliferation, lipid accumulation, and connective tissue deposition. Because plaque has features similar to those associated with chronic inflammation, such as the accumulation of macrophages,[1,2] anti-inflammatory agents have been evaluated in the treatment of atherosclerosis.[3] Anti-inflammatory drugs, including corticosteroids, have been found to suppress the development of atherosclerosis in both cholesterol-fed New Zealand White rabbits[4,5] and Watanabe heritable hyperlipidemic rabbits.[6] In a different model of experimental atherosclerosis, dexamethasone inhibited both the leukocyte accumulation and intimal thickening induced by cuff sheathing in the rabbit carotid artery; indomethacin, a cyclooxygenase inhibitor, had little effect.[7] However, the mechanisms by which corticosteroids exert an inhibitory effect on atherosclerotic plaque formation remain to be elucidated. In particular, the phenomenon of reduced plaque formation in the presence of enhanced hyperlipidemia in corticosteroid-treated, cholesterol-fed rabbits[3,4] has not been explained. Since monocyte-derived macrophages are thought to play an important role in atherogenesis, we attempted to clarify the mechanism of action of corticosteroids by focusing on the effect of corticosteroid treatment on macrophages. We investigated the effects of dexamethasone on plasma lipoproteins and on the distribution of macrophages and T lymphocytes in plaques of cholesterol-fed rabbits. We also conducted in vitro experiments using monocyte/macrophage-like cells.

From the Department of Geriatrics (K.A., C.F., T.H., K.Y., M.N., M.K., N.Y.) and the Third Department of Internal Medicine (F.Y.), Nagoya University School of Medicine, and the Nakatsugawa Municipal Hospital (F.K.), Nagoya, Japan.

Supported in part by the Japanese Ministry of Education.

Address for correspondence: Kanichi Asai, MD, PhD, Department of Geriatrics, Nagoya University School of Medicine, 65 Tsuruma-cho, Showa-ku, Nagoya, 466 Japan.

Received March 17, 1992; revision accepted March 10, 1993.

Methods

Animal Experiments

Twenty male New Zealand White rabbits weighing 2.2–2.5 kg were divided into two groups: a dexamethasone-treated group ($n=10$) and a control group ($n=10$). Both groups were fed a 1% cholesterol diet for 8 weeks. During those 8 weeks, the dexamethasone-treated group received daily injections of 0.125 mg i.m. (0.050–0.057 mg/kg body wt) of dexamethasone (Banyu Pharmaceutical Co., Tokyo) in 0.1 mL of vehicle. The control group received only vehicle, which contained sodium bisulfate (0.5 mg/mL), methyl *p*-hydroxybenzoate (1.5 mg/mL), propyl *p*-hydroxybenzoate (0.2 mg/mL), and creatinine (8 mg/mL). Blood was sampled at 4-week intervals for the determination of hemoglobin, serum total cholesterol (TC), total protein, and glucose. Very low density lipoprotein (VLDL, $d<1.006$ g/mL) was separated from plasma by ultracentrifugation,[8] and the concentrations of protein, TC, and triglyceride (TG) were measured. TC/TG was calculated as an index of the composition of lipids in VLDL. After 8 weeks, all rabbits were killed by injection of sodium pentobarbital (150 mg i.v.); the whole aorta was removed and incised longitudinally. The aortic surface involved by plaque was traced within 12 hours of removal of the aortas, assessed quantitatively by planimetry with a computer, and expressed as the proportion (percent) of the area of

plaque involvement to that of the entire area of the aorta.

All experiments were conducted in accordance with institutional guidelines for animal studies.

Immunofluorescence Study of Aortic Specimens

Small portions were obtained from the aortic base from two representative animals in each group with the highest or the second highest serum cholesterol level, snap-frozen in liquid nitrogen, and stored at −80°C until studied. Frozen tissues were cut into 2-μm sections with a cryostat. Sections were fixed with acetone at room temperature for 10 minutes and air-dried. After being washed with 0.01 mol/L phosphate-buffered saline (PBS), the sections were incubated for 20 minutes with an optimal concentration of the mouse monoclonal anti-macrophage immunoglobulin M (IgM) antibody (HAM-56, Enzo Diagnostics, New York). The sections were washed three times with PBS and then incubated with fluorescein isothiocyanate (FITC)–conjugated rabbit antibody against mouse IgM (HAM-56). Similarly, to stain the T lymphocytes in plaques, the sections were first incubated with goat anti-rabbit T-lymphocyte polyclonal antibody (CL-8800, Cedarlane Laboratories, Hamby, Canada) and then stained with FITC-conjugated rabbit anti-goat IgG. In addition, small portions from the aortic base were fixed in 10% formalin, embedded in paraffin, and stained with hematoxylin and eosin.

Proliferation and Differentiation of U937

Proliferation of U937 cells and [^{3}H]thymidine incorporation into cellular DNA. U937 cells (CRL 1593, American Type Culture Collection, Rockville, Md.) were cultured in RPMI 1640 (Nissui Pharmaceutical Co., Tokyo) supplemented with 10% fetal calf serum (FCS, Cell Culture Laboratories, Cleveland, Ohio) in a humidified CO_2 (5%) incubator at 37°C. Cell growth was arrested in cultures of U937 cells at a cell concentration of $\approx 1\times10^6$ cells/mL by transfer of cells to RPMI 1640 with 0.5% FCS; cells were incubated in this medium for 48 hours. The incubated cells were seeded in RPMI 1640 with 10% FCS (growth medium) at a density of $1.5–1.6\times10^5$/mL and were incubated for 48 hours with dexamethasone in concentrations of 10^{-9} to 10^{-6} mol/L (Sigma Chemical Co., St. Louis, Mo.) dissolved in ethanol. The final concentration of ethanol in the incubation medium was 0.1% (vol/vol). After 48 hours of treatment, the cells were counted with a hemocytometer (model CC-130, Sysmex, Tokyo).

DNA synthesis during dexamethasone treatment was evaluated by [^{3}H]thymidine (TdR) incorporation. The U937 cultures, which had been growth arrested and incubated for 48 hours in RPMI 1640 with 0.5% FCS, were incubated in a growth medium containing 10^{-9} to 10^{-6} mol/L dexamethasone and incubated for 24 hours. Aliquots (1 mL) with a density of 4×10^5 cells/mL were incubated with 3.7 kBq/mL of [^{3}H]TdR (NEN Research Products, Boston) for 2 hours at 37°C. The cells were then washed twice with Dulbecco's PBS, and the radioactivity in trichloroacetic acid (TCA, Katayama Chemical, Osaka, Japan)–insoluble fractions was measured.

Differentiation of U937 by phorbol esters. The U937 cell line is a well-characterized representative of monocytic cells that, on stimulation with differentiation-inducing agents such as phorbol esters, mature along the monocytic pathway.[9] When stimulated by phorbol 12-myristate 13-acetate (PMA, Sigma), these cells adhere

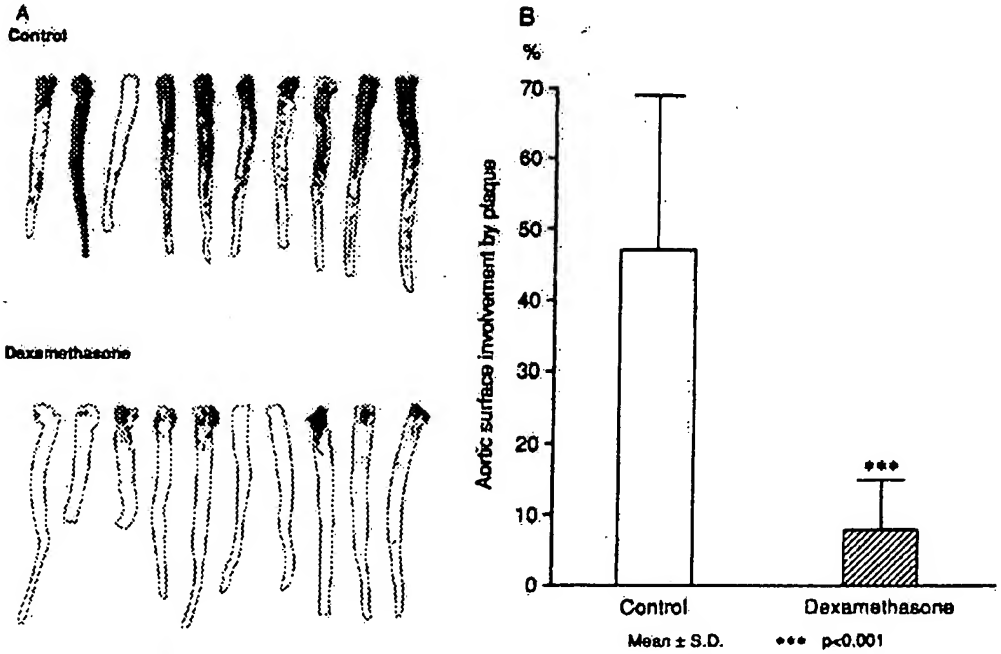

FIGURE 1. *Plaque involvement of aortic surface. Panel A: Drawing showing aortic surface plaque involvement traced within 12 hours of removal of aortas. Black portions represent areas of plaque. Panel B: Bar graph showing aortic surface involvement expressed as the proportion (percent) of the area of aortic plaque involvement to the entire aortic area.*

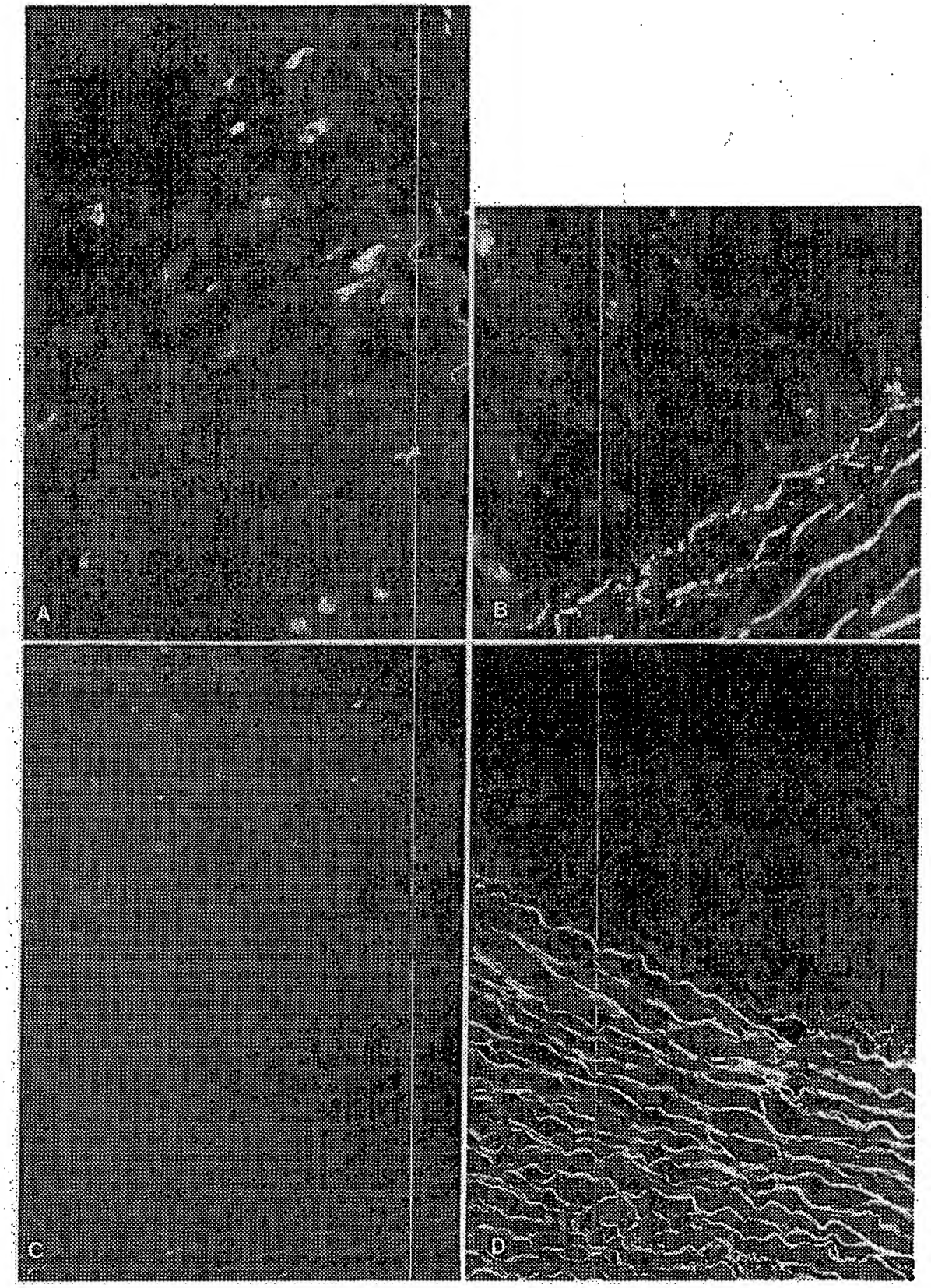

FIGURE 2. *Facing page. Immunofluorescence photomicrographs. Panel A: Aortic plaque lesions from a representative control rabbit (anti-macrophage antibody; HAM-56; original magnification, ×400). Note the cluster of positively stained cells in core lesions of atheromatous plaques. Panel B: Dexamethasone-treated rabbit. Few positive cells were observed in lesions (original magnification, ×400). Panel C: Plaque lesions from a control rabbit (anti-T-lymphocyte antibody; CL-8800; original magnification, ×200). Round, positively stained cells were seen in plaques. Panel D: Lesions from a dexamethasone-treated rabbit showed no positively stained cells (original magnification, ×200).*

to plastic and exhibit macrophage-like characteristics.[10] To assess the effect of dexamethasone on the PMA-induced differentiation, we counted the number of the adherent cells[10] after they were cultured for 72 hours with 10^{-9} to 10^{-6} mol/L dexamethasone and 10^{-9} mol/L PMA dissolved in dimethyl sulfoxide (DMSO, Katayama Chemical). The final concentration of DMSO in the incubation medium was 0.1% (vol/vol). Percentage of adherent cells was calculated as number of adherent cells divided by number of nonadherent cells plus adherent cells times 100 (%).

In each experiment, the viability of U937 cells was determined by trypan blue dye exclusion. Results are given as the average of triplicate incubations.

Binding, Uptake, and Degradation of β-VLDL by Mouse Peritoneal Macrophages

Unstimulated ddY mice weighing 25–30 g were anesthetized with ethyl ether in air, and peritoneal cells were harvested in Dulbecco's PBS.[11] Cells were collected by centrifugation (400g, 10 minutes) and washed once with Dulbecco's modified Eagle's medium (DMEM, Nissui Pharmaceutical Co.). Aliquots (1 mL) were dispensed into 12-well dishes (Corning 25815, Corning, N.Y.) in DMEM containing 20% (vol/vol) FCS and then incubated in a humidified CO_2 (5%) incubator at 37°C for 2 hours. After being washed to remove the nonadherent cells, the monolayers were incubated with or without 10^{-7} mol/L dexamethasone for 36 hours at 37°C in DMEM containing 20% FCS and then used in experiments.[11] Each dish contained about 70–90 μg cell protein, which was not substantially altered by dexamethasone treatment.

β-VLDL separated from the plasma of cholesterol-fed rabbits was labeled with 37 MBq of [^{125}I]NaI (NEN Research Products) by the iodine monochloride method.[12] The specific activity of ^{125}I–β-VLDL ranged from 20 to 40 cpm/ng iodine monochloride protein. Treatment with 15% TCA consistently precipitated >97% of the radioactivity. An average of 3.5% radioactivity was present in the lipid, as determined by chloroform/methanol extraction. After the medium was replaced by DMEM containing 0.3% bovine serum albumin (BSA, Sigma) with or without 10^{-7} mol/L dexamethasone, the cells were incubated with ^{125}I–β-VLDL for 5 hours. The total cellular content (cellular uptake) of ^{125}I–β-VLDL in the peritoneal macrophages was measured.[13] The proteolytic degradation of ^{125}I–β-VLDL by the cells was determined by assaying the amount of the ^{125}I-labeled, TCA-soluble material excreted into the medium from the cells.[13] For the binding study, the cells were incubated with ^{125}I–β-VLDL at 4°C for 2 hours. Each dish was washed six times with 2 mL of buffer containing 50 mmol/L tris(hydroxymethyl)aminomethane chloride (pH 7.4), 0.15 mol/L NaCl, and 6 mg BSA. The cells were then dissolved in 1 mL of 0.1N NaOH and incubated for 1 hour at room temperature. The entire sample was assayed to determine the radioactivity associated with the cells.[13,14] In all cases, the cells were incubated with the indicated concentration of ^{125}I–β-VLDL in the presence or absence of a 20-fold excess of unlabeled β-VLDL. Specific binding, uptake, or degradation was calculated by subtracting the amount of ^{125}I–β-VLDL measured in the presence of unlabeled β-VLDL from the amount measured in the absence of unlabeled β-VLDL.

Each data point represents the average of duplicate incubations. The protein content of the lipoproteins and cell extracts was determined by the method of Lowry et al.[15]

Other Assays

Serum levels of cholesterol,[16] TG,[17] total protein, and glucose were determined by established procedures. Data are expressed as mean±SD. Statistical significance was determined by Student's *t* test, with the probability level set at $p<0.05$.

TABLE 1. Effects of Dexamethasone Administration on Body Weight, Organ Weight, and Major Laboratory Parameters in Cholesterol-Fed Rabbits

	Control	Dexamethasone
Body weight (g)	2,924±134	2,447±111*
Organ weight		
Liver (g)	126±11	118±10
Adrenal gland (g)	0.53±0.23	0.21±0.13†
Hemoglobin (g/dL)	10.4±11.2	11.0±0.8
Total protein (g/dL)	6.4±0.8	7.6±0.4*
Total cholesterol (mg/dL)	1,804±612	4,089±1,181*
Glucose (mg/dL)	146±28	124±22

Values are mean±SD. $n=10$. Dexamethasone (0.125 mg) was injected intramuscularly for 8 weeks.
*$p<0.001$; †$p<0.01$.

Results

Macroscopic and Microscopic Findings

As illustrated in Figures 1A and 1B, dexamethasone suppressed plaque involvement of the aortic surface by 83% compared with control rabbits ($p<0.001$). Microscopic study of plaques from the aortic base showed a markedly raised intima with proliferation of foam cells in control rabbits. In dexamethasone-treated rabbits, the lesions consisted of fewer layers of foam cells.

Immunofluorescence Study

Immunofluorescence microscopic study using anti-macrophage monoclonal antibody (HAM-56) showed clusters of positively stained cells in atherosclerotic plaques of the control animals (Figure 2A). There was a marked decrease in these cells in the dexamethasone-treated rabbits (Figure 2B). Similarly, aortic specimens

TABLE 2. Effects of Dexamethasone Administration on Fractions of Very Low Density Lipoprotein

	Protein (mg/mL)	TC (mg/dL)	TG (mg/dL)	TC/TG
Control				
4 Weeks	3.8±1.0	1,064.5±548.7	51.3±25.5	21.3±6.2
8 Weeks	5.4±2.1	1,443.3±538.4	143.0±55.3	10.6±4.0
Dexamethasone				
4 Weeks	6.0±1.8*	1,985.7±671.0*	323.3±108.8†	6.5±2.3†
8 Weeks	8.0±2.7*	3,623.5±1,540.2*	254.9±270.1	32.0±21.2‡

TC, total cholesterol; TG, triglyceride. Values are mean±SD.
*$p<0.01$, †$p<0.001$, ‡$p<0.05$, control vs. dexamethasone.

stained with anti-T-lymphocyte polyclonal antibody (CL-8800) showed some T lymphocytes in the plaques of the control rabbits but almost no T lymphocytes in aortic specimens from dexamethasone-treated animals (Figures 2C and 2D).

Body Weight, Organ Weight, and Laboratory Parameters

The serum TC level in the dexamethasone-treated group was more than twice that of the control group (Table 1): 1,804±612 mg/dL (control) versus 4,089±1,181 mg/dL (dexamethasone-treated) ($p<0.001$). Serum total protein levels in the dexamethasone-treated group were significantly higher than in the control group ($p<0.001$). Hemoglobin and serum glucose did not differ significantly between the two groups. Baseline body weights were similar in both groups: 2,266±163 g (control) versus 2,266±111 g (dexamethasone-treated). At autopsy, the body weight of the dexamethasone-treated animals was significantly ($p<0.001$) decreased compared with control, indicating that the dexamethasone-treated rabbits gained less weight during the experimental period. The weights of major organs did not differ between the groups, with the exception of the adrenal gland, which was significantly ($p<0.01$) smaller in the dexamethasone-treated group.

Analysis of VLDL Fractions

Analysis of VLDL fractions revealed a significant increase in protein ($p<0.01$), TC ($p<0.01$), and TG ($p<0.001$) in the dexamethasone-treated group compared with the control group at 4 weeks (Table 2). In the dexamethasone-treated group, the TC/TG was significantly lower ($p<0.001$) at 4 weeks but was significantly higher ($p<0.05$) at 8 weeks.

Proliferation and Differentiation of U937 Cells

The U937 cells used in this study consistently showed a viability of >95%, as determined by trypan blue dye exclusion. As shown in Figure 3, top panel, dexamethasone at concentrations of 10^{-8} to 10^{-6} mol/L significantly (10^{-8} mol/L, $p<0.05$; 10^{-7} to 10^{-6} mol/L, $p<0.001$) suppressed the increase in number of U937 cells after 48 hours of culture. Cell viability was >90% after treatment with 10^{-9} to 10^{-6} mol/L dexamethasone, similar to cell viability in the control group (Figure 3, top). When DNA synthesis was evaluated by [^{3}H]TdR incorporation, U937 cells incubated with 10^{-6} mol/L dexamethasone for 24 hours showed a significantly ($p<0.05$) decreased DNA synthesis (Figure 3, bottom). Again, cell viability did not differ between the control and dexamethasone-treated cells. These results suggest that dexamethasone suppressed the proliferation of U937 cells without causing significant toxic effects.

The U937 cells incubated with 10^{-9} mol/L PMA for 72 hours showed a sixfold increase (from 4.9% to 29.9%) in adherence, as measured by percent adherence to plastic dishes (Figure 4). Dexamethasone at concentrations of 10^{-7} to 10^{-6} mol/L significantly ($p<0.001$) reduced the percentage of adherent U937 cells. When the viability of residual nonattached cells was examined, the PMA-treated cells showed a slight decrease after 72 hours of incubation: 95.2% (0.1% DMSO control) versus 91.6% (0.1% ethanol control with PMA). The dexamethasone-treated cells showed at least 88.5% viability (10^{-7} mol/L), indicating that dexamethasone treatment did not produce any significant decrease in the viability of nonattached cells.

Binding, Uptake, and Degradation of ^{125}I-β-VLDL by Mouse Peritoneal Macrophages

The effects of dexamethasone at 10^{-7} mol/L on ^{125}I-β-VLDL binding, uptake, and degradation as a function of ligand concentration appear in Figure 5. Treatment with 10^{-7} mol/L dexamethasone did not alter the binding of ^{125}I-β-VLDL to mouse peritoneal macrophages (Figure 5, top panel). In contrast, dexamethasone treatment reduced ^{125}I-β-VLDL uptake and degradation (Figure 5, middle and bottom panels). The saturation curve of ^{125}I-β-VLDL degradation showed a pattern in the effect on receptor activity: the apparent $V_{maximum}$ was reduced, whereas the K_m did not change.

Discussion

The mechanism by which corticosteroids inhibit diet-induced atherosclerosis in rabbits has not been established. Our results showed that dexamethasone reduced the development of grossly visible atherosclerotic plaques by an average of 83% in cholesterol-fed rabbits, despite the development of a greater degree of hyperlipidemia in treated animals. These findings are consistent with previous reports.[4-6] Less plaque formation in the presence of more highly elevated serum cholesterol levels contradicts the assumption that the severity of atherosclerosis is proportional to serum cholesterol levels. We performed lipoprotein analysis, an immunofluorescence study of plaques, and in vitro experiments to examine the effects of dexamethasone on U937 cells and mouse peritoneal macrophages in an attempt to explain this paradox. Our analysis of VLDL fractions indicated that VLDL concentration was increased in dexamethasone-treated animals, but there was no con-

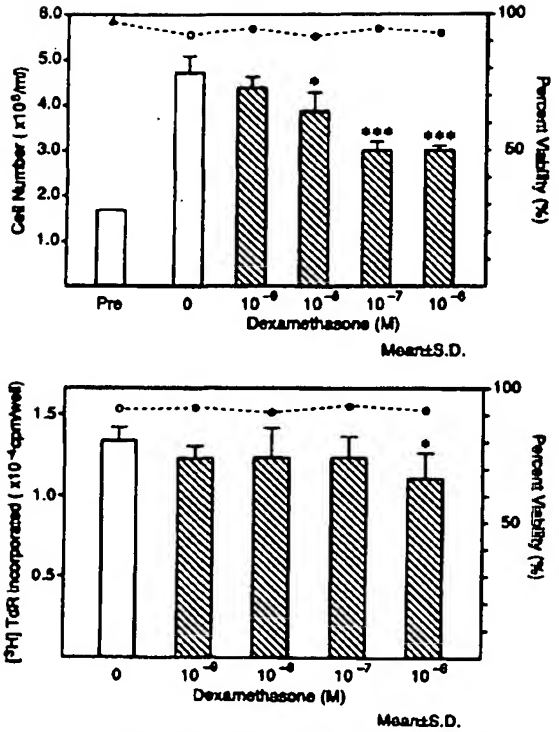

FIGURE 3. *Bar graphs showing effects of dexamethasone on proliferation of U937 cells. Upper panel: Cell count after 48 hours of culture. Cultures of U937 cells at a concentration of ≈1×10⁶/mL were growth arrested by being transferred to RPMI 1640 with 0.5% fetal calf serum and were then incubated for 48 hours. The incubated cells in a concentration of 1.5–1.6×10⁵/mL (pre) were then incubated in the growth medium with or without (control cells) the indicated concentration of dexamethasone for 48 hours. The number of cells was counted by hemocytometer. Lower panel: [³H]Thymidine (TdR) incorporation into cellular DNA. U937 cells, growth arrested and incubated as in upper panel, were incubated in growth medium containing the indicated concentration of dexamethasone for 24 hours. Aliquots (1 mL, 4×10⁵ cells/mL) were incubated with 3.7 kBq/L [³H]TdR for 2 hours. After aliquots were washed with Dulbecco's phosphate-buffered saline, radioactivity in trichloroacetic acid–insoluble fractions was counted. Each point represents the mean of five incubations. The cell viability was determined by trypan blue dye exclusion. Each point represents the average of triplicate determinations. △, Cell viability (pre); ○, cell viability without dexamethasone (0, control); ●, cell viability with the indicated concentration of dexamethasone. *p<0.05; ***p<0.001 (vs. control).*

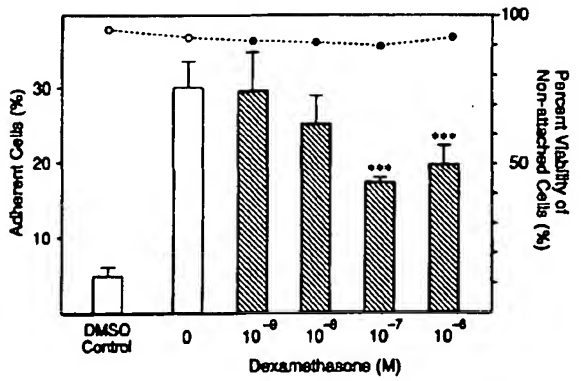

FIGURE 4. *Bar graph showing adherent U937 cells (%) after 72 hours of incubation with phorbol 12-myristate 13-acetate (PMA) and dexamethasone. U937 cells (3.5–3.6×10⁵/mL) were incubated with 10⁻⁹ mol/L PMA for 72 hours in the absence or presence of the indicated concentration of dexamethasone. For the dimethyl sulfoxide (DMSO) control, the cells were incubated in growth medium containing only 0.1% DMSO and ethanol. Percent of adherent cells is expressed as number of adherent cells divided by number of nonadherent cells plus adherent cells times 100 (%). Each point represents the mean of six incubations. The viability of residual nonadherent cells is expressed as the average of triplicate determinations. ○, Cell viability without dexamethasone; ●, cell viability with dexamethasone. ***p<0.001 (vs. 0).*

sistent difference in TC/TG of VLDL fractions between the two groups throughout the experiment.

Macrophages specifically and saturably bind glucocorticoids via their cytosol receptors,[18] which, in turn, modulate numerous macrophage functions.[19] Our in vitro results using the monocyte/macrophage cell line U937 showed that dexamethasone suppressed not only proliferation of these cells but also their PMA-induced differentiation without significantly affecting cell viability. These observations are consistent with previous reports.[10,20] It has been shown that proliferating macrophages exist in atherosclerotic lesions from cholesterol-fed rabbits.[21] The systemic administration of corticosteroids has induced a prolonged monocytopenia in blood and a characteristic reduction of mononuclear phagocytes at the site of inflammation during steroid treatment.[22] Moreover, corticosteroids have also been found to reduce monocyte chemotaxis in response to various inducers.[23] Together with these findings, our immunofluorescence study data suggest that dexamethasone inhibited the recruitment and proliferation of monocyte-derived macrophages in the aortic wall.

Although dexamethasone did not alter the binding of ^{125}I-β-VLDL to mouse peritoneal macrophages, it reduced ^{125}I-β-VLDL uptake and degradation. Related studies conducted under somewhat different experimental conditions have shown that exposure of cultured fibroblasts and arterial smooth muscle cells to physiological concentrations of hydrocortisone (4.1×10^{-8} mol/L),[24] of cultured human monocyte-derived macrophages to dexamethasone,[25] and of cultured human fibroblasts to serum from glucocorticoid-treated patients[26] reduces their capacity to degrade low density lipoprotein (LDL). Recent reports indicate that uptake of β-VLDL is mediated by the LDL receptor,[27–29] suggesting that, in our experiments, dexamethasone suppressed the degradation of β-VLDL via the LDL pathway. Our results with dexamethasone are similar to those in an earlier report[24] showing that hydrocortisone reduced LDL uptake and degradation by cultured human fibroblasts without affecting binding. A decreased uptake of β-VLDL to macrophages in association with unchanged binding suggests a dexamethasone-related internalization defect of β-VLDL, as Henze et al[24] demonstrated

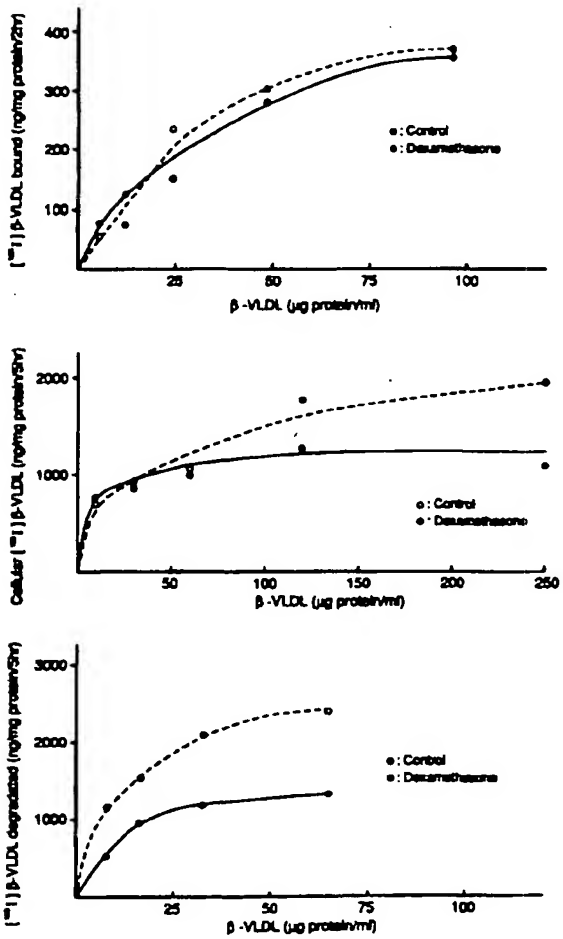

FIGURE 5. *Top panel: Binding curve of ^{125}I–β–very low density lipoprotein (VLDL) to mouse peritoneal macrophages. Monolayers of mouse peritoneal macrophages were preincubated with or without 10^{-7} mol/L dexamethasone for 36 hours at 37°C. Then cells were incubated at 4°C for 2 hours with the indicated concentration of ^{125}I–β-VLDL with or without 10^{-7} mol/L dexamethasone. Cell-associated ^{125}I–β-VLDL was determined. Middle panel: Uptake of ^{125}I–β-VLDL. Mouse peritoneal macrophages were incubated with ^{125}I–β-VLDL at 37°C for 5 hours, and cell-associated ^{125}I–β-VLDL was measured. Bottom panel: Degradation of ^{125}I–β-VLDL. After cells were incubated at 37°C for 5 hours with the indicated concentration of ^{125}I–β-VLDL, the amount of ^{125}I-labeled trichloroacetic acid–soluble materials excreted into the medium was determined. In all studies of binding, uptake, and degradation, incubation with ^{125}I–β-VLDL was carried out in the presence or absence of a 20-fold excess of unlabeled β-VLDL. Each point is the average of duplicate determinations.*

using LDL. When Henze et al measured the net LDL uptake to cultured fibroblasts and arterial smooth muscle cells by trypsinization, they found that hydrocortisone reduced the internalization of LDL. In addition to an enhanced hepatic production or secretion of VLDL caused by dexamethasone administration,[30] these alterations in β-VLDL metabolism in macrophages may play a role in the dexamethasone-induced enhancement of hyperlipidemia. It is conceivable that, despite the enhanced hyperlipidemia induced by a high-cholesterol diet, dexamethasone suppressed macrophages that would be expected to take up and degrade excess β-VLDL in the aortic wall, leading to a decrease in the formation of foam cells. However, a toxic effect of dexamethasone on macrophages can be excluded, since we observed no difference in the amount of cell protein or the number of cells (data not shown).

These observations suggest that dexamethasone enhances the accumulation of β-VLDL in plasma but suppresses the recruitment of monocyte-derived macrophages to the aortic wall, as evidenced by the presence of fewer macrophages in the plaques of the dexamethasone-treated rabbits. In addition, this agent may have inhibited foam cell formation via a reduction in the uptake of β-VLDL by macrophages.

The T lymphocytes frequently found in association with macrophages in plaques[31] may be involved in atherogenesis.[2] Immunofluorescence study in our experiments showed that dexamethasone greatly diminished T lymphocytes in plaques. Since corticosteroids suppress the production of interleukin-1 by macrophages,[32] they may thus exert an inhibitory effect on T-cell accumulation in plaques.

Corticosteroids have been used to treat a variety of chronic diseases, such as rheumatoid arthritis and systemic lupus erythematosus, over long periods. Nevertheless, there is little information on the effects of corticosteroids on atherosclerosis. In humans, retrospective studies, including pathological data obtained at autopsy, suggested that these agents, through their hyperlipidemic action, adversely affected atherogenesis.[33–35] The inconsistency between such reports and our experimental findings raises the question of whether corticosteroids may exert a different action on atherogenesis in humans versus cholesterol-fed rabbits. Although we have no data to answer that question, recent studies[25] using cultured human monocyte-derived macrophages have shown that dexamethasone stimulates acetyl-LDL receptor activity. If this were true in vivo, dexamethasone would augment the scavenger receptor activity of the macrophages for the denatured LDL, which is thought to play a central role in atherogenesis,[36] and would thus accelerate atherosclerosis in humans. Therefore, differing atherogenic lipoproteins in humans and cholesterol-fed rabbits may account for the different response of macrophages to corticosteroid treatment.

The dose of dexamethasone (0.050–0.057 mg/kg) used in our animal experiment is comparable to that administered clinically. However, when administered in vivo for long periods as in this experiment, dexamethasone causes a variety of side effects, including growth retardation or atrophy of adrenal glands (Table 1), indicating that the antiatherogenic effect of dexamethasone cannot be practically applied in the clinical setting. Nonetheless, our data show that, irrespective of the presence of hyperlipidemia, atherosclerotic plaque formation can be suppressed by modulating the function of macrophages. Recently, the suppression of aortic atherosclerosis by purified rabbit interferon was observed in cholesterol-fed rabbits[37] in which, interestingly, interferon administration did not change the

serum lipid levels but decreased the number of foam cells of macrophage origin in the atherosclerotic lesions. This result, as well as our findings, suggests that approaches other than the lowering of serum cholesterol that may affect the inflammatory aspects of atherosclerosis may protect against atherogenesis.

In conclusion, our observations suggest that dexamethasone suppresses the recruitment and proliferation of macrophages and the formation of foam cells in atherosclerotic lesions, thereby inhibiting the development of aortic atherosclerosis in cholesterol-fed rabbits. These findings may provide new insights into the pharmacological control of atherosclerosis.

Acknowledgments

We would like to thank S. Aoyama, M. Doi, and K. Adachi for their excellent technical assistance.

References

1. Munro JM, Cotran RS: The pathogenesis of atherosclerosis: Atherogenesis and inflammation. *Lab Invest* 1988;58:249–261
2. Hansson GK, Jonasson L, Seifert PS, Stemme S: Immune mechanisms in atherosclerosis. *Arteriosclerosis* 1989;9:567–578
3. Bailey JM, Butler J, Macnamara T, Roe N: Anti-inflammatory steroids in experimental atherosclerosis. *Fed Proc* 1968;27:440–448
4. Bailey JM, Butler J: Anti-inflammatory drugs in experimental atherosclerosis: 1. Relative potencies for inhibiting plaque formation. *Atherosclerosis* 1973;17:515–522
5. Naito M, Yasue M, Asai K, Yamada K, Hayashi T, Kuzuya M, Funaki C, Yoshimine N, Kuzuya F: Effects of dexamethasone on experimental atherosclerosis in cholesterol-fed rabbits. *J Nutr Sci Vitaminol (Tokyo)* 1992;38:255–264
6. Makheja AN, Bloom S, Muesing R, Simon T, Bailey JM: Anti-inflammatory drugs in experimental atherosclerosis: 7. Spontaneous atherosclerosis in WHHL rabbits and inhibition by cortisone acetate. *Atherosclerosis* 1989;76:155–161
7. Hagihara H, Nomoto A, Mutoh S, Yamaguchi I, Ono T: Role of anti-inflammatory responses in initiation of atherosclerosis: Effects of anti-inflammatory drugs on cuff-induced leukocyte accumulation and intimal thickening of rabbit carotid artery. *Atherosclerosis* 1991;91:107–116
8. Hatch FT, Lees RT: Practical methods for plasma lipoprotein analysis. *Adv Lipid Res* 1968;6:1–68
9. Kochler L, Hass R, Goppelt SM, Kaever V, Resch K: Differential effect of dexamethasone on the regulation of phospholipase A_2 and prostanoid synthesis in undifferentiated and phorbol ester-differentiated U937 cells. *J Cell Biol* 1989;40:397–406
10. Dodd RC, Winslow BT: Corticosteroids inhibit the differentiation of U937 cells induced by the combination of lymphocyte-conditioned media and calcitriol. *Bone Miner* 1987;2:281–290
11. Goldstein JL, Ho YK, Brown MS, Innerarity TL, Mahley RW: Cholesteryl ester accumulation in macrophages resulting from receptor-mediated uptake and degradation of hypercholesterolemic canine β-very low density lipoproteins. *J Biol Chem* 1980;255: 1839–1848
12. Bilheimer DW, Eisenberg S, Levy RI: The metabolism of very low density lipoproteins: 1. Preliminary in vitro and in vivo observations. *Biochim Biophys Acta* 1972;260:212–221
13. Goldstein JL, Brown MS: Binding and degradation of low density lipoproteins by cultured human fibroblasts: Comparison of cells from a normal subject and from a patient with homozygous familial hypercholesterolemia. *J Biol Chem* 1974;249:5153–5162
14. Goldstein JL, Ho YK, Basu SK, Brown MS: Binding site on macrophages that mediates uptake and degradation of acetylated low density lipoprotein, producing massive cholesterol deposition. *Proc Natl Acad Sci U S A* 1979;76:333–337
15. Lowry OH, Rosebrough NJ, Farr AL, Randall RJ: Protein measurement with the Folin phenol reagent. *J Biol Chem* 1951;193: 265–275
16. Allain CC, Poon LS, Chan CSG, Richmond W, Fe PC: Enzymatic determination of total serum cholesterol. *Clin Chem* 1974;20: 470–475
17. Sardesai VM, Manning JA: The determination of triglyceride in plasma and tissues. *Clin Chem* 1968;14:156–161
18. Werb Z, Foley R, Munck A: Interaction of glucocorticoids with macrophages: Identification of glucocorticoid receptors in monocytes and macrophages. *J Exp Med* 1978;147:1684–1694
19. Schreiber AD, Parsons J, McDermott P, Cooper RA: Effects of corticosteroids on the human monocyte IgG and complement receptors. *J Clin Invest* 1975;56:1189–1197
20. Duval D, Lynde P, Hatzfeld A, Hatzfeld J: Dexamethasone-induced stimulation of arachidonic acid release by U937 cells grown in defined medium. *Biochim Biophys Acta* 1986;887:204–213
21. Rosenfeld ME, Ross R: Macrophage and smooth muscle cell proliferation in atherosclerotic lesions of WHHL and comparably hypercholesterolemic fat-fed rabbits. *Arteriosclerosis* 1990;10: 680–687
22. Leibovich SJ, Ross R: The role of the macrophage in wound repair. *Am J Pathol* 1975;78:71–100
23. Rinehart JJ, Balcerzak SP, Sagone AL, LoBulio AF: Effects of corticosteroids on human monocyte function. *J Clin Invest* 1974;54: 1337–1343
24. Henze KA, Chait A, Albers J, Bierman EL: Hydrocortisone decreases the internalization of low density lipoprotein in cultured human fibroblasts and arterial smooth muscle cells. *Eur J Clin Invest* 1983;13:171–177
25. Hirsch LJ, Mazzone T: Dexamethasone modulates lipoprotein metabolism in cultured human monocyte-derived macrophages. *J Clin Invest* 1986;77:485–490
26. Bagdade JD, Albers JJ, Subbaiah PV: Glucocorticoid-related impairment in the metabolism of low density lipoprotein by human fibroblast. *Horm Metab Res* 1986;18:768–770
27. Koo C, Hammond MEW, Innerarity TL: Uptake of canine β-very low density lipoproteins by mouse peritoneal macrophages is mediated by a low density lipoprotein receptor. *J Biol Chem* 1986;261: 11194–11201
28. Ellsworth JL, Kraemer FB, Cooper AD: Transport of β-very low density lipoproteins and chylomicron remnants by macrophages is mediated by low density lipoprotein receptor pathway. *J Biol Chem* 1987;262:2316–2325
29. Koo C, Hammond MEW, Garcia Z, Molloy MJ, Uauy R, East C, Bilheimer DW, Mahley RW, Innerarity TL: Uptake of cholesterol-rich remnant lipoproteins by human monocyte-derived macrophages is mediated by low density lipoprotein receptors. *J Clin Invest* 1988;81:1332–1340
30. Reaven EP, Kolterman OG, Reaven GM: Ultrastructural and physiological evidence for corticosteroid-induced alterations in hepatic production of very low density lipoprotein particles. *J Lipid Res* 1974;15:74–83
31. Jonasson L, Holm J, Skalli O, Bondjers G, Hansson GK: Regional accumulation of T cells, macrophages, and smooth muscle cells in the human atherosclerotic plaque. *Arteriosclerosis* 1986;6:131–138
32. Snyder DS, Unanue ER: Corticosteroids inhibit murine macrophage Ia expression and interleukin 1 production. *J Immunol* 1982; 129:1803–1805
33. Nashel DJ: Is atherosclerosis a complication of long-term corticosteroid treatment? *Am J Med* 1986;80:925–929
34. Kalbak K: Incidence of atherosclerosis in patients with rheumatoid arthritis receiving long-term corticosteroid therapy. *Ann Rheum Dis* 1972;31:196–201
35. Bulkley BH, Roberts WC: The heart in systemic lupus erythematosus and the changes induced in it by corticosteroid therapy. *Am J Med* 1975;58:246–264
36. Steinberg D, Parthasarathy S, Carew TE, Khoo JC, Witztum JL: Beyond cholesterol: Modification of low density lipoprotein that increases its atherogenicity. *N Engl J Med* 1989;320:915–924
37. Wilson AC, Schaub RG, Goldstein RC, Kuo PT: Suppression of aortic atherosclerosis in cholesterol-fed rabbits by purified rabbit interferon. *Arteriosclerosis* 1990;10:208–214

Summary: Federal Circuit hears In re Seagate

On Thursday, June 7, 2007, an en banc Federal Circuit panel heard arguments on In re Seagate. This case presented questions about the scope of the waiver of attorney-client privilege and work-product doctrine that results from asserting an advice-of-counsel defense to willful infringement and the extent, if any, that such a waiver extends to trial counsel. The court also raised the question of whether it should reevaluate the affirmative duty of care to avoid patent infringement established in Underwater Devices, Inc. v. Morrison-Knudsen, 717 F.2d 1380 (Fed. Cir. 1983). It was the creation of this affirmative duty that gave rise to the heavy reliance on opinions of counsel. Eliminating or revising the affirmative duty could have a profound impact on the patent litigation landscape. Judges Newman, Mayer, Lourie, Rader, Schall, Bryson, Gajarsa, Linn, Dyk, and Prost were present at the hearing.

At the onset of Petitioner Seagate's argument, Judge Mayer, referring to Federal Circuit precedent as "Swiss cheese," indicated that it may make sense for the court to eliminate the holes in the law surrounding the affirmative duty of care. This theme continued throughout the oral argument, as the judges often inquired about the effectiveness of current Federal Circuit law surrounding the duty of care and how a change to this standard could potentially change patent litigation.

Should the advice of counsel defense waive communications with trial counsel?

The panel first focused on whether waiver of the attorney-client privilege or work product doctrine should extend to trial counsel when a defendant asserts an advice of counsel defense in response to a willfulness charge. When questioning Petitioner, the panel focused on the situation where trial counsel provides a contrary opinion to that of opinion counsel, even though those facts are not found in this case. Petitioner indicated that the court must balance the defendant's right to retain privileged information with the plaintiff's need to discover evidence about the defendant's state of mind. In many situations, Petitioner argued, the opposing party can use means other than deposing trial counsel to gather essential information. The panel responded to this contention by asking how a plaintiff would even know about a contrary opinion unless the defendant were actually required to disclose communications with trial counsel.

Respondents, Convolve, Inc. and Massachusetts Institute of Technology, replying to similar questioning about trial counsel waiver, indicated that such a contrary opinion by trial counsel is very relevant to the potential infringer's state of mind and should be discoverable. Respondents indicated that this same reasoning applies to in-house counsel. The Petitioner, however, maintained that waiving the privilege with regards to trial counsel presents the defendant with an unwarranted Hobson's choice when defending against willful infringement – it must decide to either assert the advice-of-counsel defense or retain privilege on trial communications with in-house and outside counsel and risk a finding of willfulness and enhanced damages.

Judge Rader asked Respondents whether the timing of an opinion is significant in determining whether a defendant waives privilege, suggesting that, in today's world of "instant suing," the defendant would always receive an opinion from counsel after suit began and so the timing is not really relevant to the inquiry. Respondents countered Judge Rader's proposition by

indicating that even though timing is very relevant, the scope of the wavier does not change regardless of when the defendant received the opinion. The waiver exists to show what the defendant knew at the time of the alleged infringement and if that knowledge changed over time.

Turning Respondents' attention to the practical difficulties that waiver presents, the panel asked counsel how the Petitioner will defend themselves if Respondents obtain unfettered access to the Petitioner's views on the subject matters contained in Seagate's opinion of counsel. Respondents' counsel indicated that under In re EchoStar Commc'n Corp., 448 F.2d 1294 (Fed. Cir. 2006), not all work product is discoverable. Furthermore, counsel continued, Federal Rule of Civil Procedure 26(b) creates a duty to supplement when a party learns of changes to its initial responses. The court reacted, stating that, while it is sympathetic to Respondents' situation here, exposing Petitioner's entire trial strategy seems "fundamentally wrong." Despite the court's opposition to such sweeping disclosures, Respondents' counsel urged against setting a bright-line between opinion counsel and trial counsel communications and work-product because the court can never anticipate every situation that could arise under such a rule.

Should the court revise or change the affirmative duty of care to avoid patent infringement?

After probing both counsels about the waiver issue, the panel then focused on whether it should modify the current duty to avoid infringement and how any change could alter willful infringement litigation.

Petitioner began by questioning whether the duty of care still serves its original intended function, citing the fact that patentees currently assert willfulness in 92.3% of patent infringement cases, and indicated that this case presents the court with a factual situation ripe to create consistency within the law. The panel proceeded to ask Respondents about this high percentage of willfulness claims, inquiring whether today's patentees are really worried about "catching people with [their] hand in the cookie jar" or if plaintiffs' claim willfulness as part of a strategy to receive more discovery. Respondents reacted by highlighting the fact that it is entirely the defendant's decision of whether to assert the advice-of-counsel defense to show it met the requisite duty of care.

The panel also focused on who holds the burden to show whether or not the defendant satisfied its duty of care and how this burden would shift should the court clarify or change the duty standard. Petitioner maintained that in practice, once a willfulness charge is made, the burden shifts to the defendant to show they met their affirmative duty and that courts often conclude that the defendant has breached its duty if the defendant does not present an opinion of counsel. Instead, the burden should be on the plaintiff to prove willfulness by clear and convincing evidence and that only when the plaintiff has made a prima facie case of willfulness should the defendant have to put forth evidence that it met its affirmative duty.

Petitioner further contended that this burden would appropriately shift to the plaintiff should the Federal Circuit adopt the Supreme Court's reckless disregard standard. Respondents appeared to agree with part of Petitioner's argument, conceding that the plaintiff currently carries the burden of showing willfulness by clear and convincing evidence. After the plaintiff sufficiently meets this burden, the burden then shifts to the defendant to defend against the

willfulness claim. Petitioners further argued, however, that allowing the defendant to engage in selective waiver would be unfair to the plaintiff.

The court aptly recognized that any change in jurisprudence surrounding the affirmative duty would not come without profound implications. The panel asked Petitioner about the impact that eliminating the duty could have on the number of opinions of counsel and if the court would still have to address the waiver issue if it eliminated the duty of care. In response, Petitioner conceded that there may be less opinions of counsel providing guidance on whether a patent infringes or not but suggested that companies may still request these opinions for investment purposes and when making decisions about entering the market. Because of this, Petitioner argued, the court would still have to address the waiver issue, regardless of any change to the duty of care.

The court further asked Petitioner whether eliminating the duty of care would continue to drain the value of patents in light of recent Supreme Court decisions. In response, the Petitioner emphasized that the court should require a plaintiff to do more in a willful infringement charge than simply provide the defendant with notice and claim willfulness, which, in effect, places the burden of proving non-willfulness on the defendant and forces the defendant to waive privilege on its opinions.

The panel and counsel often referred to the Supreme Court's June 4, 2007 decision in Safeco v. Burr, which evaluated the meaning of "willful" and determined that, in the context of Safeco, willful meant "reckless." The Seagate panel spent time examining the duty of care standard with both counsel to determine whether the affirmative duty to avoid infringement and whether it amounts to a statutory duty, a negligence standard, or whether it is synonymous with reprehensibility and recklessness. To this end, Judge Dyk probed Respondents' counsel to determine the basis for reading the duty of care into the willfulness statute. Respondents indicated that the duty of care follows a strict liability standard – the defendant must show that it complied with the law.

Conclusion

The panel's overall questioning seemed to illustrate that the court is uncomfortable with exposing trial counsel's mental impressions. However, the court's inquiries also suggested that contrary advice by trial counsel should be discoverable. The panel appeared split on whether it would change the affirmative duty of care standard, recognizing the reduction such a change could have on the value of patents and the number of opinions, but at the same time acknowledging that a plaintiff may sometimes claim willfulness simply to receive more discovery before trial begins. Neither party agreed with the court's suggestion that eliminating the duty would moot the wavier issue – if the defendant chose to rely on opinion of counsel in defense to a charge of willfulness regardless of the standard of proof necessary for willfulness, the scope of waiver and the defendant's state of mind would still be relevant. Regardless of the Federal Circuit's ultimate findings on the facts of this case, the court's decision will significantly impact the future of willful infringement claims.

Effect of indomethacin on serum lipids, lipoproteins, prostaglandins and the extent and severity of atherosclerosis in Rhesus monkeys

VEENA DHAWAN, PHD, NIRMAL KUMAR GANGULY, MD, SIDDHARTHA MAJUMDAR, MD, PHD, ROBINDRA NATH CHAKRAVARTI, MD, PHD

V DHAWAN, NK GANGULY, S MAJUMDAR, RN CHAKRAVARTI. Effect of indomethacin on serum lipids, lipoproteins, prostaglandins and the extent and severity of atherosclerosis in monkeys. Can J Cardiol 1992;8(3):306-312.

The present study evaluated indomethacin therapy – a nonsteroidal anti-inflammatory drug – on experimental hyperlipidemia and atherosclerosis in Rhesus monkeys. Twenty-four monkeys were divided randomly into four groups of six. Two groups received stock pellet diet and two were given an atherogenic diet for six months. After this period, one stock diet-fed group and one atherogenic diet-fed group were treated with oral indomethacin (2.5 mg) on alternate days for a further six months. Serum lipids and lipoproteins were markedly elevated in atherogenic diet-fed monkeys. Generally, indomethacin did not exert a hypocholesterolemic effect; however, liver cholesterol was decreased ($P<0.05$) in atherogenic diet-fed monkeys treated with indomethacin. High density lipoprotein cholesterol was increased in stock diet-fed, indomethacin-treated monkeys but not in atherogenic diet-fed, indomethacin-treated monkeys. Apoprotein A-I was not affected by indomethacin in either stock or atherogenic diet-fed monkeys; however, the drug produced a significant ($P<0.01$) reduction of serum thromboxane B_2 in stock diet-fed monkeys, without restoring the 6-keto-prostaglandin $F_{1\alpha}$ to pretreatment levels. A protective role of the drug was noted on both the extent and severity of aortic and coronary atherosclerosis.

(*Pour résumé, voir page 307*)

Key Words: *Atherosclerosis, Indomethacin, Lipoproteins, Prostacyclin, Rhesus monkey, Thromboxane*

Department of Experimental Medicine, Postgraduate Institute of Medical Education and Research, Chandigarh-160012, India

Correspondence and reprints: Dr RN Chakravarti, Emeritus Scientist, Department of Experimental Medicine, Postgraduate Institute of Medical, Education and Research, Chandigarh-160012, India

Received for publication January 30, 1991. Accepted October 15, 1991

NUMEROUS ANIMAL STUDIES HAVE documented the importance of diet-induced hyperlipidemia in atherosclerosis. Humans and subhuman primates are phylogenetically and metabolically related and present similarities in the morphological features of naturally occurring atherosclerosis (1). Hence, their response to agents used for reversing hypercholesterolemia and atherosclerosis may also be similar.

There is little doubt that serum lipids and lipoproteins are intimately related to atherogenesis. Independent positive association between total cholesterol and low density lipoprotein (LDL) cholesterol levels and ischemic heart disease has been clearly established in numerous epidemiological and clinical studies (2,3). In contrast, elevated levels of high density lipoprotein (HDL) cholesterol appear to be protective (4,5).

In 1971, Alaupovic (6) suggested that apolipoproteins should be considered as important indicators in the evaluation of lipoprotein disorders. Since then, abnormalities in lipoproteins with respect to apoproteins

Effet de l'indométacine sur les lipides, les lipoprotéines et prostaglandines sériques et étendue et gravité de l'athérosclérose chez le singe

RÉSUMÉ: La présente étude évalue l'indométacine — anti-inflammatoire non stéroïdien — dans le traitement de l'hyperlipidémie et de l'athérosclérose expérimentales du singe. Vingt-quatre singes ont été répartis au hasard en quatre groupes de six. Deux groupes ont reçu un régime normal d'aliments secs pour animaux et deux ont suivi un régime athérogène pendant six mois. Au terme de cette période, un premier groupe au régime d'aliments secs et un second groupe au régime athérogène ont reçu de l'indométacine par voie orale à la posologie de 2,5 mg tous les deux jours pendant six mois supplémentaires. Les lipides et lipoprotéines sériques se sont élevés de façon marquée dans le deuxième groupe. En général, l'indométacine n'a pas eu d'effet hypocholestérémique; on a cependant noté une diminution du cholestérol hépatique ($P<0,05$) chez les singes sous régime athérogène traités par l'indométacine. Les lipoprotéines de haute densité ont augmenté chez les singes alimentés normalement et traités par l'indométacine, mais pas chez les singes sous régime athérogène, également traités par l'indométacine. Le médicament n'a eu d'effet sur l'apoprotéine A-I ni pour les uns ni pour les autres, mais il a entraîné une baisse significative ($P<0,01$) des valeurs de la thromboxane B_2 chez les singes alimentés normalement sans rétablir les concentrations de 6-cétoprostaglandine $F_{1\alpha}$ d'avant le traitement. Le rôle protecteur du médicament était notable à la fois sur l'étendue et la gravité de l'athérosclérose aortique et coronaire.

have assumed greater importance as predictors of ischemic heart disease (7). The plasma total apoB and LDL apoB levels have been reported to correlate positively with ischemic heart disease (8,9), whereas HDL apoA-I and HDL apoA-II have a negative correlation (10,11).

Platelets play a key role in the development of atherosclerotic disease as well as in terminal events (12,13). The sequence of events following endothelial damage promotes the adhesion and aggregation of platelets with the formation of microthrombi and release of several vasoactive and mitogenic products. The latter stimulate the migration of smooth muscle cells of the media to the intima which proliferate and cause the formation of a plaque (14). Thus a critical balance between thromboxane and prostacyclin is an important factor for maintaining circulatory homeostasis and inhibiting plaque formation.

Among the therapeutic agents used to counter atherosclerosis in human subjects and experimental animals, those lowering serum cholesterol and LDL cholesterol levels have been used extensively (15). Recently, recognizing the importance of the interaction of vascular injury and platelet adhesion and hyperaggregability, several non-steroidal anti-inflammatory agents (NSAIDs) have been used in atherosclerotic disease — acetylsalicylic acid (ASA) has been the most extensively used of this class (16,17). Another potent NSAID is indomethacin which has not been used extensively as an anti-atherosclerotic agent.

The present study was undertaken to elucidate the effect of a low dose of indomethacin on lipid and lipoprotein profile, prostaglandin level and extent and severity of experimentally-induced atherosclerosis in Rhesus monkeys.

MATERIALS AND METHODS

Twenty-four adult male Rhesus monkeys with body weight ranging from 4 to 5 kg were maintained on a stock pellet diet (Hindustan Lever Ltd, Bombay, India). Water was given ad libitum. Before starting the experiment monkeys were acclimatized in the animal house for one month (termed 0 h). They were then randomly divided into four groups of six monkeys so that each group contained animals of similar body weight and serum lipid profile.

Monkeys of groups 1 and 3 were fed stock diet only, while those of groups 2 and 4 were put on the atherogenic diet comprising 1 g cholesterol and 15 g butter incorporated into the stock diet. This diet provided 1.8 mg cholesterol per kilocalorie per animal per day. After six months, groups 3 and 4 monkeys were given 2.5 mg oral indomethacin (Indian Drugs and Pharmaceuticals Limited, Haridwar, India) on alternate days. Group 1 and 2 monkeys did not receive any drugs. All four groups continued with their respective diets for six months.

The clinical and biochemical parameters recorded for each monkey included body weight, a 12-lead electrocardiogram, blood pressure, serum lipids, lipoproteins, apoproteins and prostaglandins at zero, six and 12 months.

Total cholesterol in serum was measured by the method of Zlatkis et al (18), triglycerides by the method of Gottfried and Rosenberg (19) and phospholipids by the method of Bartlett (20). For lipoprotein analysis, serum HDL fraction was prepared by the double precipitation technique of Lopes-Virella et al (21), and the cholesterol content measured (15). LDL cholesterol and very low density lipoprotein (VLDL) cholesterol were determined by the subtraction method of Friedwald (22):

$$TC - (HDL\text{-}C + 1/5\,TG) = LDL\text{-}C$$
$$TC - (HDL\text{-}C + LDL\text{-}C) = VLDL\text{-}C$$

where TC is total cholesterol and TG is triglycerides.

Serum apoproteins of HDL, ie, apoA-I and apoA-II were measured by radial immunodiffusion method using Daiichi plates (Tokyo, Japan). The standards were procured from Sigma Chemical Company (St Louis). Daiichi plates for apoB could not be procured so apoB could not be determined.

Prostaglandin metabolites, thromboxane B_2 (thromboxane A_2) and 6-keto-prostaglandin$F_{1\alpha}$ (prostacyclin) were measured at zero, six and 12 months. Briefly, samples of plasma/serum were extracted in ethyl acetate, pH 3 to 4 and the organic layer dried under nitrogen gas. After dissolving the

TABLE 1
Effect of indomethacin on serum lipids in Rhesus monkeys

Group (n=6)	Total lipids (mg/dL)			Total cholesterol (mg/dL)			Triglycerides (mg/dL)			Phospholipids (mg/dL)		
	0 months	6 months	12 months	0 months	6 months	12 months	0 months	6 months	12 months	0 months	6 months	12 months
1	397.0 ±18.34	434.0 ±14.18	447.0 ±5.17	111.8 ±3.5	129.0 ±3.26	134.0 ±6.54	39.7 ±2.64	67.6 ±5.02	66.8 ±2.1	182.0 ±10.23	177.8 ±8.6	202.7 ±6.89
2	400.0 ±25.0	654.0* ±32.0	698.0* ±4.2	119.8 ±10.0	212.2* ±14.7	246.2* ±14.7	39.8 ±2.84	63.8 ±2.10	84.7* ±4.07	186.7 ±15.17	157.7* ±8.39	272.0* ±7.83
3	401.0 ±15.77	435.0 ±7.7	471.0 ±13.27	124.3 ±3.28	137.5 ±3.4	147.3 ±4.38	39.2 ±1.62	64.7 ±1.33	66.0 ±1.42	158.5 ±3.32	160.8 ±4.35	174.0† ±5.02
4	438.0 ±22.64	571.0†§ ±8.86	653.0†§ ±6.80	115.3 ±2.71	230.8† ±9.0	264.3† ±6.30	59.0 ±1.4	67.3 ±6.39	89.0† ±1.01	153.0 ±7.98	262.3† ±6.12	275.0† ±7.59
F value	0.898	34.0	242.7	0.9011	33.90	55.52	19.57	0.1916	23.67	4.58	56.59	58.12

*Group 1 Normal diet no indomethacin; Group 2 Atherogenic diet no indomethacin; Group 3 Normal diet plus indomethacin after six months; Group 4 Atherogenic diet plus indomethacin after six months. Values are mean±SEM; n Number of monkeys. *P<0.05 group 1 versus 2; †P<0.05 group 3 versus 4; §P<0.05 group 1 versus 3; ¶P<0.05 group 2 versus 4*

TABLE 2
Effect of indomethacin on aortic and liver cholesterol content

Group (n=6)	Liver cholesterol (mg/g wet weight of tissue)	Aortic cholesterol (mg/g wet weight of tissue)
1	6.4±0.18	2.65±0.17
2	10.6±0.53*	3.95±0.29*
3	5.3±0.22	2.9±0.17
4	9.3±0.26†§	4.0±0.27†§
F value	33.93	8.60

*Group 1 Normal diet no indomethacin; Group 2 Atherogenic diet no indomethacin; Group 3 Normal diet plus indomethacin after six months; Group 4 Atherogenic diet plus indomethacin after six months. Values are mean±SEM; n Number of monkeys. *P<0.05 group 1 versus 2; †P<0.05 group 3 versus 4; §P<0.05 group 1 versus 3; ¶P<0.05 group 2 versus 4*

residues in their respective buffers prostaglandin metabolites were radioimmunoassayed (23,24). The antisera for prostaglandin metabolites were obtained from the Pasteur Institute (Paris, France), and radioactive prostaglandin from Amersham, United Kingdom.

After one year the animals were killed by intravenous sodium pentothal. On necropsy the viscera were examined and the heart and aorta along with its major arteries were dissected out. The aorta was opened dorsally in its long axis and stained with freshly prepared Sudan IV solution. The extent of aortic sudanophilia was mapped on graph paper, from which the percentage involvement of intimal lipid deposition was calculated (25).

The following histological parameters were also taken into consideration for quantification of aortic and coronary atherosclerosis: coronary atherosclerosis index, frequency of aortic and coronary plaques and the size of atheromatous/fibrous plaques. The coronary atherosclerosis index, frequency of plaques and plaque size were determined as previously described (26,27).

The heart and aorta were sampled in 10% buffered formalin solution. From each heart eight transversely cut slices were taken, processed and embedded in paraffin wax. The sections of these blocks were stained with hematoxylin and eosin, elastic Van Geison and phosphotungstic acid hematoxylin. To determine the extent of coronary atherosclerosis, one section from the basal, middle and apical regions of the heart of each animal was scanned and the number of atherosclerotic and non-atherosclerotic arteries counted. The coronary atherosclerosis index was calculated as the ratio of 'number of coronary arteries in sections of heart showing atherosclerosis' to 'total number of coronary arteries in sections of heart examined' multiplied by 100.

The size of the atherosclerotic plaques in each section was measured under the microscope using an ocular micrometer standardized against a stage micrometer. The plaque with maximum vertical dimension was taken for comparison in each animal.

Overall atherosclerosis score: To assess the overall effect of the drug on aortic and coronary atherosclerosis a scoring system was evolved (28). In this, the individual parameters as stated above were scored from 1 to 6 and their product divided by body weight in kilograms (reflecting approximate age). This provided the overall atherosclerosis score.

Statistical analysis: Statistical analysis of the data was made via ANOVA followed by post hoc analysis for biochemical parameters. Histological data were analyzed via the Student's paired t test except frequency of plaques both in aorta and coronary arteries where the χ^2 test was employed.

RESULTS

At the beginning of the study the monkey's body weights were comparable in all the groups. Group 2 and 4 monkeys gained significantly more weight than the animals fed stock pellet diet only ($P<0.05$). Indomethacin did not influence either body weight or blood pressure. No changes in the ECG were noted.

Effect of atherogenic diet on serum lipids and lipoproteins: Serum lipid levels at six months were considered baseline values, ie, before indomethacin dosing, and the results have been compared with these. The atherogenic

TABLE 3
Effect of indomethacin on serum lipoproteins in Rhesus monkeys

Group (n=6)	High density lipoprotein cholesterol (mg/dL)			Low density lipoprotein cholesterol (mg/dL)			Very low density lipoprotein cholesterol (mg/dL)		
	0 months	6 months	12 months	0 months	6 months	12 months	0 months	6 months	12 months
1	55.8±2.08	56.5±3.37	46.2±4.32	47.8±3.51	60.2±5.7	75.2±7.37	7.3±0.41	13.5±1.0	13.6±0.38
2	52.1±2.61	56.0±2.08	56.0±2.62	51.3±5.37	142.0±12.96*	167.3±13.31*	7.9±0.57	12.8±0.41	16.8±0.79*
3	46.0±2.21	49.5±1.87†	61.8±2.15†	70.5±3.20	75.2±2.66	72.0±6.56	7.8±0.32	12.8±0.30	13.2±0.30
4	51.0±1.95	65.6±1.57§	58.0±4.46	52.4±2.77	144.8±10.05†	189.5±10.3†	11.6±0.33	15.2±0.44*†§	17.7±0.21†*
F value	3.19	3.2	3.5	7.0	25.27	39.34	22.72	3.25	22.61

*Group 1 Normal diet no indomethacin; Group 2 Atherogenic diet no indomethacin; Group 3 Normal diet plus indomethacin after six months; Group 4 Atherogenic diet plus indomethacin after six months. Values are mean±SEM; n Number of monkeys. *P<0.05 group 1 versus 2; §P<0.05 group 3 versus 4; †P<0.05 group 1 versus 3; §P<0.05 group 2 versus 4*

diet resulted in a significant increase ($P<0.05$) in all fractions of serum (Table 1) and tissue lipids (Table 2). LDL cholesterol and VLDL cholesterol were increased ($P<0.05$), whereas HDL cholesterol decreased marginally ($P>0.05$) (Table 3). ApoA-I did not show any significant difference but ApoA-II was decreased in group 2 compared to group 1 (Table 4).

Again, indomethacin therapy did not significantly effect serum cholesterol, triglycerides and phospholipids but total lipid values were decreased in group 4. Liver cholesterol content was also decreased ($P<0.05$) in group 4 monkeys without affecting the aortic content (Table 2). ApoA-I and A-II values were not affected by indomethacin (Table 4).

Effect of stock diet: In stock diet-fed monkeys not treated with indomethacin, no effect on serum lipids was noted. However, with indomethacin serum phospholipids were decreased, HDL cholesterol increased ($P<0.05$) and apoA-II decreased. The other parameters were not significantly affected (Tables 1-4).

Effect of indomethacin on prostaglandins: Plasma 6-keto-prostaglandin$F_{1\alpha}$, a stable metabolite of prostacyclin, decreased significantly ($P<0.05$) in atherogenic diet-fed monkeys not treated with indomethacin. In stock diet-fed monkeys, the decline in this value was less marked. Indomethacin had no significant effect on this parameter.

On the contrary, serum thromboxane B2, a stable metabolite of thromboxane A2, was significantly increased in all groups during the experiment ($P<0.05$). The rise was much greater in atherogenic diet-fed groups compared with stock diet-fed monkeys ($P<0.05$). After indomethacin therapy, thromboxane B2 levels were reduced significantly in group 3 compared to group 1. In atherogenic diet-fed drug-treated monkeys, the decrease in thromboxane B2 levels was much less compared to group 2 ($P<0.05$) (Table 5).

Aortic atherosclerosis: Aortic sudanophilia was increased significantly ($P<0.01$) in group 2 and 4 monkeys which were fed an atherogenic diet. The frequency and size of aortic atherosclerotic plaques showed a similar increase in group 2 monkeys; however, indomethacin treatment of atherogenic diet-fed monkeys produced a significant decrease in both the frequency and size of plaques in group 4 ($P<0.01$) (Table 6). A similar decrease in atherosclerotic lesions was not observed in stock-diet fed indomethacin-treated monkeys.

The overall score of aortic atherosclerosis revealed a significant increase in group 2 versus group 1. Treatment with indomethacin produced a marked decline in this score in group 4 monkeys; however, the variation was

TABLE 4
Effect of indomethacin on serum apoproteins in Rhesus monkeys

Group (n=6)	Apoprotein A-I			Apoprotein A-II		
	0 months	6 months	12 months	0 months	6 months	12 months
1	128.3±13.45	162.0±10.73	233.2±18.09	34.8±2.12	42.5±3.21	67.2±4.62
2	133.5±9.97	176.2±2.54	201.3±10.00	36.0±3.83	43.8±1.22	55.2±2.65
3	129.3±7.70	162.0±10.1	231.7±17.3	32.3±3.44	41.6±3.19	52.2±1.60
4	136.2±3.9	164.6±7.7	213.0±14.67	36.0±1.8	43.3±3.54	53.0±3.08
F value	0.629	0.1505	0.996	0.833	0.105	4.74

Group 1 Normal diet no indomethacin; Group 2 Atherogenic diet no indomethacin; Group 3 Normal diet plus indomethacin after six months; Group 4 Atherogenic diet plus indomethacin after six months. Values are mean±SEM; n Number of monkeys

TABLE 5
Effect of indomthacin on prostaglandin metabolites in Rhesus monkeys

Group (n=6)	Thromboxane B_2 (ng/mL)			6-keto-prostaglandin$F_{1\alpha}$ (ng/mL)		
	0 months	6 months	12 months	0 months	6 months	12 months
1	1.02±0.08	2.35±0.47	4.84±0.50	1.78±0.186	1.50±0.26	1.45±0.09
2	1.38±0.11	6.21±0.17*	7.60±0.77*	2.20±0.60	2.18±0.50*	1.01±0.16*
3	1.12±0.16	4.30±0.19	2.63±0.25†	1.57±0.15	1.40±0.15	1.20±0.07
4	1.06±0.10	7.70±0.99†	5.70±0.40†§	1.74±0.10	1.20±0.07	1.07±0.076
F value	6.32	28.86	27.76	5.02	16.64	5.26

*Group 1 Normal diet no indomethacin; Group 2 Atherogenic diet no indomethacin; Group 3 Normal diet plus indomethacin after six months; Group 4 Atherogenic diet plus indomethacin after six months. Values are mean±SEM; n Number of monkeys. *P<0.05 group 1 versus 2; †P<0.05 group 3 versus 4; †P<0.05 group 1 versus 3; §P<0.05 group 2 versus 4*

TABLE 6
Effect of six months' indomethacin therapy on aortic atherosclerosis in Rhesus monkeys

Group (n=6)	Sudanophilia (%)	Frequency of plaques (%)	Size of plaques (μm)	Aortic atherosclerosis score
1	9.5±1.8	25.0	164±42.0	1.05±0.36
2	40.7±7.3*	83.3*	277±1.8*	7.4±2.0*
3	9.0±1.2	22.2	126±20.5	0.9±0.24
4	32.0±7.0†	26.7†	87.5±21.5†	2.4±0.7

*Group 1 Normal diet no indomethacin; Group 2 Atherogenic diet no indomethacin; Group 3 Normal diet plus indomethacin after six months; Group 4 Atherogenic diet plus indomethacin after six months. Values are mean±SEM; n Number of monkeys. *P<0.05 - 0.01 group 1 versus 2; †P<0.05 - 0.01 group 2 versus 4; †P<0.01 group 3 versus 4.*

TABLE 7
Effect of six months' indomethacin therapy on coronary atherosclerosis in Rhesus monkeys

Group (n=6)	Coronary atherosclerosis index (%)	Frequency of plaques (%)	Size of plaques (μm)	Coronary atherosclerosis score
1	5.8±0.7	10.4	31.2±6.3	0.96±0.4
2	8.23±0.8*	23.0*	51.4±16.9	3.79±0.48†
3	6.2±0.46	19.0	45.6±8.8	1.8±0.5
4	5.7±1.3	20.0	29.4±6.7	2.6±0.07‡

*Group 1 Normal diet no indomethacin; Group 2 Atherogenic diet no indomethacin; Group 3 Normal diet plus indomethacin after six months; Group 4 Atherogenic diet plus indomethacin after six months. Values are mean±SEM; n Number of monkeys. *P<0.05 group 1 versus 2; †P<0.01 group 1 versus 2; ‡P<0.01 group 2 versus 4.*

not significant compared with group 2. No effect of indomethacin was seen in stock-diet fed monkeys (Table 6).

Coronary atherosclerosis: The coronary atherosclerosis index and frequency of plaques were significantly increased (P<0.05 - 0.01) in group 2 monkeys compared with group 1. With indomethacin treatment, these parameters showed a decrease in group 4 monkeys, but the change was not significant (P>0.05). A marked decrease in coronary atherosclerotic plaque size was noted in group 4 monkeys compared with group 2, but the difference was not significant (P>0.05) (Table 7).

The overall coronary atherosclerosis score showed a significant increase (P<0.01) in group 2 monkeys compared with group 1. In atherogenic diet-fed indomethacin-treated monkeys (group 4), this score was significantly reduced versus the untreated monkeys (group 2) (P<0.01) (Table 7).

DISCUSSION

Atherosclerotic lesions that occur spontaneously in humans have many common features to those induced in experimental animals by a high fat and cholesterol diet. Narrowing of the vessel lumen is produced by the deposition of cholesterol in and around the intimal cells of the arterial wall in association with proliferation of smooth muscle cells followed by fibrosis. There are many factors which may contribute to the development of atherosclerotic plaques, but two key factors which take an active part in this process are lipoproteins and platelets. Therefore, to understand the mechanisms involved in atherogenesis, it is important to identify the specific lipoproteins responsible for the delivery of cholesterol to the intimal cells.

In the present study, the monkeys which developed atherosclerosis following high fat and cholesterol feeding did not present any clinical symptoms and signs (blood pressure and ECG changes). There was a highly significant increase in all serum lipid fractions in monkeys which were fed an atherogenic diet. These findings confirm the earlier observations that high fat and cholesterol diet induces hyperlipidemia in each species of monkey studied to date (29). In control groups, serum lipids also increased gradually throughout the experiment which could be the result of ageing (30).

Hyperlipidemia is associated with alterations of the hemostatic balance (31-33) and, more specifically, with changes in platelet aggregability and thromboxane A_2 generation (34,35) as well as changes in prostacyclin production by vascular tissue (36).

Experimental hyperlipidemia produced increased secretion of thromboxane B_2 from platelets and decreased level of prostacyclin as evidenced by significantly lower values of 6-keto-prostaglandin$F_{1\alpha}$ (37). These findings support that there was hyperfunction of platelets in hyperlipidemic monkeys which could have contributed to enhanced atheroma formation in atherogenic diet fed monkeys. In addition, the vascular prostacyclin liberation appeared to be decreased in atherogenic diet-fed monkeys, indicating that the balance between thromboxane A_2 and prostaglandin I_2 was disturbed as a result of hyperlipidemia.

Indomethacin therapy in atherogenic diet-fed monkeys did not influence serum cholesterol or triglycerides but slightly decreased total lipids. In stock diet-fed animals phospholipids only were lowered, suggesting that indomethacin produced only marginal effects on serum lipids which is in agreement with the findings of Hollander et al (38) and Pick et al (39) who fed ASA to cynomolgus monkeys.

Serum lipoproteins were not affected in atherogenic diet-fed, indomethacin-treated monkeys, while stock diet-fed animals given indomethacin had increased HDL cholesterol. LDL and VLDL cholesterol were not effected by indomethacin, suggesting that there was only marginal effect of the drug on the mobilization and transport of lipids in circulation. As such the drug appears to exert its anti-atherogenic effect in this model via a different mechanism than that of standard hypolipidemic drugs such as clofibrate and probucol (40).

No significant alterations were noted in apoA-I and A-II whether the animals were fed atherogenic or stock

diet or given indomethacin. These findings agree with the HDL cholesterol patterns except for group 3 for which there is no obvious explanation. The insignificant increase of apoA-I and A-II preterminally from their basal levels seems to be the effect of ageing. The present results are not in agreement with those reported by De Backer et al (41) in humans who showed that apoA-I and apoA-II levels were significantly decreased with lowering of HDL cholesterol in patients suffering from coronary artery disease.

In the present study the significant increase in cholesterol content of both aorta and liver of atherogenic diet-fed animals is in line with earlier reports published from the authors' laboratory (26,28). Indomethacin treatment revealed an interesting effect on tissue cholesterol content in group 3 monkeys. Although aortic cholesterol was not influenced by the drug, liver cholesterol content was significantly decreased – the mechanism is unclear.

The presence of aortic sudanophilia and atherosclerotic plaques in some stock diet-fed animals parallels earlier findings of Chakravarti and associates (1) of spontaneously occurring atherosclerosis in monkeys. It was noted that atherogenic diet feeding aggravated significantly both aortic and coronary atherosclerosis. The overall atherosclerosis score (aortic and coronary) was also significantly increased.

Although some parameters showed significant reduction with indomethacin therapy, the overall score of atherosclerosis was not significantly affected by the drug. Indomethacin treatment, however, significantly decreased coronary atherosclerosis in atherogenic diet-fed monkeys reflected by the overall atherosclerosis score in this group.

The cause of reduction of aortic and coronary plaques following indomethacin therapy possibly could be explained by the anti-inflammatory property of the drug which decreased edema in the lesion and retarded other inflammatory reactions associated with its genesis. However, since there was no change in aortic tissue cholesterol content in the treated animals, it is unlikely that the drug acted through mobilization of tissue lipid through enhanced reverse transport of cholesterol. This was also reflected by an insignificant change in aortic sudanophilia in the indomethacin-treated animals. Further, Bailey et al (42) reported other NSAIDs could suppress plaque size in atherogenic diet-fed rabbits, even when the degree of hypercholesterolemia remained unaffected. In an earlier publication, the present authors reported that indomethacin retards thromboxane generation by platelets and provides significant protection against atherosclerosis (37). In the light of the above findings the authors conclude that indomethacin is an effective anti-atherosclerotic drug.

REFERENCES

1. Chakravarti RN, Kukreja RS. Naturally occurring atherosclerosis in rhesus monkeys. Ind J Med Res 1981;73:603-9.
2. Carlson LA, Ericson M. Quantitative and qualitative serum lipoprotein analysis. Part 2. Studies in male survivors of myocardial infarction. Atherosclerosis 1975;21:435-50.
3. Gordon T, Kannel WB, Castelli WP, Dawber TR. Lipoproteins, cardiovascular disease and death. The Framingham Study. Arch Intern Med 1981;141:1128-31.
4. Gordon T, Castelli WP, Hjortland MC, Kannel WB, Dawber TR. High density lipoprotein as a protective factor against coronary heart disease. The Framingham Study. Am J Med 1977;62:707-11.
5. Miller NE. Associations of high density lipoprotein subclasses and apolipoproteins with ischaemic heart disease and coronary atherosclerosis. Am Heart J 1987;113:589.
6. Alaupovic P. Apolipoproteins and lipoproteins. Atherosclerosis 1971;13:141-5.
7. Brunzell JD, Sniderman AD, Albers JJ, Kwiterovich PO. Apoproteins B and A-I and coronary artery disease in humans. Arteriosclerosis 1984;4:79-83.
8. Avogaro P, Bittolo Bon G, Cazzalato G, Quinci GB. Are apolipoproteins better discriminators than lipids for atherosclerosis? Lancet 1979;i:901-3.
9. Kukita H, Hamada M, Hiwada K, Kokubu T. Clinical significance of measurement of serum apolipoproteins A-I, A-II and B in hypertriglyceridemic male patients with and without coronary artery disease. Atherosclerosis 1985;55:143-9.
10. Noma A, Yokosuta T, Kitamura K. Plasma lipids and apolipoproteins as discriminators for presence and severity of angiographically defined coronary artery disease. Atherosclerosis 1983;49:1-7.
11. Sniderman A, Shapiro S, Marpole D, Skinner B, Teng B, Kwiterovich PO. Association of coronary atherosclerosis with hyperapobetalipoproteinemia (increased protein but normal cholesterol levels in human plasma low density [B] lipoproteins). Proc Natl Acad Sci USA 1980;77:604-7.
12. Haerem JM. Mural platelet microthrombi and major acute lesions of main epicardial arteries in sudden coronary death. Atherosclerosis 1974;19:529-36.
13. Ross R. Atherosclerosis: A problem of the biology of arterial wall cells and their interactions with blood components. Arteriosclerosis 1981;1:293-311.
14. Ross R. The pathogenesis of atherosclerosis – An update. N Engl J Med 1986;314:488-500.
15. Lavie CJ, Gau GT, Squires CRW, Kottke BA. Management of lipids in primary and secondary prevention of cardiovascular disease. Mayo Clin Proc 1988;63:605-21.
16. Fuster V, Adams PC, Badiman JJ, Chesebro JH. Platelet inhibitor drugs: Role in coronary artery disease. Prog Cardiovasc Dis 1987;29:325-46.
17. The Persantine-Aspirin Reinfarction Study Research Group. Persantine and aspirin in coronary heart disease. Circulation 1980;62:449-61.
18. Zlatkis A, Zak B, Boyle AJ. A new method for direct determination of serum cholesterol. J Lab Clin Med 1953;41:486-92.
19. Gottfried SP, Rosenberg B. Improved manual spectrophotometric procedure for determination of serum triglycerides. Clin Chem 1973;19:1077-8.
20. Bartlett GR. Phosphorus assay in column chromatography. J Biol Chem 1969;234:466-8.
21. Lopes-Virella MFL, Stone PG, Colwell JA. Serum high density lipoprotein in diabetic patients. Diabetologia 1977;13:285-91.
22. Friedwald WT, Levy RI, Fredrickson DS. Estimation of the concentration of low density lipoprotein cholesterol in plasma without use of preparative ultracentrifuge. Clin Chem 1972;18:499-502.
23. Salmon JA. A radioimmunoassay for 6-keto-prostaglandin $F_{1\alpha}$. Prostaglandins 1978;15:383-98.
24. Viinikka L, Ylikorkala O. Measurement of thromboxane B_2 in

human plasma or serum by radioimmunoassay. Prostaglandins 1980;20:759-66.
25. Chakravarti RN, Mohan AP, Kumal HS. Atherosclerosis in *Macaca mulatta* – Histopathological, morphometric and histochemical studies in aorta and coronary arteries of spontaneous and induced atherosclerosis. Exp Mol Pathol 1976;25:390-401.
26. Kukreja RS, Datta BN, Chakravarti RN. Catecholamine induced aggravation of aortic and coronary atherosclerosis in monkeys. Atherosclerosis 1981;40:291-4.
27. Mohan AP, Chakravarti RN. Serum and aortic lipid profiles in spontaneous and cholesterol induced atherosclerosis in rhesus monkeys. Atherosclerosis 1975;22:39-46.
28. Bansal N, Majumdar S, Chakravarti RN. Frequency and size of atherosclerotic plaques in vasectomized diabetic monkeys. Int J Fertil 1986;34:298-304.
29. Jokinen MP, Clarkson TB, Prichard RW. Animal models in atherosclerosis research. Exp Mol Pathol 1985;42:1-28.
30. Dhawan V. Experimental atherosclerosis: Effect of prostaglandin inhibitor in vasectomised monkeys. Postgraduate Institute of Medical Education and Research, Chandigarh. 1990. (Thesis)
31. Nordoy A, Rodset JM. Platelet function and platelet phospholipids in patients with hyperbetalipoproteinemia. Acta Med Scand 1971;189:385-91.
32. Beitz J, Forster W. Influence of human low density and high density lipoprotein cholesterol on the in vivo prostaglandin I_2 synthetase activity. Biochim Biophys Acta 1980;620:352-5.
33. Carvalho A, Colman RW, Rees RS. Platelet function in hyperlipoproteinemia. N Engl J Med 1974;290:434-8.
34. Tremoli E, Folco GC, Agradi E, Galli C. Platelet thromboxane and serum cholesterol. Lancet 1979;i:107-8.
35. Tremoli E, Maderna SM, Sirtori CR. Platelet aggregation and malondialdehyde formation in type IIa hypercholesterolemic patients. Haemostasis 1979;8:47-9.
36. Zmuda A, Dembinska-kiec A, Chytkowski A, Gryglewski RJ. Experimental atherosclerosis in rabbits: Platelet aggregation, thromboxane A_2 generation and antiaggregatory potency of prostacyclin. Prostaglandins 1977;14:1035-41.
37. Dhawan V, Ganguly NK, Majumdar S, Chakravarti RN. Short-term therapy of atherosclerosis with low dose indomethacin: An experimental study. J Med Primatol 1990;19:663-73.
38. Hollander W, Kirkpatric B, Paddok J, Colombo M, Nagraj S, Prusty S. Studies on the progression and regression of coronary and peripheral atherosclerosis in the cynomolgus monkeys. I. Effects of dipyridamole and aspirin. Exp Mol Pathol 1979;30:55-73.
39. Pick R, Johnson PJ, Glick G. Deleterious effects of hypertension and oil induced atherosclerosis in the chick. In: Roberts JC Jr, Straus R, eds. Comparative Atherosclerosis. New York: Harper and Row, 1974:77-84.
40. Guiridy SM, Ahrens ZN, Salem GJ. Mechanism of action of clofibrate on cholesterol metabolism in patients with hyperlipidemia. J Lipid Res 1972;13:531-5.
41. De Backer G, Rosseneu M, Deslypere JP. Discriminative value of lipids and apoproteins in coronary heart disease. Atherosclerosis 1982;42:197-203.
42. Bailey JM. Anti-inflammatory drugs in experimental atherosclerosis: Part 6. Combination therapy with steroid and nonsteroid agents. Atherosclerosis 1985;54:205-12.